

# Advances in the Treatment of Dental Diseases with New Dental Biomaterials and Oral Tissue Engineering

Lead Guest Editor: Angelo Mariotti

Guest Editors: Gaurav Goyal and Deepak Gupta





---

**Advances in the Treatment of Dental Diseases  
with New Dental Biomaterials and Oral Tissue  
Engineering**

Journal of Healthcare Engineering

---

**Advances in the Treatment of Dental  
Diseases with New Dental Biomaterials  
and Oral Tissue Engineering**

Lead Guest Editor: Angelo Mariotti

Guest Editors: Gaurav Goyal and Deepak Gupta



---

Copyright © 2023 Hindawi Limited. All rights reserved.

This is a special issue published in "Journal of Healthcare Engineering." All articles are open access articles distributed under the Creative Commons Attribution License, which permits unrestricted use, distribution, and reproduction in any medium, provided the original work is properly cited.

## Associate Editors

Xiao-Jun Chen , China  
Feng-Huei Lin , Taiwan  
Maria Lindén, Sweden

## Academic Editors

Cherif Adnen, Tunisia  
Saverio Affatato , Italy  
Óscar Belmonte Fernández, Spain  
Sweta Bhattacharya , India  
Prabadevi Boopathy , India  
Weiwei Cai, USA  
Gin-Shin Chen , Taiwan  
Hongwei Chen, USA  
Daniel H.K. Chow, Hong Kong  
Gianluca Ciardelli , Italy  
Olawande Daramola, South Africa  
Elena De Momi, Italy  
Costantino Del Gaudio , Italy  
Ayush Dogra , India  
Luobing Dong, China  
Daniel Espino , United Kingdom  
Sadiq Fareed , China  
Mostafa Fatemi, USA  
Jesus Favela , Mexico  
Jesus Fontecha , Spain  
Agostino Forestiero , Italy  
Jean-Luc Gennisson, France  
Badicu Georgian , Romania  
Mehdi Gheisari , China  
Luca Giancardo , USA  
Antonio Gloria , Italy  
Kheng Lim Goh , Singapore  
Carlos Gómez , Spain  
Philippe Gorce, France  
Vincenzo Guarino , Italy  
Muhammet Gul, Turkey  
Valentina Hartwig , Italy  
David Hewson , United Kingdom  
Yan Chai Hum, Malaysia  
Ernesto Iadanza , Italy  
Cosimo Ieracitano, Italy

Giovanni Improta , Italy  
Norio Iriguchi , Japan  
Mihajlo Jakovljevic , Japan  
Rutvij Jhaveri, India  
Yizhang Jiang , China  
Zhongwei Jiang , Japan  
Rajesh Kaluri , India  
Venkatachalam Kandasamy , Czech Republic  
Pushpendu Kar , India  
Rashed Karim , United Kingdom  
Pasi A. Karjalainen , Finland  
John S. Katsanis, Greece  
Smith Khare , United Kingdom  
Terry K.K. Koo , USA  
Srinivas Koppu, India  
Jui-Yang Lai , Taiwan  
Kuruva Lakshmanna , India  
Xiang Li, USA  
Lun-De Liao, Singapore  
Qiu-Hua Lin , China  
Aiping Liu , China  
Zufu Lu , Australia  
Basem M. ElHalawany , Egypt  
Praveen Kumar Reddy Maddikunta , India  
Ilias Maglogiannis, Greece  
Saverio Maietta , Italy  
M.Sabarimalai Manikandan, India  
Mehran Moazen , United Kingdom  
Senthilkumar Mohan, India  
Sanjay Mohapatra, India  
Rafael Morales , Spain  
Mehrbakhsh Nilashi , Malaysia  
Sharnil Pandya, India  
Jialin Peng , China  
Vincenzo Positano , Italy  
Saeed Mian Qaisar , Saudi Arabia  
Alessandro Ramalli , Italy  
Alessandro Reali , Italy  
Vito Ricotta, Italy  
Jose Joaquin Rieta , Spain  
Emanuele Rizzuto , Italy

Dinesh Rokaya, Thailand  
Sébastien Roth, France  
Simo Saarakkala , Finland  
Mangal Sain , Republic of Korea  
Nadeem Sarwar, Pakistan  
Emiliano Schena , Italy  
Prof. Asadullah Shaikh, Saudi Arabia  
Jiann-Shing Shieh , Taiwan  
Tiago H. Silva , Portugal  
Sharan Srinivas , USA  
Kathiravan Srinivasan , India  
Neelakandan Subramani, India  
Le Sun, China  
Fabrizio Taffoni , Italy  
Jinshan Tang, USA  
Ioannis G. Tollis, Greece  
Ikram Ud Din, Pakistan  
Sathishkumar V E , Republic of Korea  
Cesare F. Valenti , Italy  
Qiang Wang, China  
Uche Wejinya, USA  
Yuxiang Wu , China  
Ying Yang , United Kingdom  
Elisabetta Zanetti , Italy  
Haihong Zhang, Singapore  
Ping Zhou , USA

## Contents

---



**Polyetherketoneketone Mesh for Alveolar Bone Augmentation: Geometric Parameter Design and Finite Element Analysis**

Xiaowen Hao, Wei Wang, Chenxi Wang, Jianmin Han , and Yu Zhang   
Research Article (12 pages), Article ID 8487380, Volume 2023 (2023)


**Value Research of NLR, PLR, and RDW in Prognostic Assessment of Patients with Colorectal Cancer**

Wanchen Chen, Shen Xin, and Baohong Xu   
Research Article (6 pages), Article ID 7971415, Volume 2022 (2022)


**Evaluation of the Effect of Nutritional Intervention on Patients with Nasopharyngeal Carcinoma**

Fan Lin , Huijun Ren, Fenfen Lin, Zhaohu Pan, Liping Wu, and Neng Yang   
Research Article (10 pages), Article ID 2531671, Volume 2022 (2022)

**Enhancement of Nursing Effect in Emergency General Surgery Based on Computer Aid**

Yan Lei, Linxiang He, and Houqiang Huang   
Research Article (10 pages), Article ID 6745993, Volume 2022 (2022)

**Correlation of HMGB1, PON-1, MCP-1, and Periodontal *P. gingivalis* with Amniotic Fluid Fecal Dye**

Zhen-Ai Jin , Ying Li, Wei-Bing Chen, Yu-Ying Wang, Yi-Kun Zhao, Xiang-Lan Sun, Jia-Jun He, Guo Jie, and Yu-Mei Sun  
Research Article (10 pages), Article ID 3143102, Volume 2022 (2022)

## Research Article

# Polyetherketoneketone Mesh for Alveolar Bone Augmentation: Geometric Parameter Design and Finite Element Analysis

Xiaowen Hao,<sup>1,2</sup> Wei Wang,<sup>3</sup> Chenxi Wang,<sup>1,2</sup> Jianmin Han ,<sup>2,4</sup> and Yu Zhang <sup>1,2</sup>

<sup>1</sup>Department of Implantology, Peking University School and Hospital of Stomatology, Beijing 100081, China

<sup>2</sup>National Clinical Research Center for Oral Diseases,

National Engineering Laboratory for Digital and Material Technology of Stomatology,

Beijing Key Laboratory of Digital Stomatology,

Research Center of Engineering and Technology for Computerized Dentistry Ministry of Health,

NMPA Key Laboratory for Dental Materials, Beijing 100081, China

<sup>3</sup>Urumqi DW Innovation InfoTech Co., Ltd., Urumqi, Xinjiang 830013, China

<sup>4</sup>Department of Dental Materials, Peking University School and Hospital of Stomatology, Beijing 100081, China

Correspondence should be addressed to Yu Zhang; zhang76yu@163.com

Received 14 June 2022; Revised 28 September 2022; Accepted 24 November 2022; Published 31 January 2023

Academic Editor: Pasi A. Karjalainen

Copyright © 2023 Xiaowen Hao et al. This is an open access article distributed under the Creative Commons Attribution License, which permits unrestricted use, distribution, and reproduction in any medium, provided the original work is properly cited.

**Objective.** To evaluate the mechanical properties of porous polyetherketoneketone (PEKK) meshes with different thicknesses, pore sizes, and porosities through finite element analysis to provide an optimal PEKK design for alveolar bone augmentation in the posterior mandibular region. **Methods.** A three-dimensional evaluation model of severe alveolar bone defects in the mandibular posterior was constructed based on cone beam computerized tomography (CBCT) data. Then, PEKK meshes with different structural designs were obtained. Two key parameters were set with different values: five levels of thickness (0.2 mm, 0.3 mm, 0.4 mm, 0.5 mm, and 0.6 mm) and three levels of pore size (1 mm, 2 mm, and 3 mm) with a corresponding porosity of 19.18%–42.67%. A 100 N physiological force was simultaneously loaded by finite element analysis (FEA), and the deformation and stress data were outputted for further analysis. **Results.** The deformation and stress of the PEKK meshes are negatively correlated with the changes in thickness and positively correlated with the changes in pore size. The FEA results show that the maximum deformation, equivalent stress, and maximum principal stress of the PEKK meshes are 0.168 mm–0.478 mm, 49.243 MPa–124.890 MPa, and 31.549 MPa–104.200 MPa, respectively. The PEKK mesh group with a thickness of 0.2 mm, pore size of 3 mm, and porosity of 42.67% is in danger of plastic deformation or even fracture during use. **Conclusion.** According to the FEA results, the PEKK meshes with larger thicknesses and smaller pore sizes and porosities behave better. In consideration of reducing soft tissue stimulation and promoting bone regeneration, an ultrathin porous PEKK mesh with a pore size of no more than 3 mm, porosity of no more than 42.67%, and thickness of 0.2 mm can be used clinically to meet the mechanical performance requirements of the guided bone regeneration (GBR) structure.

## 1. Introduction

To reestablish dentition function, dental implant surgery is a widely accepted treatment with predictable effects [1] and has become the main choice for patients. As stable bone volume has been considered a prerequisite for successful implant surgery [2], severe periodontal disease, trauma, and tumors often cause severe atrophy or large alveolar bone defects, which are the main challenges for the current

implantology based on osseointegration. Guided bone regeneration (GBR), one of the most commonly used methods, has clinically reliable outcomes regarding alveolar bone augmentation [3]. When performing GBR surgery for the bone augmentation of severe bone defects, a barrier membrane scaffold with a certain mechanical strength is often required to maintain the stability of the osteogenic space. The rigidity of the titanium-reinforced expanded polytetrafluoroethylene (e-PTFE) membrane ensures its



stability during use, and this type of membrane is widely used for bone augmentation. However, the manual bending and trimming of the 2D scaffold material is required during traditional surgery, and bent shapes are often difficult to fit into complex anatomical structures. The time-consuming shaping process and possible sharp edges also increase the risk of soft tissue dehiscence and infection [4], predisposing patients to varying degrees of bone augmentation failure [5].

With the progress in materials science and digital technology, individualized barrier membrane scaffolds that can accurately fit the shape of the reconstructed alveolar ridge can be obtained, enabling restoration-oriented bone augmentation surgery and the design of implant restoration. The individualized scaffold materials that can be digitally designed include metals, such as titanium, and high-performance polymer materials. In recent years, high-performance polymer materials with excellent physicochemical properties and good machinability have become a popular research topic in the application of individualized barrier membrane scaffolds. Among these materials, polyaryletherketone (PAEK) is a stand-out thermoplastic composite due to its ultrahigh mechanical properties and chemical resistance, and its main component, polyetheretherketone (PEEK), exhibits excellent mechanical properties and biological activity and is widely used in the biomedicine field. Recently, there have been clinical studies on the application of individualized PEEK in alveolar bone defect reconstruction, and satisfactory clinical results have been obtained [6, 7]. A recent finite element analysis (FEA) showed that under the load of occlusal force, it is possible for a porous PEEK mesh with a thickness of 0.6 mm to remain relatively stable and have abilities to maintain space and form new bone similar to those of titanium mesh [8].

Space maintenance ability and stability are the key functions of the GBR membrane scaffold, and mechanical properties are one of its primary reference indicators. However, due to the lack of relevant research on the structural design and mechanical properties of individualized PEEK, there is not yet a clear understanding of the mechanical properties of PEEK materials. In addition, the reported PEEK obtained by computer-assisted design/computer-assisted manufacturing (CAD/CAM) with redundant thickness not only increases the difficulty of the clinical operation but also may affect the healing and osteogenesis of the bone graft due to a potentially insufficient blood supply. Moreover, the FEA results suggest that ultrathin PAEK materials have the potential to be barrier membrane scaffolds, and their optimal design needs to be urgently studied. Not only do pore size and porosity have profound impacts on biological properties, such as bone ingrowth and cell and nutrient transport [9], but also thickness is a key design parameter that affects the mechanical properties of barrier membrane scaffolds. Therefore, for their common clinical applications, it is necessary to explore their geometric parameter design to obtain better clinical operability while meeting the biomechanical property requirements.

Polyetherketoneketone (PEKK) is a polyarylether polymer similar to PEEK. Compared with those of PEEK materials, the superior mechanical properties and

antibacterial properties of PEKK materials endow them with greater potential as barrier membrane scaffold materials. In the process of evaluating the mechanical properties of PEKK meshes by traditional mechanical property tests, we found that 3D printing PEKK technology is not yet mature, with high raw material requirements and a high cost. Additionally, the precision of the test PEKK sample obtained by computer numerical control (CNC) machining is poor and cannot meet the experimental design requirements. Finally, we chose the FEA method, which has unique advantages for studying biomechanical behavior, to evaluate the mechanical properties of individualized PEKK meshes.

In this study, we selected severe bone defects in the posterior mandibular area, which is the most common in clinical practice, as the mechanics evaluation model for bone defect reconstruction. We evaluated the mechanical properties of PEKK meshes with different thicknesses, pore sizes, and porosities under simulated physiological loads through FEA to provide a reference for the geometric parameter design of individualized PEKK structures for alveolar bone augmentation in the posterior mandibular area.

## 2. Materials and Methods

**2.1. Geometric Reconstruction.** A 3D geometrical model was constructed based on cone-beam computerized tomography (CBCT) data from a patient who had severe alveolar bone defects in the mandibular posterior area (Figure 1). The authors confirmed that the patient provided informed consent for data collection. The CBCT images (slice thickness 0.2 mm and pixel size 0.200 mm) were input as digital imaging and communications in medicine (DICOM) files for 3D model reconstruction into Mimics 20.0 software (Materialise NV, Belgium). For further noise reduction and smoothing, a standard tessellation language (STL) file was input into Geomagic Studio 2014 software (3D System, USA) and NX 1911 software (Siemens, Germany). A 3D model of the periodontal ligament with a thickness of 0.2 mm was obtained by expanding outward from the tooth surface, and the mandibular bone defect model was shifted inward by 1.5 mm as the cancellous bone model. The periodontal ligament and cancellous bone models were obtained by Boolean operation, and based on the virtual bone augmentation morphology (Figure 2), the PEKK mesh design was obtained. The height of the bone graft was 3 mm at the bottom of the dental crown restoration, and the width of the bone graft was at least 10 mm. The specifications of the titanium screws were designed to be 1.4 mm in diameter and 7 mm in length, and the adjusted positions of the titanium screws were at least 2 mm away from the adjacent teeth, mental foramen, and mandibular canal [10]. Finally, a virtual mandible bone augmentation model was obtained, which contained cortical bone, teeth, periodontal ligament, cancellous bone, bone graft, PEKK mesh, and titanium screws.

**2.2. Finite Element Modeling.** The special FE software ANSYS Workbench 2019 (ANSYS, USA) was used to calculate the models, which were defined as isotropic,

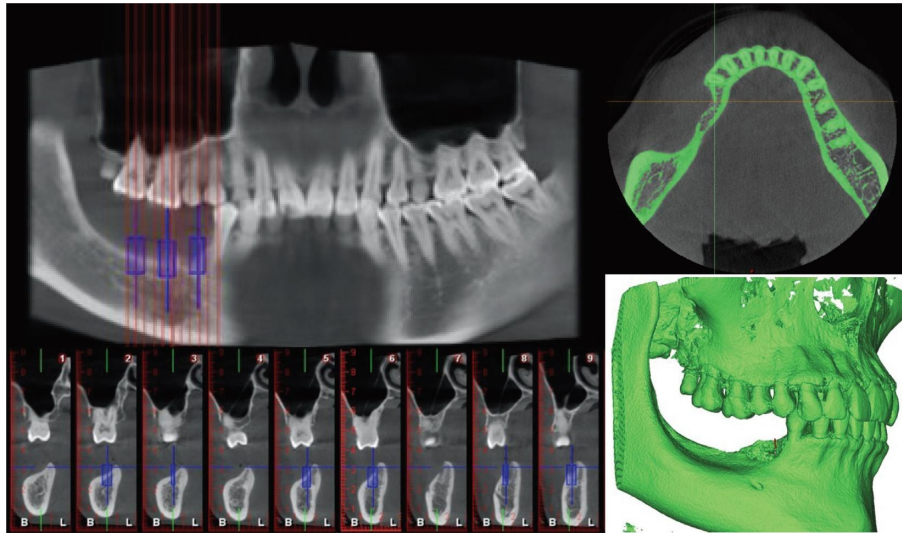


FIGURE 1: CBCT screenshot and 3D reconstruction of severe bone defects in the posterior mandibular area.

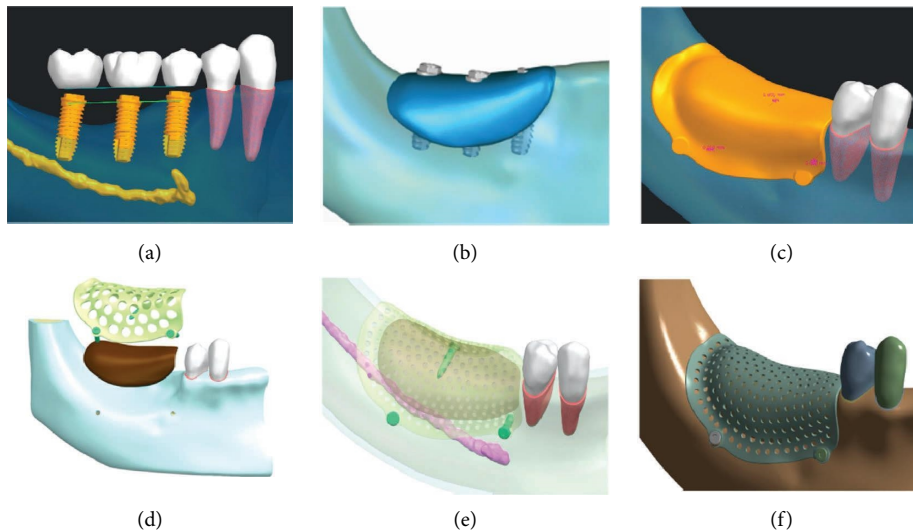


FIGURE 2: Steps involved in the individualized PEKK mesh design. (a) Virtual implants; (b) virtual bone augmentation; (c) formation of bone graft and PEKK shell; (d) assembly of PEKK mesh, titanium screws, and bone graft; (e) adjustment of model position; (f) model of PEKK mesh.

homogeneous, continuous elastic materials. We designed and built fifteen 3D-FE models of the PEKK mesh with thicknesses of 0.2 mm, 0.3 mm, 0.4 mm, 0.5 mm, or 0.6 mm and a pore size of 1.0 mm, 2.0 mm, or 3.0 mm (Table 1).

To achieve greater simulation accuracy, the interface between the PEKK mesh with the cortical bone and the graft bone was set to be in frictional contact with a friction coefficient of 0.2 [11]. The junctions between other models were set to be rigidly connected, such as the connection between the PEKK mesh with titanium screws. According to the literature, Table 2 lists the material properties of the PEKK, cortical bone, periodontal ligament, bone graft, teeth, cancellous bone, and titanium.

The ascending mandibular ramus, the lower edge of the mandible, and the median symphysis were set as the boundaries to limit the movement of the model. In the

axial direction, we applied a functional loading force of 100 N to the model [17] (Figure 3). Then, the deformation and stress data of the PEKK mesh were output for follow-up analysis.

### 3. Results

**3.1. Establishment of the Mechanics Evaluation Model.** By establishing a mechanical evaluation model based on virtual bone augmentation through advanced digital imaging technology combined with a variety of software, we successfully built fifteen 3D-FE individualized PEKK mesh models under strict boundary conditions (Figure 4). The models can simulate the mechanical performance of the barrier membrane and have good geometric similarity.

TABLE 1: Design parameters of the PEKK mesh.

Thickness (mm)	Porosity (%)		
	Pore size = 1 mm	Pore size = 2 mm	Pore size = 3 mm
0.2	19.56	34.31	42.67
0.3	19.40	33.95	42.18
0.4	19.27	33.79	41.98
0.5	19.19	33.62	41.72
0.6	19.18	33.54	41.61

TABLE 2: Material properties of model materials.

Materials	Young's modulus (MPa)	Poisson's ratio
PEKK	5100 [12–14]	0.40
Cortical bone	13700 [13, 14]	0.30
Cancellous bone	1370 [12–14]	0.30
Teeth	18600 [15]	0.31
Periodontal ligament	69 [15]	0.45
Bone graft	10 [16]	0.30
Titanium	110000 [10, 12, 13, 15]	0.30

3.2. *3D-FEA Results of the PEKK Meshes.* Taking the deformation of two groups of PEKK meshes with a pore size of 1 mm and a thickness of 0.6 mm and a pore size of 3 mm and a thickness of 0.2 mm as examples (Figure 5), the displacement from the lingual side to the alveolar ridge and then to the buccal side increases gradually, and the maximum displacement occurs when the alveolar crest migrates to the buccal bone plate. Figure 6 shows the overall deformation distribution of 15 PEKK mesh groups, ranging from 0.168 mm to 0.478 mm.

The equivalent stress of different PEKK meshes ranges from 49.243 MPa to 124.89 MPa (Figure 7), and the maximum principal stress ranges from 31.549 MPa to 104.2 MPa (Figure 8). The two figures show that the distribution trend of the equivalent stress is the same as that of the maximum principal stress, and the maximum stress is concentrated at the turning point of the buccal alveolar ridge. The group with the largest maximum principal stress of 104.2 MPa, which is very close to the extreme tensile strength, is the group of PEKK meshes with a pore size of 3 mm, thickness of 0.2 mm, and porosity of 42.67%, suggesting that this PEKK mesh group may suffer plastic deformation or even fracture during use.

### 3.3. Influences of Thickness and Pore Size on the PEKK Meshes.

The FEA results show that with decreasing thickness (0.6 mm–0.2 mm) and increasing pore size and porosity (1 mm–3 mm; 19.18–42.67%), the maximum deformation and stress values of the PEKK meshes increase (Figure 9). These changes are negatively correlated with the changes in thickness and positively correlated with the changes in pore size.

Moreover, by using multiple linear regression analysis, the deformation, equivalent stress, and maximum principal stress of the PEKK meshes are used as dependent variables to analyze the corresponding influences of the thickness and

pore size (Tables 3–5). The regression models have a statistical significance ( $P < 0.05$ ), which means that both thickness and pore size significantly affect the deformation and stress distributions of the PEKK meshes. The  $F$  change of the multiple regression analysis model of the deformation of PEKK is 152.149, and the adjusted  $R$  squared value is 0.956. The  $F$  change of the multiple regression analysis model of the equivalent stress of PEKK is 42.155, and the adjusted  $R$  squared value is 0.855. The  $F$  change of the multiple regression analysis model of the maximum principal stress of PEKK is 36.777, and the adjusted  $R$  squared value is 0.836.

## 4. Discussion

PAEK is a linear aromatic polyetherketone with a stable para-aromatic ring structure that results in superior mechanical properties and chemical resistance as a thermoplastic composite [13]. Moreover, its good biocompatibility has made it an alternative material for titanium in the field of orthopedics and a promising restorative material in stomatology, and PAEK materials have been applied in removable partial dentures, full-crown restorations, implant abutments, root posts, and cores [18–20]. Both PEEK and PEKK have aromatic ring structures, but their ratios of ether groups and ketone groups are different. Compared with PEEK, PEKK not only exhibits superior mechanical properties in terms of flexural, tensile, and compressive strength [21] but also its elastic modulus is closer to that of the bone tissue, and it has better antibacterial properties [20]. Therefore, in terms of mechanical properties and biological activities, PEKK is more suitable as a barrier membrane scaffold material than PEEK. However, the individualized PEKK structure design and application is still lacking and determining how to obtain an optimal scaffold structure design while meeting biomechanical performance requirements is crucial for its clinical application.

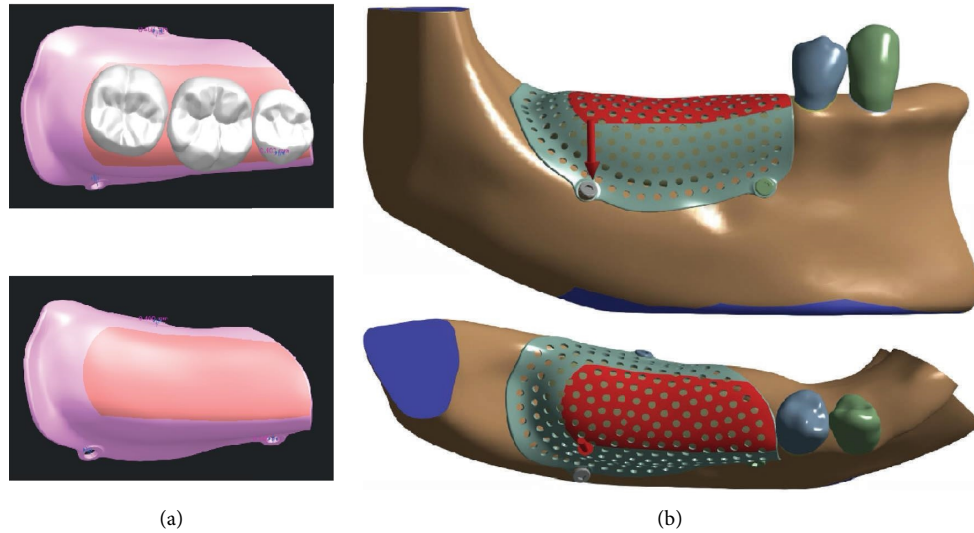


FIGURE 3: (a) Range of functional loading force. (b) The arrow indicates the direction of force, and the blue area represents the border.

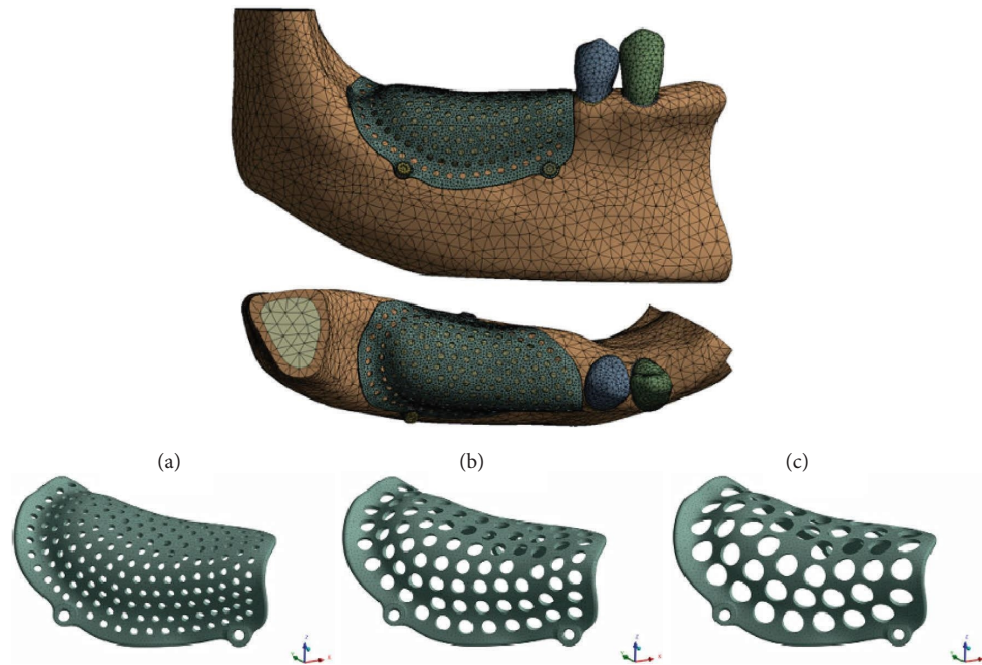


FIGURE 4: 3D-FE model of the PEKK mesh with different pore sizes: (a) pore size of 1 mm; (b) pore size of 2 mm; (c) pore size of 3 mm.

It is known that as design parameters, the thickness, pore size, and porosity of barrier membrane scaffolds significantly affect their mechanical properties, but the effects of these factors on clinical applications are complex and even contradictory in some cases [9, 22]. For example, increasing membrane thickness increases membrane stability but reduces the clinical management and volume of new bone; increasing pore size and porosity may enhance the efficiency of bone regeneration but substantially reduce membrane stiffness and strength. Therefore, the ideal PEKK scaffold should achieve better clinical operability on the basis of ensuring space maintenance. Among the methods for evaluating the

mechanical properties of materials, the standard mechanical properties test is the most common and effective method, including tensile, compression, bending, and fatigue tests. Since Friedenber first applied the finite element method to the medical field in 1969, with the development of computer technology and related software, the FEA has become a very effective analysis tool in the oral biomechanics field [23]. Therefore, because the existing methods of additive manufacturing and CNC machining cannot produce a test sample that meets experimental design requirements, 3D-FEA was used to investigate the stress distribution of PEKK meshes between the bone graft interfaces in this study, aiming at

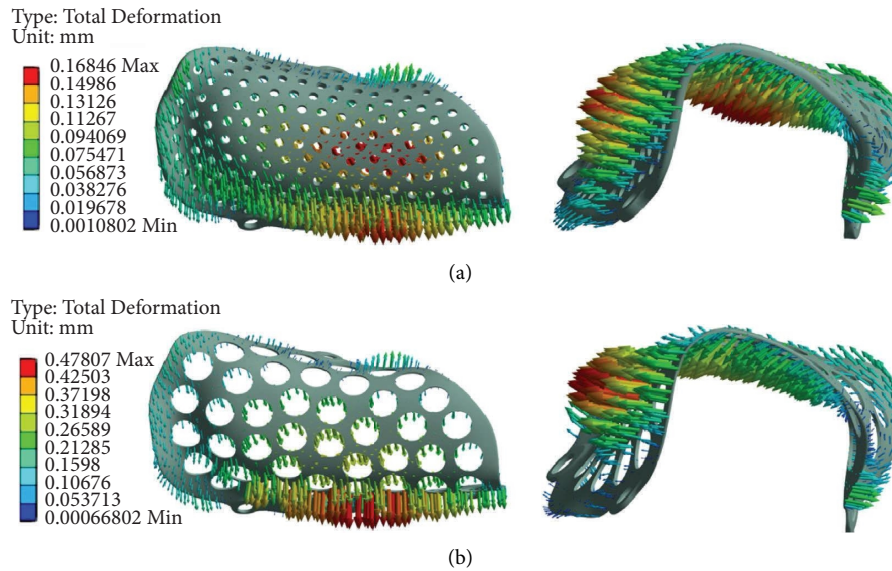


FIGURE 5: (a) Deformation of the PEKK mesh with a thickness of 0.6 mm and a pore size of 1 mm; (b) deformation of the PEKK mesh with a thickness of 0.2 mm and a pore size of 3 mm.

efficiently and quickly finding the optimal structure and providing a reference for clinical application. Our study takes full advantage of the structural advantages of FEA and reduces the dependence on a large number of human or animal experiments. A mechanical evaluation model for alveolar bone augmentation with good geometric similarity and biosimulation was successfully established.

PEKK is a new type of polymer material, and there is still a lack of preliminary clinical and experimental data relevant to its use as a barrier membrane scaffold. Therefore, when designing the thickness of PEKK, we refer to the titanium and PEEK meshes that have been clinically used. Under most circumstances, a thickness of 0.2 mm is enough for titanium mesh application [24], and another study reported that a 0.6 mm thick PEEK mesh was sufficient to maintain relative stability [8]. Therefore, considering that the mechanical properties of PEKK are between those of titanium and PEEK, this study set a thickness range from 0.2 to 0.6 mm to explore the mechanical properties of PEKK meshes. Moreover, the pore size of the barrier membrane scaffolds directly affects their mechanical strength, and their porous structures also affect vascularization and bone ingrowth. On the premise of ensuring mechanical properties, high porosity and large pore size tend to be selected to enhance bone regeneration. At present, the pore size of commercially available titanium meshes is usually at the millimeter level (usually 1–3 mm), which is why the author selected the pore size range from 1 to 3 mm. For the assignment of load force, considering that the Chinese usual bite force (UBF) is 100–150 N, the bone graft area does not directly

bear the bite force but generally bears light pressure from food, tooth brushing, or chewing when speaking and swallowing that would not exceed the average bite force of the normal dentition. Finally, we set the 100 N physiological load force as the limit value of the PEKK's compressive capacity for the simulation.

According to the FEA results, with increasing mesh pore size and porosity (1–3 mm; 42.67–19.18%) and decreasing thickness (0.6–0.2 mm), there was a decrease in the mechanical behavior of the PEKK mesh. Furthermore, the thickness had a greater effect on the deformation and maximum principal stress than pore size, but the effect of pore size on the equivalent stress was greater than that of the thickness. All 15 groups of PEKK meshes showed good space maintenance ability under a 100 N physiological loading force; the maximum deformation was 0.478 mm, and the degree of displacement did not show the adverse effect of maintaining the osteogenic space, indicating that PEKK can remain relatively stable when used as a barrier membrane scaffold. The equivalent stress, also known as the von Mises stress, is related to the yield strength of the material; the maximum principal stress, also known as the tensile stress, is related to the tensile strength of the material. According to the literature [13, 25–27], the tensile strength of PEKK is approximately 102 MPa–115 MPa, which is much smaller than its compressive strength of 172 MPa–246 MPa and yield strength of 175 MPa. Since the edge of the PEKK mesh was fixed by titanium screws, when the stress was transmitted to the lateral displacement of the buccal and lingual, it was transformed into tensile stress. Therefore,

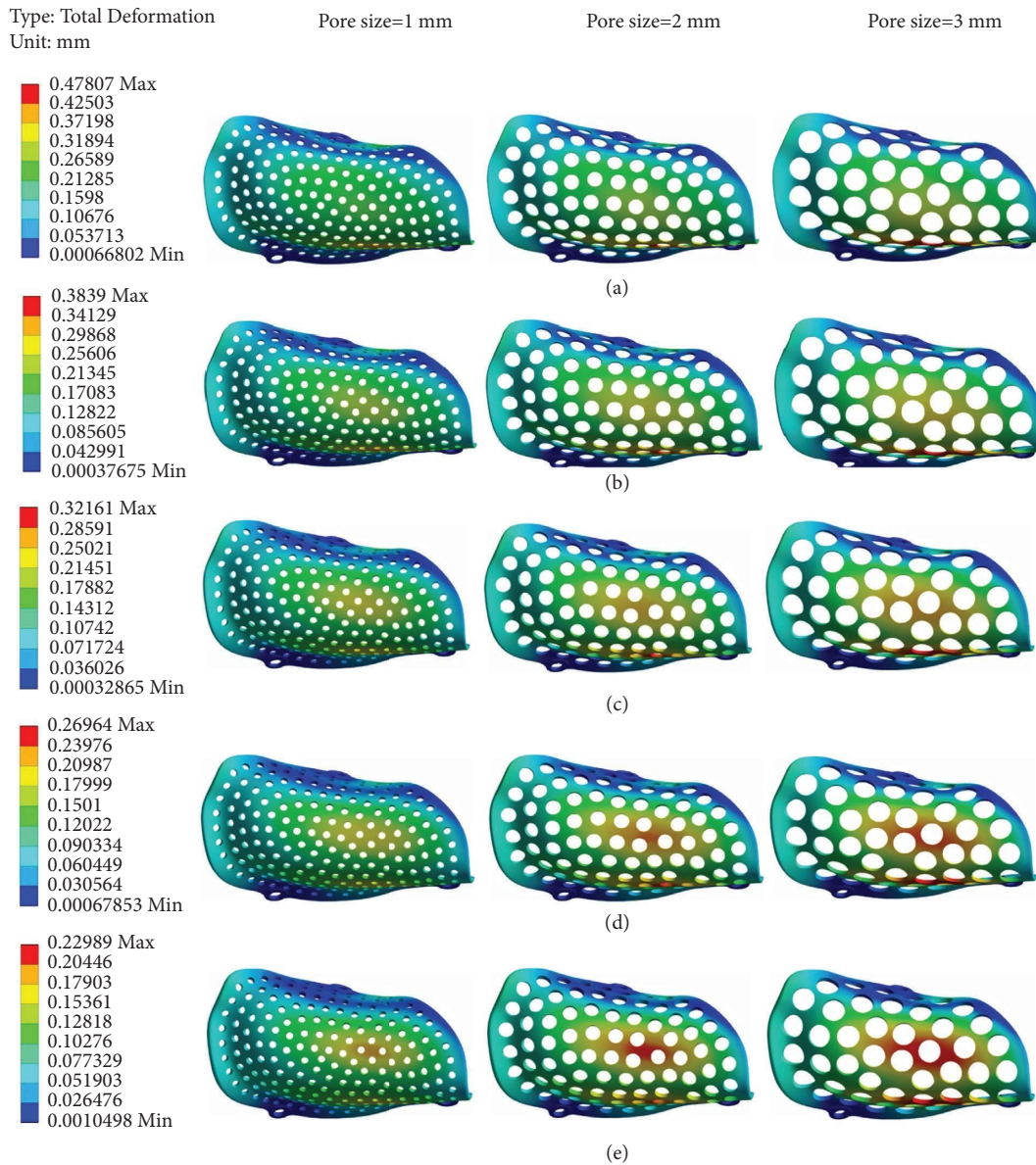


FIGURE 6: Deformation distributions of PEKK meshes with different thicknesses: (a) 0.2 mm. (b) 0.3 mm. (c) 0.4 mm. (d) 0.5 mm. (e) 0.6 mm.

the force leading to the breakage of the PEKK mesh should be tensile stress, and the broken site should be located at the turning point of the buccal and lingual sides, as the good toughness of PEKK may provide a certain buffer for compression in the alveolar ridge area. The group of PEKK meshes with a thickness of 0.2 mm, diameter of 3 mm, and porosity of 42.67% may be in danger of plastic deformation or even fracture during use, which is detrimental to the bone augmentation process. The maximum principal stress of the remaining groups

ranged from 31.549 MPa to 72.91 MPa, which is far less than the tensile strength of PEKK, indicating that there is no danger of fracture during use.

Our study has its inevitable limitations as an FEA study. The loading condition was simplified to a single vertical loading force, but in clinical practice, the motor force of muscles such as the buccal muscles acting in the bone graft area after tension reduction and suture cannot be ignored. Therefore, it is necessary to further establish the masticatory muscle system and design different working

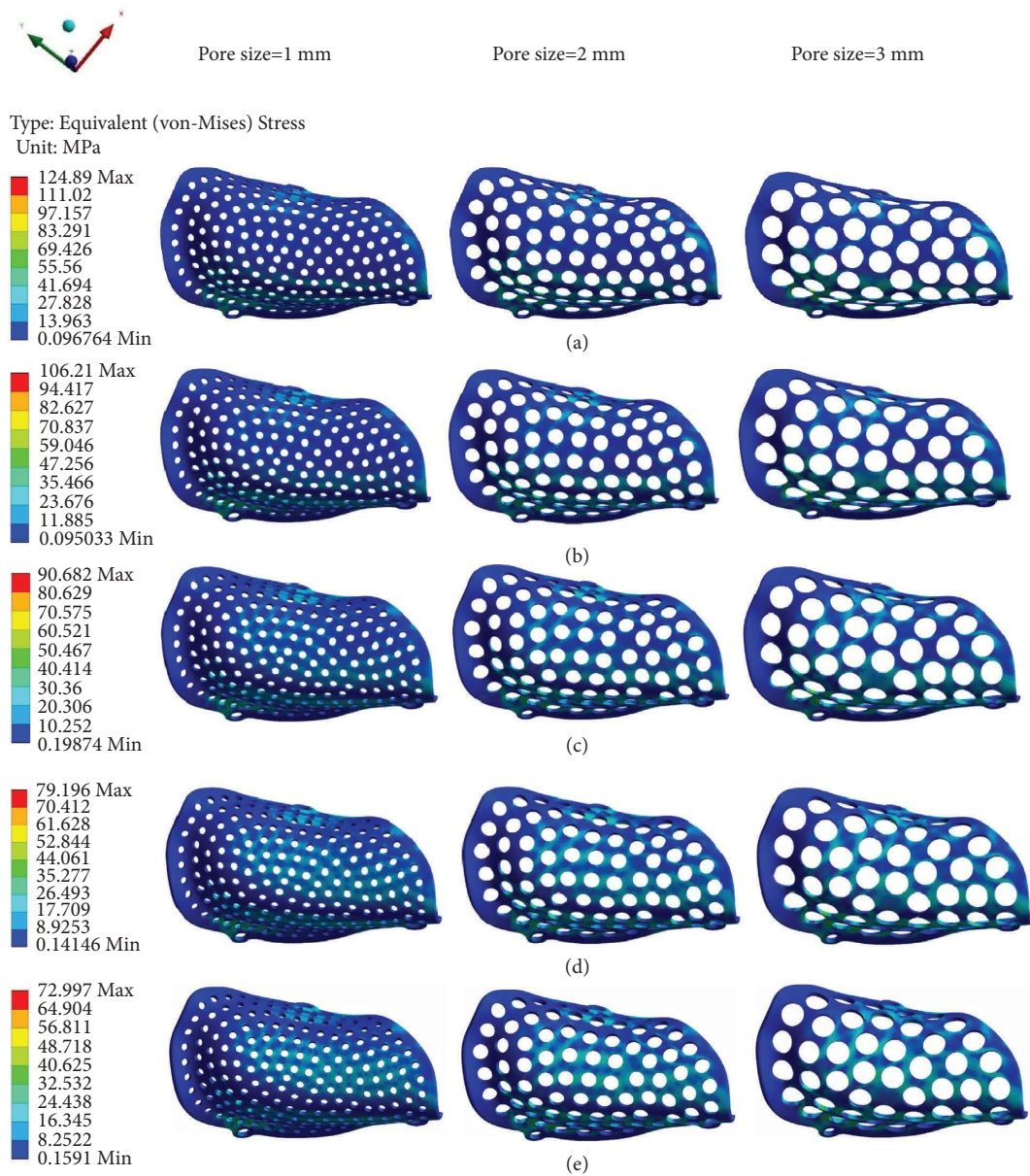


FIGURE 7: Equivalent stress distributions of PEKK meshes with different thicknesses: (a) 0.2 mm. (b) 0.3 mm. (c) 0.4 mm. (d) 0.5 mm. (e) 0.6 mm.

conditions under clinical conditions to simulate the oral and jaw systems more realistically, such as alveolar bone defects in different regions, different stress angles, or placing implants simultaneously according to patient needs. Furthermore, since the finite element method is a computer numerical simulation, there are other

limitations: changes in temperature, pH, load incidence, and fatigue are not taken into consideration, and the material is assumed to be homogeneous, linear, and free of defects. As a preclinical study of PEKK materials, the results of this study are limited to evaluating the feasibility of PEKK as a barrier membrane scaffold. Therefore, further

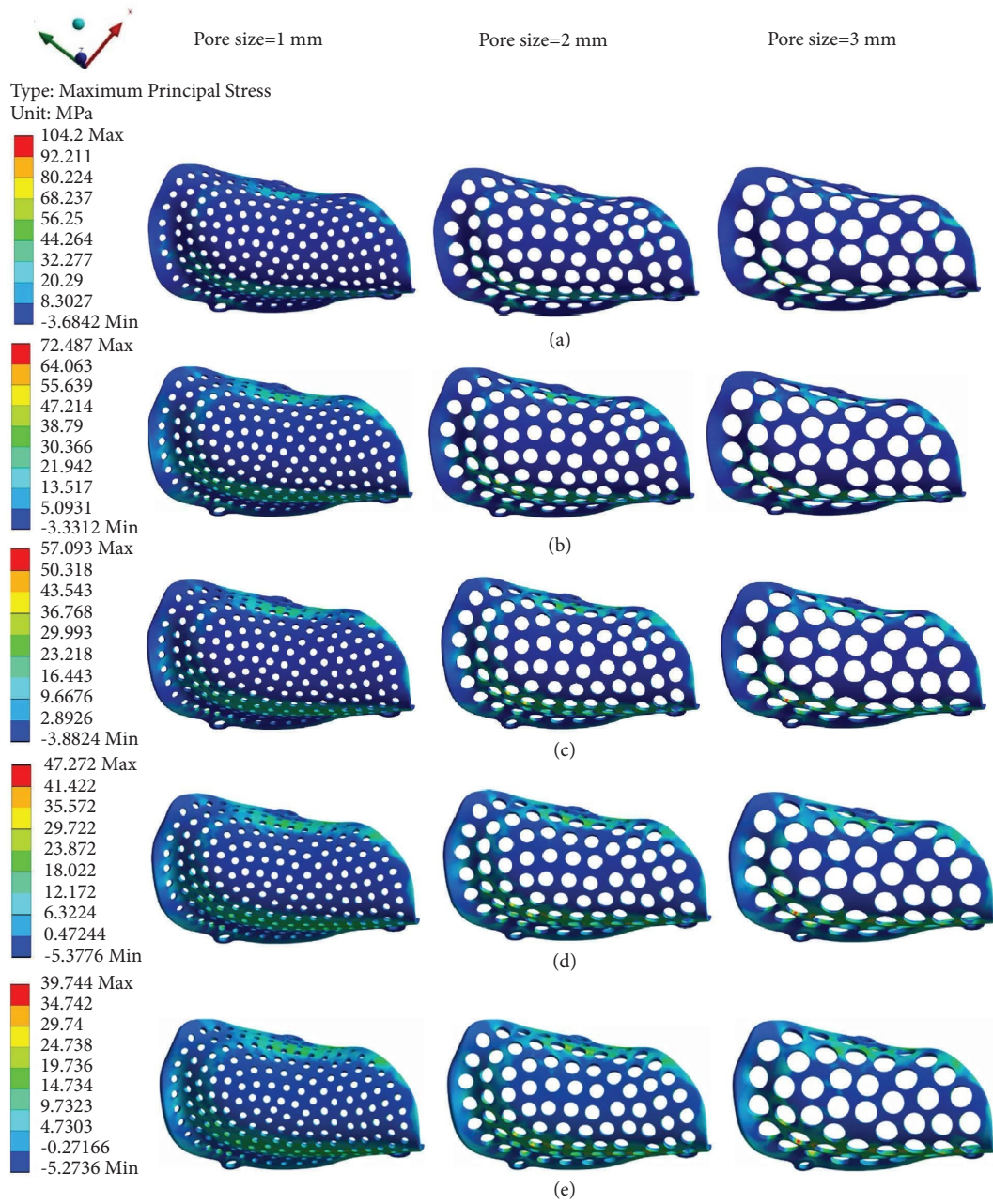


FIGURE 8: Maximum principal stress distributions of PEKK meshes with different thicknesses: (a) 0.2 mm. (b) 0.3 mm. (c) 0.4 mm. (d) 0.5 mm. (e) 0.6 mm.



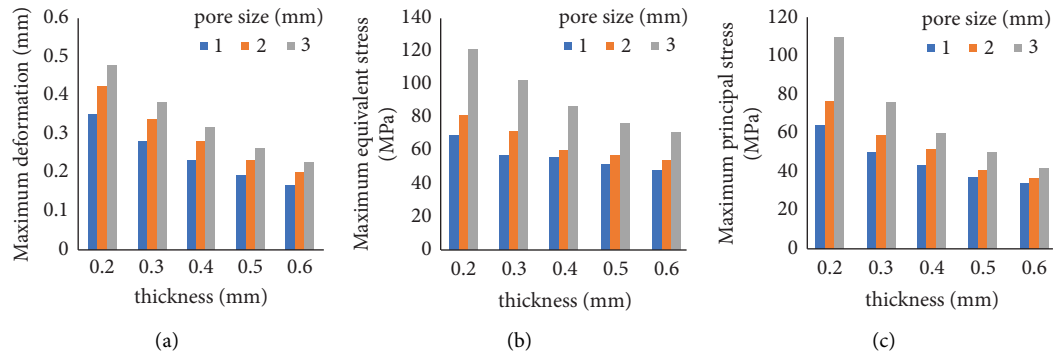


FIGURE 9: Relationship between the deformation (a), equivalent stress (b), and maximum principal stress (c) and the thickness and pore size of the PEKK meshes.

TABLE 3: Multiple regression model of the deformation of the PEKK meshes.

	Unstandardized B	Coefficients std. error	Standardized coefficient beta <sup>1</sup>	Sig	95.0% confidence interval for B	
					Lower bound	Upper bound
(Constant)	0.411	0.019		<0.05	0.370	0.451
Pore size	0.046	0.006	0.442	<0.05	0.034	0.059
Thickness	-0.531	0.034	-0.876	<0.05	-0.065	-0.457

<sup>1</sup>The beta is the standardized regression coefficient, which is used to compare the absolute effect or absolute contribution between the coefficients. The larger the beta value is, the greater the absolute effect or absolute contribution. All beta values in the tables have the same meaning.

TABLE 4: Multiple regression model of the equivalent stress of the PEKK meshes.

	Unstandardized B	Coefficients std. error	Standardized coefficient beta	Sig	95.0% confidence interval for B	
					Lower bound	Upper bound
(Constant)	70.353	8.019		<0.05	52.882	87.824
Pore size	18.248	2.536	0.733	<0.05	12.724	23.773
Thickness	-83.484	14.640	-0.581	<0.05	-115.382	-51.587

TABLE 5: Multiple regression model of the maximum principal stress of the PEKK meshes.

	Unstandardized B	Coefficients std. error	Standardized coefficient beta	Sig	95.0% confidence interval for B	
					Lower bound	Upper bound
(Constant)	73.752	7.791		<0.05	56.776	90.728
Pore size	10.528	2.464	0.462	<0.05	5.160	15.896
Thickness	-105.779	14.225	-0.804	<0.05	-136.772	-74.785

animal experiments and clinical studies are needed to verify the real biomechanical and osteogenic performance of the PEKK mesh used for alveolar bone augmentation.

## 5. Conclusion

Our study successfully constructed a mechanical evaluation model with high simulation and good geometric similarity for alveolar bone defect reconstruction, which takes full advantage of the structural benefits of FEA and is also applicable for other GBR barrier membrane scaffold materials, such as polymers and metals. In addition, this is the first attempt at studying the biomechanics of individualized PEKK scaffolds.

From a biomechanics perspective, this study provides a new option for the use of individualized barrier membrane scaffolds and provides a reference for the optimal design of PEKK as a barrier membrane scaffold material. The FEA results showed that the thickness, pore size, and porosity, as geometric parameters for the structural design of the PEKK mesh, are closely related to biomechanical performance. Within the range of FEA results, the larger the thickness and smaller the pore size and porosity are, the better the performance of the PEKK meshes, and PEKK has great potential for clinical application in terms of biomechanical properties. Considering that a barrier membrane should minimize soft tissue stimulation and maximize tissue integration functions, under the

precondition of meeting the needs of alveolar bone defect reconstruction, ultrathin porous PEKK meshes with a 0.2 mm thickness, pore size of not more than 3 mm, and porosity of not more than 42.67% are preferred for clinical practice.

### Data Availability

The data analyzed in this study are available from the corresponding author upon request.

### Conflicts of Interest

The authors declare that they have no conflicts of interest.

### Acknowledgments

The authors would like to thank the Dental Medical Devices Testing Center of Peking University School of Stomatology and Urumqi DW Innovation InfoTech Co., Ltd. for their technical consulting and design guidance. This work was supported by the National Program for Multidisciplinary Cooperative Treatment on Major Diseases (grant number PKUSSNMP-202012).

### References

- [1] G. E. Romanos, R. Delgado Ruiz, A. Sculean, R. Delgado-Ruiz, and A. Sculean, "Concepts for prevention of complications in implant therapy," *Periodontology 2000*, vol. 81, no. 1, pp. 7–17, 2000.
- [2] P. Brånemark, R. Adell, T. Albrektsson, U Lekholm, S Lundkvist, and B Rockler, "Osseointegrated titanium fixtures in the treatment of edentulousness," *Biomaterials*, vol. 4, no. 1, pp. 25–288, 1983.
- [3] F. Briguglio, D Falcomata, S Marconcini, L Fiorillo, R Briguglio, and D Farronato, "The Use of Titanium Mesh in Guided Bone Regeneration: A Systematic Review of titanium mesh in guided bone regeneration: a systematic review," *International Journal of Dentistry*, vol. 2019, pp. 1–8, 2019.
- [4] A. Hartmann, H Hildebrandt, JU Schmohl, and PW Kammerer, "Evaluation of Evaluation of Risk Parameters in Bone Regeneration Using a Customized Titanium Mesh: Results of a Clinical Study. isk parameters in bone regeneration using a customized titanium mesh: results of a clinical study," *Implant Dentistry*, vol. 28, no. 6, pp. 543–550, 2019.
- [5] M. Chiapasco and P. Casentini, "Horizontal bone-augmentation procedures in implant dentistry: prosthetically guided regeneration," *Periodontology 2000*, vol. 77, no. 1, pp. 213–240, 2018.
- [6] M. Mounir, M Shalash, S Mounir, Y Nassar, and O El Khatib, "Assessment of three dimensional bone augmentation of severely atrophied maxillary alveolar ridges using prebent titanium mesh vs customized poly- ether-ether-ketone (PEEK) mesh: Assessment of three dimensional bone augmentation of severely atrophied maxillary alveolar ridges using prebent titanium mesh vs customized poly-ether-ether-ketone (PEEK) mesh: A randomized clinical trial randomized clinical trial," *Clinical Implant Dentistry and Related Research*, vol. 21, no. 5, pp. 960–967, 2019.
- [7] O. A. EL Morsy, A. Barakat, S. Mekhemer, and M Mounir, "Assessment of 3-dimensional bone augmentation of severely atrophied maxillary alveolar ridges using patient-specific poly ether-ether ketone (PEEK) sheets," *Clinical Implant Dentistry and Related Research*, vol. 22, no. 2, pp. 148–155, 2020.
- [8] L. Li, *Clinical and Preclinical Study of Individualized Titanium and PEKK Meshes for Complex Alveolar Bone Augmentation*, Chongqing Medical University, Chongqing, China, 2021.
- [9] X. Wang, S Xu, S Zhou et al., "Topological design and additive manufacturing of porous metals for bone scaffolds and orthopaedic implants: Topological design and additive manufacturing of porous metals for bone scaffolds and orthopaedic implants: A review review," *Biomaterials*, vol. 83, pp. 127–14141, 2016.
- [10] L. Bai, P Ji, X Li, H Gao, L Li, and C Wang, "Mechanical Mechanical Characterization of 3D-Printed Individualized Ti-Mesh (Membrane) for Alveolar Bone Defectsharacterization of 3D-printed individualized Ti-mesh (membrane) for alveolar bone defects," *Journal of healthcare engineering*, vol. 2019, pp. 1–13, 2019.
- [11] A. Ramalho, P. V. Antunes, and P. Antunes, "Reciprocating wear test of dental composites against human teeth and glass," *Wear*, vol. 263, no. 7–12, pp. 1095–1104104, 2007.
- [12] H. Alqurashi, Z Khurshid, AUY Syed, S Rashid Habib, D Rokaya, and MS Zafar, "Polyetherketoneketone (PEKK): Polyetherketoneketone (PEKK): An emerging biomaterial for oral implants and dental prostheses emerging biomaterial for oral implants and dental prostheses," *Journal of Advanced Research*, vol. 28, pp. 87–95, 2021.
- [13] S. C. Dayan, O. C. Geckili, and O. Geckili, "The influence of framework material on stress distribution in maxillary complete-arch fixed prostheses supported by four dental implants: a three- dimensional finite element analysis," *Computer Methods in Biomechanics and Biomedical Engineering*, vol. 24, no. 14, pp. 1606–1617, 2021.
- [14] K. S. Lee, "Comparative evaluation of a four-implant-supported polyetherketoneketone framework prosthesis: a three-dimensional finite element analysis based on cone beam computed tomography and computer-aided design," *International Journal of Prosthodontics*, vol. 30, no. 6, pp. 581–585, 2017.
- [15] C. L. Lin, J C. Wang, S. H. Chang, and S. T. Chen, "Evaluation of stress induced by implant type, number of splinted teeth, and variations in periodontal support in tooth-implant-supported fixed partial dentures: a non-linear finite element analysis," *Journal of Periodontology*, vol. 81, no. 1, pp. 121–13030, 2010.
- [16] S. Checa, P. J. Prendergast, G. Duda, N. J. Prendergast, and G. N. Duda, "Inter-species investigation of the mechano-regulation of bone healing: comparison of secondary bone healing in sheep and rat," *Journal of Biomechanics*, vol. 44, no. 7, pp. 1237–124545, 2011.
- [17] L. y. Bai et al., "Three dimensional finite element analysis of customized titanium mesh with different thicknesses," *Journal of Oral Science Research*, vol. 35, no. 1, p. 75, 2019.
- [18] S. Najeeb, MS Zafar, Z Khurshid, and F Siddiqui, "Applications of polyetheretherketone (PEEK) in oral implantology and prosthodontics," *Journal of Prosthodontic Research*, vol. 60, no. 1, pp. 12–19, 2016.
- [19] M. Sakihara, Y. Taira, and T. Sawase, "Effects of sulfuric and vinyl sulfonic acidetchants on bond strength of resin composite to polyetherketoneketone," *Odontology*, vol. 107, no. 2, pp. 158–164, 2019.
- [20] M. Wang, G. Bhardwaj, and T. J. Webster, "Antibacterial properties of PEKK for orthopedic applications," *International Journal of Nanomedicine*, vol. 12, pp. 6471–6476, 2017.

- [21] G. Fuhrmann, M Steiner, S Freitag Wolf, and M Kern, "Resin bonding to three types of polyaryletherketones (PAEKs)— durability and influence of surface conditioning," *Dental Materials*, vol. 30, no. 3, pp. 357–363, 2014.
- [22] M. M. Dewidar, J. M. Lim, and J. K. Lim, "Properties of solid core and porous surface Ti–6Al–4V implants manufactured by powder metallurgy," *Journal of Alloys and Compounds*, vol. 454, no. 1-2, pp. 442–446, 2008.
- [23] J. P. Geng, K. B. Tan, G. R. Liu, K. B. Tan, and G. R. Liu, "Application of finite element analysis in implant dentistry: a review of the literature," *The Journal of Prosthetic Dentistry*, vol. 85, no. 6, pp. 585–598, 2001.
- [24] Y. Xie, S Li, T Zhang, C Wang, and X Cai, "Titanium mesh for bone augmentation in oral implantology: current application and progress," *International Journal of Oral Science*, vol. 12, no. 1, p. 37, 2020.
- [25] D. K. Deng and Y. Liu, "Properties of Special Engineering Plastic Polyether Ketone Ketone," *Eng Plast Appl*, vol. 44, no. 09, pp. 83–86, 2016.
- [26] D.-a. Gu and W. Lu, "Research progress on oral clinical application and stock devices of Polyaryletheretherketone," *Chinese Journal of Stomatological Research(Electronic Edition)*, vol. 14, pp. 265–270, 2020.
- [27] Z. Y.-M. Qi Man-lin, "Properties of polyetherketoneketone and its application in stomatology," *Journal of Oral Science Research*, vol. 34, no. 09, pp. 939–942, 2018.

## Research Article

# Value Research of NLR, PLR, and RDW in Prognostic Assessment of Patients with Colorectal Cancer

Wanchen Chen, Shen Xin, and Baohong Xu 

Department of Gastroenterology, Beijing Luhe Hospital, Capital Medical University, Beijing 101149, China

Correspondence should be addressed to Baohong Xu; [bxu22@ccmu.edu.cn](mailto:bhxu22@ccmu.edu.cn)

Received 22 January 2022; Revised 10 March 2022; Accepted 21 March 2022; Published 16 April 2022

Academic Editor: Angelo Mariotti

Copyright © 2022 Wanchen Chen et al. This is an open access article distributed under the Creative Commons Attribution License, which permits unrestricted use, distribution, and reproduction in any medium, provided the original work is properly cited.

**Objective.** This study aimed to investigate the relevance of the study with the neutrophil count and lymphocyte count ratio (NLR), platelet count and lymphocyte count ratio (PLR), and red blood cell distribution width (RDW) in the prognostic evaluation of colorectal cancer patients. **Methods.** 143 patients with colorectal cancer from January 2016 to January 2019 were selected by our hospital, and then, other 143 cases of physical examiners as normal groups were selecting to proceed colonoscopic biopsy to diagnose 106 cases of precancerous diseases related to colorectal cancer. Among them were the inflammatory bowel group ( $n = 56$ ) and the colorectal polyp group ( $n = 50$ ). Analysis of the survival impact factors of patients with carcinoma of the rectum, preoperative NLR, ROW, PLR, and prognostic relationship, and comparison of NLR, PLR, and RDW diagnostic rate and expression were performed. **Results.** Tissue type, TNM stage, lymph node metastasis, NLR, RDW, and PLR had a predictive influence on patients with colorectal cancer ( $P < 0.05$ ). There was no link between gender, age, aetiology, pathological type, and prognosis in patients with colorectal cancer ( $P > 0.05$ ). Multiple variables in patients with colorectal cancer are affected by tissue categorization (poor differentiation), TNM stages (III, IV), lymph node metastases, NLR, ROW, and PLR ( $P < 0.05$ ). When compared to solo NLR, Row, and PLR diagnostics, the combination diagnosis and malignancy rates were greater, and the differences were statistically significant ( $P < 0.05$ ). Diagnostic sensitivity, specificity, and accuracy were greater when compared to single NLR, ROW, and PLR. When compared to the normal control group, NLR, ROW, and PLR have greater levels, and the differences are statistically significant ( $P < 0.05$ ). The patient survival declines more slowly as PLR, NLR, and the severity of the condition rises. **Conclusion.** NLR, ROW, and PLR combined diagnosis has high accuracy in colorectal cancer diagnosis, and the prognosis of patients with NLR, ROW, and PLR levels has a tight association; so, clinically, the above signs should be identified, and the optimal treatment time is grasped.

## 1. Introduction

The colorectal cancer is a higher incidence of malignant tumor disease. The mortality rate and incidence rate are high; therefore, the clinical exploration of effective methods diagnosis and the treatment is critical [1]. Studies have confirmed that tumor-related inflammatory cells can have a direct role in tumors and play an important role in tumor metastasis, angiogenesis, and extracellular matrix [2].

NLR and RDW can reflect the system of anti-inflammatory response, tumor presence, invasion, metastasis, and recurrence, and NLR, PLR, and clinical response to the body promoted tumor and antitumor immune response' evaluation [3]. Another scholar confirms that RDW will have significant abnormalities in malignant tumors [4]. Nevertheless, the clinical report is not much in this area; in order to investigate the prognosis of NLR, PLR, and RDW levels and the colorectal cancer patient, the study selected colorectal cancer patients, colorectal cancer-related cancer, and

analyzed NLR, PLR, and RDW levels change trend, hoping to provide a theoretical foundation for disease diagnosis, and the relevant content will be reported as follows.

## 2. Data and Methods

**2.1. General Information.** From January 2016 to January 2019, 143 colorectal cancer cases in our hospital were selected and other 143 cases were selected as the normal group, and colonoscopic biopsy was selected as 106 cases of precancerous lesions are related to colorectal cancer Among them were the inflammatory bowel disease group ( $n=56$ ) and a colorectal polyp group ( $n=50$ ). 143 patients with rectal cancer, 76 males, 67 female, ( $53.6 \pm 3.8$ ) years old, tissue classification: 25 patients with low-differentiated patients, high, medium differential patients; onset: 45 cases of rectum, rising 39 cases of colon, 27 ethyl colon, 13 cases designed, and 19 cases. The research object agreed with the study; in the meanwhile, the research data are comparable ( $P > 0.05$ ), and the hospital ethics committee agreed with the study. Informed consent was obtained from the patients who were participating.

### 2.2. Inclusion Criteria

- (1) No hypertension
- (2) No cellular hyperthyroidism
- (3) No active hemorrhage and no bleeding quality
- (4) Clinical data are complete and patients signed informed consent
- (5) No autoimmune system diseases

### 2.3. Exclusion Criteria

- (1) Patients with liver and kidney or cardiopulmonary function
- (2) Age <18-year-old patient
- (3) Patients with malignant tumor disease
- (4) Folic acid or vitamin lack patient
- (5) Causes straightening reactive disease

## 3. Methods

Fasting for 12 hours before detection was advised, and after extracting 3 mL of fasting venous blood, lymphocyte count, platelet count, RDW, neutrophil count, peripheral blood, and white blood cell count (Model: Beckman Cul Special LH-750) were observed. Following the completion of the detection, the PLR value is derived using the NLR and RDW detection results. Patients are followed up on for two years by WeChat, phone, and other means, and the patient's survival time is reported.

### 3.1. Observation Indicator

**3.1.1. Explosion Factors Affecting Rectal Cancer Patients.** The explosion factors affecting renal cancer patients include gender, age, tissue classification, pathogenesis, TNM stage,

pathological type, lymph node metastasis, NLR, RDW, PLR, and other factors.

**3.1.2. Preoperative NLR, ROW, PLR, and Prognosis.** In preoperative NLR, ROW, PLR, and prognosis, add up tissue classification (low differentiation), TNM stages (III and IV), lymph node metastasis, NLR, ROW, PLR, and other factors.

**3.1.3. NLR, PLR, and RDW Diagnostic Rate.** Calculate the calculation rate of diagnosis examples of benign and malignant patients.

**3.1.4. NLR, PLR, and RDW Expression.** Add up 0, 20, 40, 60, and 80 months to correspond to NLR, PLR, and RDW survival rate, respectively. PLR normal range [5] is ( $1.5 \pm 0.9$ ),  $PLR > 103.7$  represents the PLR abnormality; NLR normal range is ( $1.5 \pm 0.9$ ),  $NLR > 2.4$  represents the NLR abnormalities; RDW normal range is ( $10.0 \pm 2.6$ ) FL,  $NLR > 12.58FL$  represents the RDW anomaly.

**3.2. Statistical Method.** Enter the acquired data into the Excel form, use statistics SPSS 22.0 software to perform data analysis, and conduct normal distribution inspection on the acquisition data, such as data compliance with normal distribution, count data, comparison ratio, and intergroup difference.

Using econometrics to carry out gender analysis, select card measurement. Selection card data were represented, and the differences of selection groups were analyzed. The data are represented, and the difference analysis of the group is chosen. The physical impact factor of the case group is calculated using logistic regression analysis, with a  $P$  value of less than 0.05 indicating that the difference is statistically significant. The image analysis software used by the Research Institute was GraphPad Prism 8.

## 4. Results

**4.1. Prognosis Analysis of the Single Survival Factor in Patients with Colorectal Cancer.** The prognosis affecting the single survival factor in patients with colorectal cancer is tissue typing, TNM stage, lymph node metastasis, NLR, RDW, PLR ( $P < 0.05$ ), gender, age, pathogenesis, and pathological type, which has no correlation with the prognosis of patients with colorectal cancer ( $P > 0.05$ ) (Table 1).

**4.2. Analysis of Multifactors of Prognostic Survival in Patients with Rectal Cancer.** The analysis of multifactors of prognostic survival in patients with rectal cancer is tissue classification (low differentiation), TNM stages (III and IV), lymph node metastasis, NLR, ROW, and PLR ( $P < 0.05$ ) (Table 2).

**4.3. Comparison of NLR, ROW, and PLR Diagnosis in Positive Rate and Malignancy.** Compared with single NLR, ROW, and PLR diagnosis, combined diagnosis, positive rate and malignancy, revealed differences which have a statistical significance ( $P < 0.05$ ) (Figure 1).

TABLE 1: Prognosis analysis of the single survival factor in patients with colorectal cancer.

Variables		Count	Death	Survivor	$X^2/t$	$P$
Gender	Male	76	37 (52.1)	39 (54.2)	0.524	>0.05
	Female	67	34 (47.9)	33 (45.8)		
Age	<65	82	34 (49.3)	48 (64.9)	0.043	>0.05
	≥65	61	35 (50.7)	26 (35.1)		
Tissue	Low differentiation	25	23 (35.9)	2 (2.5)	6.327	<0.05
	High, midphase	118	41 (64.1)	77 (97.5)		
	Rectum	45	20 (31.3)	25 (31.6)		
Constraint	Jigged	39	17 (26.6)	22 (27.9)	0.728	>0.05
	Ethyl colon	27	13 (20.3)	14 (17.7)		
	Colon	13	6 (9.4)	7 (8.9)		
TNM staging	Other	19	8 (12.5)	11 (13.9)	5.634	<0.05
	I, II	18	4 (6.3)	14 (17.7)		
	III, IV	125	60 (93.7)	65 (82.3)		
Pathological type	Aden cancer	138	61 (96.8)	77 (97.5)	1.724	>0.05
	Other (printed ring) cellular carcinoma, tubular cancer, and high-level epithelial tumor	5	2 (3.2)	2 (2.5)		
Lymph node metastasis	Yes	63	58 (92.1)	5 (6.3)	6.247	<0.05
	No	80	5 (7.9)	75 (93.7)		
NLR	—	—	5.0 ± 1.3	2.9 ± 0.6	13.854	<0.05
RDW (FL)	—	—	17.3 ± 2.2	13.9 ± 1.4	16.724	<0.05
PLR	—	—	4181.6 ± 35.8	106.3 ± 2.4	20.838	<0.05

TABLE 2: Analysis of multifactors of prognostic survival in patients with rectal cancer.

Influencing factors	B value	SE	Wald $X^2$ value	OR value	95% CI	$P$ value
Organizational profile: low differentiation	0.914	0.204	21.343	2.48	1.66–3.74	<0.001
TNM stages: III, IV	1.592	0.416	12.285	4.90	2.16–11.14	<0.001
Lymph node metastasis	0.501	0.124	19.533	1.64	1.28–2.12	<0.001
NLR	0.417	0.121	14.725	1.50	1.18–1.93	<0.001
Row (FL)	0.724	0.144	19.414	2.05	1.54–2.75	<0.001
PLR	0.711	0.313	21.545	2.02	1.09–3.78	<0.001

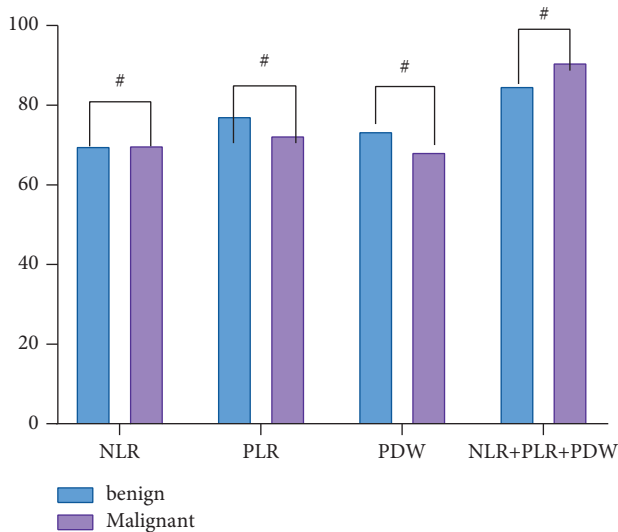


FIGURE 1: Comparison of NLR, ROW, and PLR diagnosis in positive rate and malignancy.

4.4. Comparison of NLR, Row, and PLR Diagnostic Sensitivity, Specificity, and Accuracy. Compared with single NLR, Row, and PLR diagnosis, combined diagnosis has higher sensitivity, specificity, and accuracy, and the differences have a statistical significance ( $P < 0.05$ ) (Figure 2).

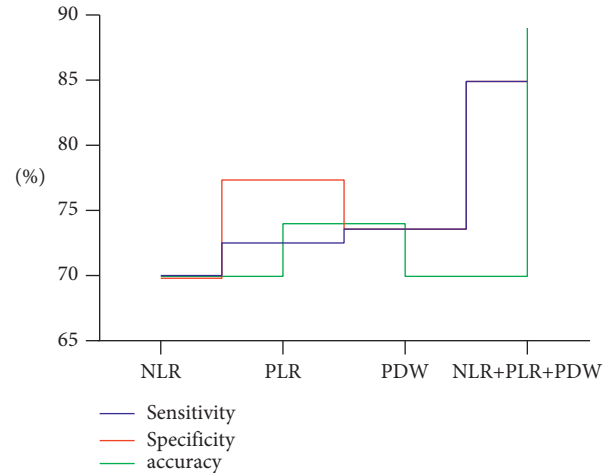


FIGURE 2: Comparison of NLR, Row, and PLR diagnostic sensitivity, specificity, and accuracy.

4.5. Comparison of NLR, ROW, and PLR Expression in Each Group. Compared to the normal control group, colorectal polyp group, and inflammatory bowel disease group, NLR, ROW, and PLR have higher levels of expression; in comparison between groups, there is a statistical significance ( $P < 0.05$ ) (Figure 3).

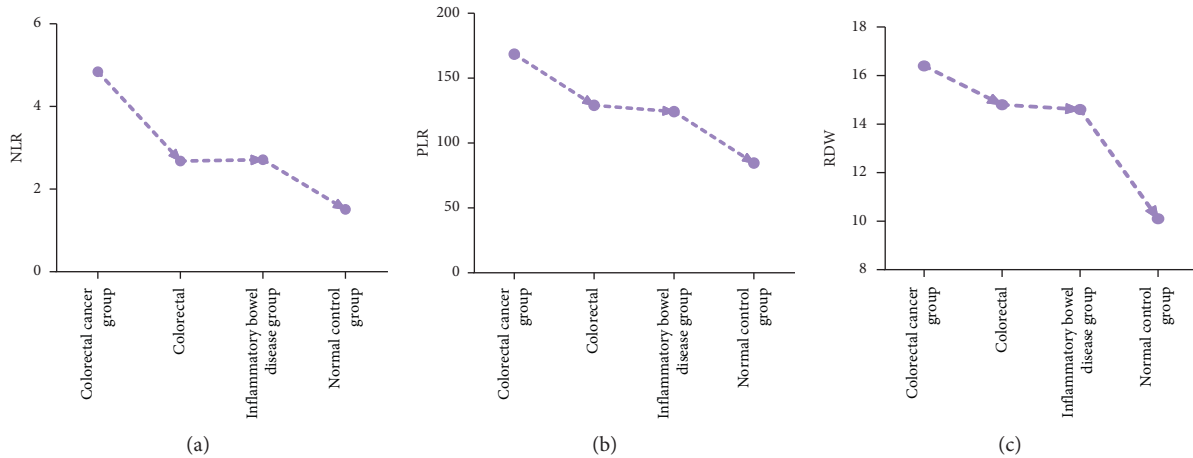


FIGURE 3: Comparison of NLR, ROW, and PLR expressions in each group.

**4.6. Preoperative NLR, ROW, PLR, and Prognosis Relationship.** Patient survival rates are steadily dropping as PLR and NLR levels rise in conjunction with increasingly severe conditions (Figure 4).

## 5. Discussion

The detrimental degree of colorectal cancer is severe, affecting the normal life of the patient. The current clinical research hotspot is to explore accurate diagnosis methods, improve prognosis, and reduce the degree of harm to patients [6, 7]. Several studies have proven the importance of NLR, PLR, and other markers in the prognosis of these cancers, which may be examined and monitored for systemic inflammatory response [8–10].

The study detected the value exploration of RDW, NLR, and PLR levels in colorectal carcinoma and analyzed the diagnosis, accuracy, and sensitivity. The results showed that there was a statistically significant significance for combined diagnosis and specificity and differences in combination diagnosis. The main reason is that Row is the platelet count and lymphocyte count ratio, and platelets can secrete due to secretion of P selector in adhesion, endothelial, and inflammatory cells, having promotion [11]. Platelet secretion of vascular endothelial growth factors, migration, and proliferation of endothelial cells have an induction effect, increased vascular permeability, tumor cell penetrating machine vascular metastasis, and invasive chances [12, 13]. RDW reflects the heterogeneous parameters of red blood cell size and peripheral blood [14, 15]. In addition, research shows that various factors will affect PLR and NLR individual test results and reduce sensitivity and specificity [16]. Therefore, PLR is carried out in patients with colorectal cancer, and NLR combination is very necessary. It has been shown that RDW is significantly expressed in several solid cancers, including lung cancer, breast cancer, esophageal squamous cell carcinoma, renal cell carcinoma, and other solid cancers, and that the prognosis of patients with solid tumors is closely associated with the expression of RDW [17]. Scholars pointed out that [18] tumor and PLR and NLR have a positive link with increasing NLR levels in the body,

and if the number of lymphocytes is lowered, the body's immunisation balancing function will be affected, leading to tumor metastasis and proliferation. The patient's prognosis is heavily influenced by these factors. The study explores a multifactor survival in rectal cancer patients. The results showed tissue classification (low differentiation), TNM stages (III and IV), lymph node metastasis, NLR, ROW, and PLR for neutral colorectal cancer prognosis ( $P < 0.05$ ). The main causes of RDW, NLR, and PLR affect the prognosis of colorectal cancer patients, the level of inflammatory factors increased, and the risk of colorectal cancer increased. Neutral granulocytes are N2 in the tumor state, which can pass base metal protease and vascular endothelial growth factor' effect on tumor cell apoptosis, which has promoted tumor angiogenesis, and tumor progression accelerates [19, 20]. Lymphocytes induce apoptosis of target cells, which is a tumor immune apoptotic cell, and the cytotoxic effect is obvious [21]. In addition, platelet aggregation increases the growth of tumor growth [22]. PLR and NLR are important markers for systemic inflammation and can be evaluated against inflammatory response [22]. The body's inflammatory response is raised by PLR and NLR levels, and the tissue infiltration and angiogenesis have promotion, which can cause tumor diffusion [23]. After the neutrophil is activated, the intravenous system reaches around tumor cells, the amount of active oxygen release increases, and the degree of cell DNA is damaged [24]. Therefore, it is necessary to create a microenvironment suitable for tumor cells. Tumor cell metastasis, growth, and platelet levels have significant correlation. PLR and NLR levels' increase will reduce the number of lymphocytes; the body's immunoassay is affected, and tumor cellular immunity is weakened, which is not conducive to the recovery of the condition [24]. In addition, scholars pointed out that PLR and NLR levels have correlation with patient survival. The results show that the survival time is negatively correlated with the survival rate, and the systemic inflammatory reaction equilibrium of patients with colorectal cancer is not high, which will inhibit anti-tumor immune response. The stage of disease and PLR and NLR have close ties with the PLR and NLR levels, which will reduce the 5-year survival rate largely. The findings revealed

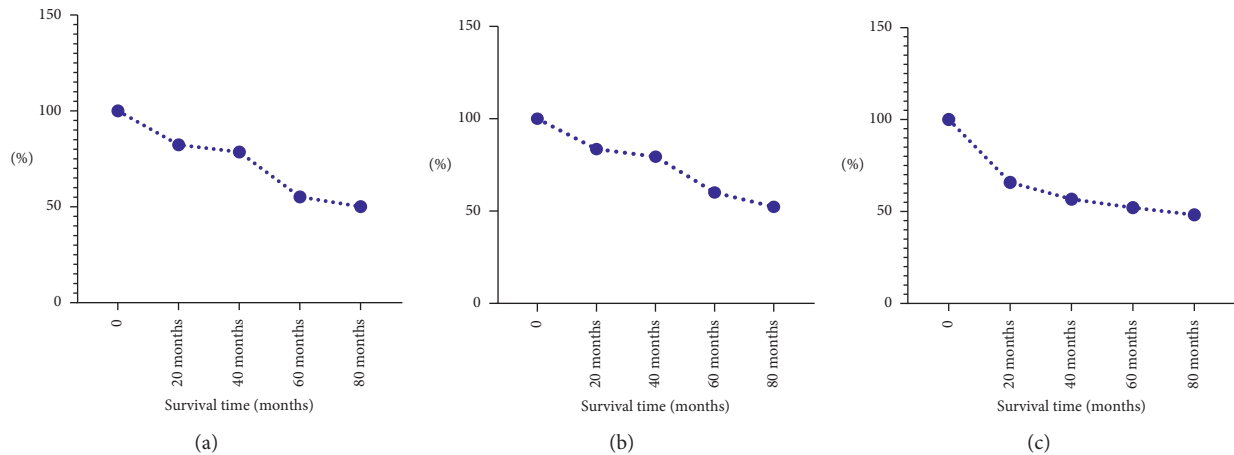


FIGURE 4: Preoperative NLR, ROW, PLR, and prognosis relationship.

that single tissue type, TNM stage, lymph node metastasis, NLR, RDW, PLR ( $P < 0.05$ ), sex, age, disease location, pathological type, and prognosis of colorectal cancer patients have no correlation ( $P < 0.05$ ). A comprehensive analysis should influence clinical prognostic factors in patients with colorectal cancer, and targeted interventions, with individual treatment, improve patient survival. The appraised value of research was analyzed using NLR, PLR, and RDW in the prognosis of patients with colorectal cancer and higher clinical feasibility, but this study is a retrospective analysis which included a limited number of cases. The accuracy of the results will have an impact. Following that, the sample should contain more qualified individuals who do a more in-depth investigation into immune inflammation; in order to increase the accuracy of research, lengthen the lifespan of the patient and improve the patient's quality of life.

In summary, in terms of diagnosis of colorectal cancer, NLR, ROW, and PLR combined diagnosis is with high accuracy, and prognosis of patient with high NLR, ROW, and PLR levels has a close relationship; so, clinically, the above indicators should be detected and grasped for the best treatment timing.

## Data Availability

The data used to support the findings of this study are available from the corresponding author upon request.

## Conflicts of Interest

The authors declare that there are no conflicts of interest.

## Acknowledgments

This work was supported by the Beijing Luhe Hospital, Capital Medical University.

## References

- [1] B. Mohebbi, K. Ashtibaghahi, M. Hashemi, and H. Asadzadeh Aghadaei, "Zali MR conditioned medium from cultured colorectal cancer cells affects peripheral blood mononuclear cells inflammatory phenotype in vitro iran," *Journal of Medical Sciences*, vol. 44, no. 4, pp. 334–341, 2019, PMID: PMC6661523.
- [2] S. Ogino, J. A. Nowak, T. Hamada et al., "Integrative analysis of exogenous, endogenous, tumour and immune factors for precision MEDICINE," *Gut*, vol. 67, no. 6, pp. 1168–1180, 2018.
- [3] R. Alamro, M. Mustafa, and A. Al-Asmari, "Inflammatory gene mRNA expression in human peripheral blood and ITS association with colorectal cancer," *Journal of Inflammation Research*, vol. 11, pp. 351–357, 2020.
- [4] C. N. Bernstein, E. I. Benchimol, A. Bitton et al., "The impact of inflammatory bowel disease in Canada 2018: extra-intestinal diseases in IBD," *Journal of the Canadian Association of Gastroenterology*, vol. 2, no. 1, pp. S73–S80, 2019.
- [5] M. Gasser, R. Lissner, K. Nawalaniec, L.-L. Hsiao, and A. M. Waaga-Gasser, "KMP01D demonstrates beneficial anti-inflammatory effects on immune cells: an ex vivo preclinical study of patients with colorectal cancer," *Frontiers in Immunology*, vol. 11, p. 684, 2020 Pmid: PMID: PMC7205007.
- [6] A. Copija, E. Nowakowska-Zajdel, K. Janion, and K. Walkiewicz, "Clinical characteristics of colorectal cancer patients in terms of selected platelet indices," *Disease Markers*, vol. 2020, PMID: PMC7568811, Article ID 6145604, 6 pages, 2020.
- [7] S. Wen, N. Chen, J. Peng et al., "Peripheral monocyte counts predict the clinical outcome for patients with colorectal cancer: a systematic review and meta-analysis," *European Journal of Gastroenterology and Hepatology*, vol. 31, no. 11, pp. 1313–1321, 2019.
- [8] J. Ge, J. Li, S. Na, P. Wang, G. Zhao, and X. Zhang, "MiR-548c-5p inhibits colorectal cancer cell proliferation by targeting PGK1," *Journal of Cellular Physiology*, vol. 234, no. 10, pp. 18872–18878, 2019.
- [9] J. Jiang, T. Ma, W. Xi et al., "Pre-treatment inflammatory biomarkers predict early treatment response and favorable survival in patients with metastatic colorectal cancer who underwent first line cetuximab plus chemotherapy," *Cancer Management and Research*, vol. 11, pp. 8657–8668, 2019.
- [10] M. S. Abdellateif, S. E. Salem, D. M. Badr et al., "The prognostic significance of 5-fluorouracil induced inflammation and immuno-modulation in colorectal cancer patients," *Journal of Inflammation Research*, vol. 13, pp. 1245–1259, 2020.



- [11] H. Luo, L. Liu, J. J. Zhao, X. F. Mi, Q. J. Wang, and M. Yu, "Effects of oxaliplatin on inflammation and intestinal floras in rats with colorectal cancer," *European Review for Medical and Pharmacological Sciences*, vol. 24, no. 20, pp. 10542–10549, 2020.
- [12] L. Liu, F. K. Tabung, X. Zhang et al., "Diets that promote colon inflammation associate with risk of colorectal carcinomas that contain f," *Clinical Gastroenterology and Hepatology*, vol. 16, no. 10, pp. 1622–1631, 2018, PMID: PMC6151288.
- [13] V. Sasidharan Nair, S. M Toor, R. Z Taha et al., "Transcriptomic ptumor-infiltrating cd4+tim+ T cells reveals their suppressive, exhausted, and metastatic characteristics in colorectal cancer patients," *Vaccines*, vol. 8, no. 1, p. 71, 2020 PMID: PMC7157206.
- [14] L. Campos Carrascosa, A. A. Van Beek, V. De Ruiter et al., "FcγRIIB engagement drives agonistic activity of Fc-engineered αOX40 antibody to stimulate human tumor-infiltrating T cells," *JImmunother Cancer*, vol. 8, no. 2, Article ID E000816, 2020.
- [15] Y. Wu, L. Yuan, Q. Lu, H. Xu, and X. He, "Distinctive profiles of tumor-infiltrating immune cells and association with intensity of infiltration in colorectal cancer," *Oncology Letters*, vol. 15, no. 3, pp. 3876–3882, 2018.
- [16] R. Ankathil, M. A. Mustapha, A. A. Abdul Aziz et al., "Contribution of genetic polymorphisms of inflammation response genes on sporadic colorectal cancer predisposition risk in Malaysian patients - a case control study," *Asian Pacific Journal of Cancer Prevention*, vol. 20, no. 6, pp. 1621–1632, 2019, Pmid: PMCID: PMC7021613.
- [17] Z. L. Wang, Y. D. Wang, K. Wang, J. A. Li, and L. Li, "KFL2 participates in the development of inhibiting inflammation via ulcerative colitis through regulating cytokines," *European Review for Medical and Pharmacological Sciences*, vol. 22, no. 15, pp. 4941–4948, 2018.
- [18] W. Peng, H. Yang, and K. Zhang, "Value of preoperative peropheral blood NLR and PLR in the prognostic assessment of colorectal cancer," *Chinese Journal of Immunology*, vol. 35, no. 4, pp. 93–97, 2019.
- [19] S. Jinendiran, H.-U. Dahms, B. S. Dileep Kumar, V. Kumar Ponnusamy, and N. Sivakumar, "Diapolycopenedioic-acid-diglucosyl ester and keto-myxocoxanthin glucoside ester: n," vol. 103, Article ID 104149, 2020.
- [20] A. Bruno, B. Bassani, D. G. D'Urso et al., "Angiogenin and the MMP9-TIMP2 axis are up-regulated in proangiogenic, decidual NK-like cells from patients with colorectal cancer," *The FASEB Journal*, vol. 32, no. 10, pp. 5365–5377, 2018.
- [21] H. Bessler and M. Djaldetti, "The impact of three commercial sweeteners on cytokine expression by mononuclears impelled by colon carcinoma cells," *International Journal of Food Sciences & Nutrition*, vol. 70, no. 8, pp. 970–976, 2019.
- [22] A. Varkaris, A. Katsiampoura, J. S. Davis et al., "Circulating inflammation signature predicts overall survival and relapse-free survival in metastatic colorectal cancer," *British Journal of Cancer*, vol. 120, no. 3, pp. 340–345, 2019.
- [23] H. Liu, Z. Liang, F. Wang et al., "Intestinal CD14+ mp+ T cells from activation-induced cell death via emc's disease," *Journal of Cohn's and Colitis*, vol. 14, no. 11, pp. 1619–1631, 2020.
- [24] F. Hidayat, I. Labeda, S. Sampetoding et al., "Correlation of interleukin-6 and C-reactive protein levels in plasma with the stage and differentiation of colorectal cancer: a cross-sectional study in east Indonesia," *Annals of Medicine and Surgery*, vol. 62, pp. 334–340, 2021.

## Research Article

# Evaluation of the Effect of Nutritional Intervention on Patients with Nasopharyngeal Carcinoma

Fan Lin <sup>1</sup>, Huijun Ren,<sup>1</sup> Fenfen Lin,<sup>2</sup> Zhaohu Pan,<sup>3</sup> Liping Wu,<sup>1</sup> and Neng Yang <sup>1</sup>

<sup>1</sup>Department of Otolaryngology, Taizhou Hospital of Zhejiang Province Affiliated to Wenzhou Medical University, Zhejiang Taizhou 317000, China

<sup>2</sup>Operating Room, Taizhou Hospital of Zhejiang Province Affiliated to Wenzhou Medical University, Zhejiang Taizhou 317000, China

<sup>3</sup>Department of Otorhinolaryngology, Taizhou Hospital of Zhejiang Province Affiliated to Wenzhou Medical University, Zhejiang Taizhou 317000, China

Correspondence should be addressed to Neng Yang; [yh\\_yangn@enzemed.com](mailto:yh_yangn@enzemed.com)

Received 23 December 2021; Revised 18 January 2022; Accepted 25 January 2022; Published 11 March 2022

Academic Editor: Gaurav Goyal

Copyright © 2022 Fan Lin et al. This is an open access article distributed under the Creative Commons Attribution License, which permits unrestricted use, distribution, and reproduction in any medium, provided the original work is properly cited.

**Aim.** The paper aims to combine mathematical statistics to assess the effect of nutritional intervention in the population of nasopharyngeal cancer patients. **Methodology.** After following the inclusion and exclusion criteria, a total of 120 patients with nasopharyngeal carcinoma were selected. All patients are treated with intensity-modulated radiotherapy (IMRT). The nurse collects relevant clinical treatment data during the radiotherapy of the patient. After the patient's radiotherapy, the nurse re-measures the patient's nutritional status indicators. Three months after the completion of radiotherapy, the patient will be reexamined by MRI, and the radiotherapist will assess the patient's radiosensitivity based on the results of the MRI examination. All the blood biochemical indicators and body measurement indicators were also assessed and coordinated with nasopharyngeal carcinoma patients. This study performs multiple linear regression analysis on treatment-related factors that affect nutritional status during radiotherapy. **Results.** The experimental results showed that the side effects of radiotherapy are independent influencing factors of nutritional status. Radiotherapy damages the DNA of cells, so that cells cannot continue to divide and grow, and all cells in the treatment area were affected by radiation. The standard radiotherapy treatment is quite long, and the oral cavity, throat, and parotid gland, are all within the irradiation range. In addition to killing the tumor cells, the radiation can also cause certain damage to the surrounding tissues of the tumor. This article takes radiosensitivity as the dependent variable (insensitivity = 0; sensitivity = 1) and takes the nutritional index NI, age, gender, education level, marriage, smoking, chronic disease history, TNM staging, whether the chemotherapy steps are the same or not, GTVnx prescription dose, and the number of radiotherapies as independent variables. AMC, albumin, hemoglobin, serum prealbumin, and transferrin are all correlated with radiosensitivity, which is consistent with the results of most studies. The results of multivariate logistic regression analysis showed that nutritional index (NI) was correlated with the radiosensitivity of nasopharyngeal carcinoma. **Conclusion.** Finally, this paper concludes that nutritional intervention has a certain effect on the treatment of patients with nasopharyngeal carcinoma.

## 1. Introduction

The incidence of nasopharyngeal carcinoma is high in central and southern regions of China. Because the early symptoms of nasopharyngeal carcinoma are not obvious, most of the patients with nasopharyngeal carcinoma have been diagnosed at middle and late stages. Moreover, due to the special physiological anatomical location of the

nasopharyngeal cancer, concurrent radiotherapy and chemotherapy is currently the most effective way to treat nasopharyngeal carcinoma [1]. Concurrent radiotherapy and chemotherapy could improve the control rate and reduce the rate of distant metastasis. However, side effects such as dry mouth, sore throat, oral mucositis, and taste changes caused by radiotherapy and gastrointestinal changes caused by chemotherapy could affect the appetite of patients, which

further results in decreased intake and absorption of nutrients by patients and affects with malnutrition [2]. Malnutrition not only affects the treatment effect and prognosis, but also reduces the patient's quality of life. Quality of life refers to a comprehensive measurement of the subjective feeling of a person or a group of physical, psychological, and social aspects of a good adaptation state. Patients with good nutritional status have a higher quality of life [3]. Therefore, effective symptom management is an important prerequisite for improving the nutritional status of patients and an important measure to improve the quality of life of patients.

At present, there have been intervention studies on improving the nutritional status of patients with nasopharyngeal carcinoma. However, no standardized nutritional intervention model has been formed. Nutritional support such as oral nutritional supplementation, intravenous nutritional support, or nasal feeding is mainly provided through health education or when patients have obvious symptoms of malnutrition. In addition, the target intake is determined based on the patient's gender, age, weight, height, and disease characteristics. There are few related studies on nutrition education, dietary guidance, and individualized dietary nutrition intervention in combination with patients' dietary habits and adverse effects of treatment.

Many methods can be used to assess the nutritional status of patients. Amongst them, the measurement of patient's body mass has been widely used because of its simplicity, ease of use, and economy and noninvasiveness. It can also be evaluated by measuring serum protein concentration, nitrogen balance, and body composition, but all of them require the assistance of a professional nutritionist. The causes of malnutrition in cancer patients are very complex. The patients experience not only the biological effects of the tumor itself, but also the side effects of anti-tumor therapy. In fact, cancer patients require more nutritional valuable foods than healthy people. It contains the nutrients needed for tumor tissue growth. In addition, factors such as infection, fever, and anemia caused by tumors and treatment reactions also aggravate the chances of malnutrition. Numerous studies have shown that patients with severe weight loss during the treatment usually have low quality of life scores, poor treatment tolerance, and increased hospital stays. In the current clinical treatment process, the nutritional status of cancer patients is often neglected, and that is why timely and effective nutritional support cannot be obtained. Moreover, there is no clear evidence-based medicine for the lack of nutritional status detection and the timing and duration of nutritional intervention. Recent studies have shown that proper nutritional support has a positive effect on the quality of life and prognosis of patients with head and neck cancer. Nutrition education is the simplest intervention method to improve nutritional status. However, this method is not only costly, but it also consumes manpower, material, and financial resources and is easy to forget or lose. International guidelines suggest intensive nutritional counseling (NC) and oral nutritional supplements as nutritional intervention for head and neck cancer patients with chemoradiotherapy. It is also suggested that if the cancer affects eating or swallowing,

enteral nutrition (EN) should be provided through tube feeding. In March 2015, the Chinese government proposed an "Internet +" action plan. In recent years, it has actively promoted the development of "Internet + medical health," which can provide online health consultation, appointment referral, chronic disease follow-up, health management, and other services to optimize the allocation of medical resources and improve the effectiveness of the medical service system. With the popularization of smartphones and the rapid development of network information, mobile medical applications with convenient portability, large amount of information, high efficiency, and low cost have been widely used in chronic disease health management, continued care, and online diagnosis and treatment.

This article combines mathematical statistics to study the effect of nutritional intervention in patients with nasopharyngeal carcinoma, which provides a theoretical reference for the effective treatment of patients with nasopharyngeal carcinoma.

## 2. Review of the Literature

Cancer patients often have varying degrees of malnutrition. The overall incidence of malnutrition in hospitalized malignant tumor patients in different countries is basically similar, such as 65.6% in Latin America, 69.2% in Argentina, 62.0% in Cuba, and 64.5% in China [4, 5]. The literature used the actual body mass to ideal body mass ratio (IBW%) to evaluate the status malnutrition and found that different malignant tumors occur at different locations, and the incidence of malnutrition is different at different stages [6]. They are 52% for gastric cancer and 48% for esophageal cancer, 46% of colon cancer, 43% of rectal cancer, 35% of lung cancer, 29% of ovarian cancer, 13% of breast cancer, and 8% of malignant lymphoma, suggesting that the weight loss rate of gastrointestinal malignant tumors is significantly higher than that of nondigestive malignant tumors. Patients with head and neck tumors could experience radioactive inflammation in the mouth, throat, and esophagus, due to the specificity of their treatment, which has a greater impact on swallowing. The combined chemotherapy has increased toxic and side effects and significantly reduced eating and absorption. Literature [7] reported that the incidence of third-degree oral mucositis in the radiotherapy and chemotherapy group was 75% and that, in the radiotherapy group, it was only 25%. Literature [8] reported that about 60% of patients with head and neck tumors who received chemotherapy and radiotherapy had moderate-to-severe eating disorders, and the diet was restricted in the following year. The researchers have [9, 10] used the subjective comprehensive evaluation method to study the nutritional status of patients with head and neck cancer after radiotherapy and found that the incidence of malnutrition was as high as 88%.

Tumor cells take up more amino acids than normal cells, reduce the protein synthesis, increase degradation, and other factors such as reduced protein intake, ascites, and protein loss from fistulas, which often trigger negative nitrogen balance. When the sugar supply in the body is consumed by

tumors, the mobilization and utilization of fatty acids as additional energy sources can cause changes in lipid metabolism. There are obvious obstacles to the metabolism of sugar, protein, and fat. The three major nutrient metabolism disorders that are vital to the human body directly lead to the patient's cachexia state [11, 12].

Malnutrition can cause decline in immune function, increase the incidence of complications such as infections, and lead to an increase in mortality and a longer recovery period and with longer hospital stay. The authors in [13] examined the results of a nutritional survey of 800 hospitalized patients and showed that the length of hospital stay was proportional to the degree of malnutrition of the hospitalized patients [13].

Studies have shown that nutritional support for patients with malnutrition or nutritional risk can improve clinical outcomes, reduce complications, and shorten hospital stays [14]. Literature [15] reported that oral nutritional supplements can reduce the occurrence of complication rate (27% vs. 12%) and fatality rate (26% vs. 17%) and shorten the length of hospital stay (28 d vs. 19 d). The authors in [16] examined the survey results of 404 adult hospitalized patients and showed that the length of hospitalization of malnourished patients was prolonged, and the per capita hospitalization expenses were significantly higher than those of well-nourished patients, which were 45,762 and 28,631 US dollars, respectively. Use of flow cytometry (FCM) technology to analyze the changes in tumor cell dynamics has been proposed by many researchers [17]. It was found that patients with head and neck tumors who received total parental nutrition (TPN) had active tumor cell proliferation, and the percentage of hyperdiploid cells in the cell cycle was significantly higher than before the TPN, while patients who took a normal diet did not have this change. So, the researchers [18] believe that although TPN may stimulate the growth of tumors, it can increase the number of cells in the S phase. In fact, the ability of tumor cells to obtain nutrients is far greater than that of normal cells of the body. Even if the supply of exogenous nutrients is insufficient or severely insufficient, the tumor can still compete with the host for limited nutrients and obtain sufficient nutrients. Satisfying its own growth needs causes the host to produce cachexia. On the other hand, even if adequate nutritional support is provided, human tumors still proliferate according to their original biological characteristics. The intake of nutrients for cancer patients is restricted, and the harm to the host body far exceeds the benefits of inhibiting tumor growth.

### 3. Materials and Methods

The samples in this paper are first-diagnosed patients with nasopharyngeal cancer admitted to the hospital from September 2019 to August 2021, and after careful consideration, a total of 120 patients with nasopharyngeal carcinoma were selected. The study was approved by the Institutional Review Board of Medical University with the Approval No.2019-VM-089. The study's reporting complies with Chinese legislation and the V2008 Helsinki Declarations.

Patient consent has been taken from each and every patient.

**3.1. Case Inclusion Criteria.** Case inclusion criteria are as follows: (1) patients with nasopharyngeal carcinoma diagnosed by clinical, imaging, and pathological examinations; (2) patients without radiotherapy contraindications; (3) patients aged 18–79 years; (4) patients receiving intensity-modulated radiotherapy; (5) patients without other malignant tumors (except skin cancer that has been cured); (6) patients with clear consciousness, no cognitive impairment, and no psychotic disorder; (7) patients had a Karnofsky Performance Status (KPS) score of 70 or above.

**3.2. Case Exclusion Criteria.** Case exclusion criteria are as follows: (1) patients who do not cooperate with the investigation and have incomplete data; (2) patients with other life-threatening diseases; (3) patients who have been diagnosed with nasopharyngeal carcinoma in other hospitals or have received treatment; (4) patients who have received radiotherapy for two weeks or less, or who had their radiotherapy interrupted for more than one week.

All patients are treated with intensity-modulated radiotherapy (IMRT): (1) CT scan and image transmission: the patient is in a supine position with the head, neck, and shoulders fixed with a conventional thermoplastic mask, and the CT scan is enhanced. The scan range is from the top of the skull to 1 cm below the clavicle head, and the layer thickness is 4 mm. The scanned images are transmitted via the network to the radiotherapy planning system (Pinnacle 9.2 m, Philips, The Netherlands). (2) Delineation of target area and dangerous organs: according to the reporting principles of ICRU 50 and ICRU 62, referring to MRI, the CT cross section is drawn layer by layer: (1) nasopharyngeal primary tumor (GTV-nx) and cervical metastatic lymph node area (GTV-nd); (2) clinical target area 1 (CTV1): the area expanded 5–10 mm outside the primary tumor; (3) clinical target area 2 (CTV2): the area of GTV extended by 10 mm, including skull base, posterior 1/3 of nasal cavity, posterior of maxillary sinus, part of posterior group of ethmoid sinus, pterygopalatine fossa, parapharyngeal space, and part of cervical vertebra or slope; (4) CTVnd: neck and clavicle-negative lymph node area; (5) planned target volume (PTV): the area expanded by 3 mm from GTV or CTV (except the posterior edge), and the area expanded by 2–3 mm outside the posterior edge; (6) peripheral organs at risk (OAR): including lens, eyeball, optic nerve, optic chiasm, parotid glands on both sides, brain stem, and spinal cord; (7) prescription dosage: GTV 66–70 Gy or above, CTV1 60–62 Gy, CTV2 and CTVnd 54–56 Gy, PTV16O-64 Gy, PTV2 57–60 Gy, PTVnx 68–72 Gy, PTVnd 66–70 Gy, 30–33 irradiations, 5 times/week; irradiation time is 6.0–6.6 weeks. According to the requirements of RTOG 02–25, the restricted dose of surrounding dangerous organs is set: 9 Gy for lens, 50 Gy for optic nerve and optic chiasm, 50 Gy for brain stem, 40 Gy for spinal cord, and D50 26 Gy for parotid gland. The physicist calculates and optimizes it through the Pinnacle reverse planning system based on the prescription dose given by the clinician. Moreover, the study uses seven fields of static intensity modulation technology to irradiate. In order to reduce human differences in plans, all IMRT

plans are completed by the same person. According to the dose volume histogram to evaluate the dose distribution of the target area and dangerous organs, it is required to receive the PTV volume of >110% of the prescribed dose <20%. The 100% prescription dose line surrounds at least 95% of the PTV volume, and the PTV volume that accepts <93% of the prescribed dose is <3%, and no more than 110% of the prescribed dose is allowed anywhere outside the PTV.

**3.3. Body Measurement Indicators.** ① Body mass index (BMI) = weight (kg)/[height (m)]<sup>2</sup>. BMI is considered to be a reliable indicator of protein-caloric malnutrition. Its main advantage is that it reduces the influence of height on weight when judging overweight or underweight. In 1997, the WHO announced that the normal BMI is 18.5–24.9, and the suitable BMI range for Chinese is 18.5–24.9. BMI between 17.0 and 18.4 is mild malnutrition, BMI between 16.0 and 16.9 is moderate malnutrition, and BMI less than 16 is severe malnutrition. ② Upper arm circumference (MAC) refers to the circumference of the midpoint of the upper arm, including subcutaneous fat and upper arm muscles. The upper arm circumference evaluates the nutritional status of protein in the skeletal muscle and somatic cell population. The normal value for men is 22.8–27.8 cm and for women is 20.9–25.5 cm. Skinfold thickness mainly indicates the thickness of subcutaneous fat, which is used to evaluate the fat content in the human body. ③ Triceps skinfold thickness (TSF) indirectly judges the amount of body fat. The normal value for men is 12.5 mm and for women 16.5 mm. A measured value greater than 90% is normal, 80%–90% of the normal value is mild malnutrition, 60%–80% is moderate malnutrition, and less than 60% is severe malnutrition. ④ Upper arm muscle circumference (AMC) = upper arm circumference (cm) – 3.14 × triceps skinfold thickness (mm). It is used to determine the number of skeletal muscles throughout the body. The average upper arm muscle circumference of adults in my country is 25.3 cm for men and 23.2 cm for women. A measured value greater than 90% of the standard value indicates normal nutrition and equivalent to 80%–90% of the normal value indicates mild muscle protein consumption. A measured value equals to 60%–80% indicates moderate muscle protein consumption and less than 60% indicates heavy muscle protein consumption.

**3.4. Blood Biochemical Indicators.** ① Albumin: the level of serum albumin represents the protein storage of internal organs and is an important indicator of the nutritional status of patients. The normal range is ≥35 g/L, serum albumin 30–35 g/L indicates mild malnutrition, 25–30 g/L indicates moderate malnutrition, and <25 g/L indicates severe malnutrition. ② Total lymphocyte count: the total lymphocyte count decreases when severe malnutrition occurs. The reference value for normal adults is  $(1-4) \times 10^9/L$  (1000–4000/mm<sup>3</sup>), and lymphocyte count <1500/mm<sup>3</sup> often indicates malnutrition. ③ Red blood cells: it is a routine examination item for diagnosing iron deficiency anemia. The normal index for men is  $4.0-5.5 \times 10^{12}/mm^3$ , and the normal index for women is  $3.5-5.0 \times 10^{12}/mm^3$ . ④ Hemoglobin:

hemoglobin is a routine examination item for diagnosing anemia caused by lack of hematopoietic substances or utilization disorders (such as iron deficiency anemia, sideroblastic anemia, megaloblastic anemia). The normal value for adult men is 120–160 g/L, and the normal value for adult women is 110–150 g/L. Generally, when adult male hemoglobin is <120 g/L or adult female hemoglobin is <110 g/L, anemia is diagnosed. Hemoglobin >90 g/L indicates mild anemia, 90–60 g/L indicates moderate anemia, 60–30 g/L indicates severe anemia, and <30 g/L indicates extreme anemia. ⑤ Serum prealbumin evaluates the nutritional metabolism of plasma and visceral proteins, reflecting protein malnutrition and liver dysfunction. The reference value for normal adults is 233.5–372.7 mg/L for men and 217.75–337.65 mg/L for women. ⑥ Transferrin evaluates the nutritional metabolism of plasma and visceral proteins and reflects the changes in nutritional status in the short term. The reference value for normal adults is 2200–4000 mg/L.

**3.5. Data Collection Methods and Steps.** (1) This paper uses a uniformly designed questionnaire. For patients with primary nasopharyngeal carcinoma who were admitted to the Department of Radiotherapy of the First Affiliated Hospital of Fujian Medical University from September 2012 to December 2013 and met the inclusion requirements, before they undergo radiotherapy, a uniformly trained radiotherapy nurse will collect the patient's baseline data and determine their nutritional status indicators. (2) The nurse collects relevant clinical treatment data during the radiotherapy of the patient. (3) After the patient's radiotherapy, the nurse remeasures the patient's nutritional status indicators. (4) Three months after the completion of radiotherapy, the patient will be reexamined by MRI, and the radiotherapist will assess the patient's radiosensitivity based on the results of the MRI examination.

**3.6. Statistical Evaluation.** SPSS software was used to do statistical analysis on the data (version 22.0; IBM SPSS, Chicago, IL, USA). For continuous variables, the Student's *t*-test was used, and for categorical variables, the chi-square test or Fisher's exact test was used. *P*0.05 was regarded as statistically significant.

## 4. Results

The radiosensitivity of patients was evaluated according to the WHO evaluation criteria for the efficacy of solid tumors. The results are as follows. Among 120 patients with nasopharyngeal carcinoma, 96 (80%) are radiosensitive patients, and 24 (20%) are insensitive patients, as shown in Figure 1 (1 means sensitive; 0 means insensitive).

Among the 120 patients before radiotherapy, the nutritional status of the subjects before radiotherapy is shown in Table 1.

After radiotherapy, the nutritional indicators after radiotherapy are shown in Table 2. The abnormal rate of various nutritional indicators increased after radiotherapy. The comparison chart is shown in Figure 2.

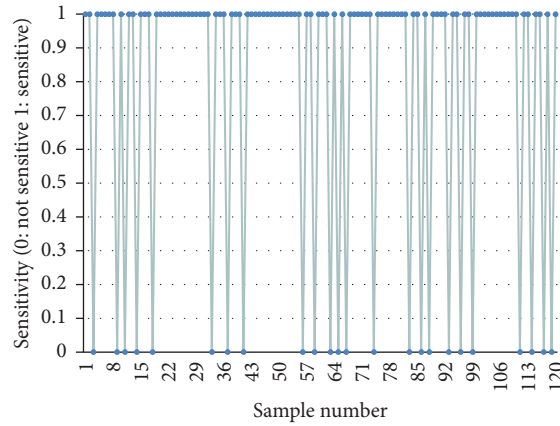


FIGURE 1: Evaluation of radiosensitivity.

TABLE 1: Nutritional status of subjects before radiotherapy.

Nutrition index	Abnormal rate (%)	Abnormal rate 95% CI	
		Lower (%)	Upper (%)
BMI	6.336	3.564	9.108
AMC	23.859	18.414	29.304
Albumin	2.475	0.891	4.059
Lymphocytes	37.026	30.69	43.362
Hemoglobin	3.366	1.485	5.247
Red blood cell	0.495	0	0.99
Serum prealbumin	14.652	10.296	19.008
Transferrin	39.996	33.462	46.53

TABLE 2: Nutritional status of subjects after radiotherapy.

Nutrition index	Abnormal rate (%)	Abnormal rate 95% CI	
		Lower (%)	Upper (%)
BMI	18.117	11.583	24.651
AMC	26.631	18.81	34.452
Albumin	3.762	1.188	6.336
Lymphocytes	98.010	94.842	100
Hemoglobin	20.988	13.959	28.017
Red blood cell	9.504	4.851	14.157
Serum prealbumin	51.381	41.976	60.786
Transferrin	69.498	60.39	78.606

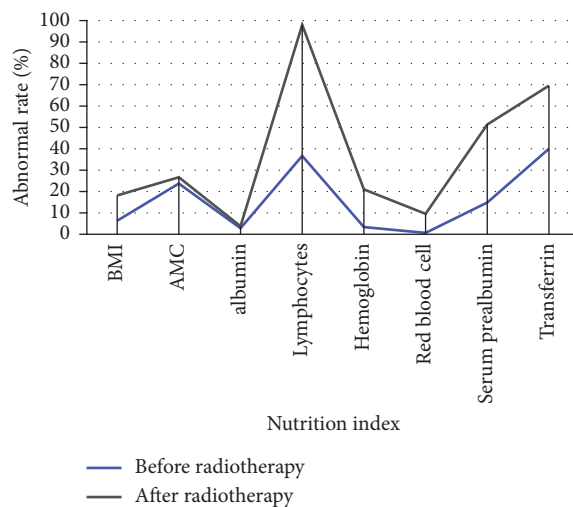


FIGURE 2: Comparison of abnormal rates of subjects before and after radiotherapy.

Before radiotherapy, the abnormal rates of AMC, lymphocytes, hemoglobin, and serum prealbumin in women are higher than those in men. However, the abnormal rates of women's BMI, albumin, red blood cells, and transferrin are lower than those of men. After radiotherapy, the abnormal rate of serum albumin in women is changed to be lower than that in men, and the abnormal rate of red blood cells is changed to be higher than that in men, and other indicators remain unchanged. The nutritional status of patients of different genders is shown in Table 3.

Before radiotherapy, in addition to AMC and hemoglobin, the abnormal rates of other nutritional indicators in patients aged 50 years or older are higher than those in patients aged younger than 50 years. However, after radiotherapy, the abnormal rates of other nutritional indicators, except hemoglobin, red blood cells, and transferrin, are higher in patients aged 50 years or older than those in patients younger than 50 years. The nutritional status of patients in different age groups is shown in Table 4.

Before and after radiotherapy, the abnormal rates of lymphocytes, serum prealbumin, and transferrin in rural patients are higher than those in urban patients, while BMI, AMC, hemoglobin, and red blood cells are lower than those in urban patients. The nutritional status of patients from different places of residence is shown in Table 5.

Before and after radiotherapy, the abnormal rates of BMI, albumin, red blood cell, serum prealbumin, and transferrin in the group whose family monthly income is less than or equal to 1,000 yuan are higher than those in the group whose family monthly income is more than 1,000 yuan. However, their AMCs are lower than those of patients whose family monthly income is more than 1000 yuan. The nutritional status of patients with different incomes is shown in Table 6.

The upper arm muscle circumference (AMC), albumin, hemoglobin, serum prealbumin, and transferrin of the radiation-sensitive group before radiotherapy are all higher than those of the radiation-insensitive group, and the difference is statistically significant ( $P < 0.05$ ). However, there is no significant difference in body mass index (BMI), total lymphocyte count, and red blood cell count between the radiation sensitive group and the insensitive group, as shown in Table 7.

Principal component analysis is used for nutritional indicators related to radiosensitivity (AMC, albumin, hemoglobin, serum prealbumin, and transferrin). Moreover, a comprehensive index to evaluate the nutritional status of patients with nasopharyngeal cancer was established, and it was defined as the nutrition index (NI). The eigenvectors of the correlation matrix of the principal component analysis are shown in Table 8.

The distribution of the nutritional index NI value obtained on this basis is shown in Figure 3.

This article takes radiosensitivity as the dependent variable (insensitivity = 0, sensitivity = 1) and takes the nutritional index NI, age, gender, education level, marriage, smoking, chronic disease history, TNM staging, whether the chemotherapy steps are the same or not, GTVnx prescription dose, and the number of radiotherapies as

independent variables. Moreover, this paper uses the non-conditional Logistic regression analysis method (Forward: LR, introduces  $\alpha = 0.05$ , removes  $\alpha = 0.10$ ) to conduct a multivariate analysis of the influencing factors of radiosensitivity. The results are shown in Table 9.

## 5. Discussion

Nasopharyngeal carcinoma is a common malignant tumor of the head and neck in China. Radiotherapy is currently the most effective treatment method. However, it will also bring about oral mucositis, saliva reduction, sore throat, and other treatment side effects, which will seriously affect the dietary intake of patients with nasopharyngeal cancer, increase the incidence of malnutrition, and affect the treatment and prognosis of patients. At present, in the process of clinical tumor treatment, the evaluation and monitoring of nutritional status and the selection of nutritional support therapy to adapt to the population still lack evidence of evidence-based medicine. Accurately predicting the radiosensitivity of nasopharyngeal carcinoma and designing and implementing individualized treatment plans accordingly have important clinical significance for improving the therapeutic effect of nasopharyngeal carcinoma.

Combining chemotherapy and other anticancer treatments can improve the killing effect on tumor cells. A large number of studies have found that the percentages of tumor cells in the S phase and proliferation phase of patients who have received nutritional support treatment are significantly increased, and the apoptosis rate is decreased, which stimulates the growth and proliferation of tumors. However, simultaneous chemotherapy is conducive to cycle-specific chemotherapy. The effect of the drug increases the efficacy, and the efficacy of the nutrition + chemotherapy group is significantly higher than that of the chemotherapy alone group.

The nutritional indicators selected in this study are three physical indicators (deltoid skinfold thickness, upper arm circumference, and body mass index) and six blood biochemical indicators (albumin, total lymphocyte count, red blood cells, hemoglobin, serum prealbumin, and transfer iron protein). The nine indicators are all commonly used in clinical practice and well-researched nutritional indicators.

Moreover, these nutritional indicators reflect the patient's nutritional status from different aspects. Body mass index is a reliable indicator of protein-caloric malnutrition, and upper arm circumference is used to evaluate the nutritional status of protein in skeletal muscle and somatic cell populations, and the thickness of triceps skinfold is used to judge body fat reserves. Serum albumin level represents the protein storage of internal organs, and red blood cells are a routine examination item for diagnosing iron deficiency anemia, and hemoglobin is commonly used to diagnose anemia caused by lack of hematopoietic substances or utilization disorders.

The results of univariate and multivariate analysis in this study showed that there is no correlation between age and radiosensitivity of nasopharyngeal carcinoma, which is consistent with the reports of Liu Kai and Wang Hao. The

TABLE 3: Nutritional status of different genders.

Nutrition index	Before radiotherapy		After radiotherapy	
	Male	Female	Male	
BMI	7.425	3.366	BMI	7.425
AMC	12.969	51.183	AMC	12.969
Albumin	3.366	0	Albumin	3.366
Lymphocytes	32.769	47.817	Lymphocytes	32.769
Hemoglobin	1.386	8.514	Hemoglobin	1.386
Red blood cell	0.693	0	Red blood cell	0.693
Serum prealbumin	14.355	15.345	Serum prealbumin	14.355
Transferrin	48.51	18.81	Transferrin	48.51

TABLE 4: Nutritional status of different age groups.

Nutrition index	Before radiotherapy		After radiotherapy	
	< 50	≥50	< 50	
BMI	6.237	6.336	BMI	6.237
AMC	29.106	17.919	AMC	29.106
Albumin	1.782	3.168	Albumin	1.782
Lymphocytes	38.115	35.838	Lymphocytes	38.115
Hemoglobin	3.663	3.168	Hemoglobin	3.663
Red blood cell	0	1.089	Red blood cell	0
Serum prealbumin	14.553	14.751	Serum prealbumin	14.553
Transferrin	39.006	41.085	Transferrin	39.006

TABLE 5: Nutritional status of patients in different places of residence.

Nutrition index	Before radiotherapy		After radiotherapy	
	Rural area	Town	Rural area	
BMI	5.742	7.623	BMI	5.742
AMC	22.275	27.423	AMC	22.275
Albumin	2.871	1.485	Albumin	2.871
Lymphocytes	37.323	36.531	Lymphocytes	37.323
Hemoglobin	2.871	4.554	Hemoglobin	2.871
Red blood cell	0	1.485	Red blood cell	0
Serum prealbumin	15.741	15.246	Serum prealbumin	15.741
Transferrin	40.194	39.6	Transferrin	40.194

TABLE 6: Nutritional status of different incomes.

Nutrition index	Before radiotherapy		After radiotherapy	
	≤1000	> 1000	≤1000	
BMI	7.92	4.356	BMI	7.92
AMC	22.077	26.136	AMC	22.077
Albumin	2.673	2.178	Albumin	2.673
Lymphocytes	37.125	39.204	Lymphocytes	37.125
Hemoglobin	3.564	3.267	Hemoglobin	3.564
Red blood cell	0	1.089	Red blood cell	0
Serum prealbumin	15.048	14.058	Serum prealbumin	15.048
Transferrin	40.689	40.293	Transferrin	40.689

reason for the difference in research results may be that the selected samples come from different regions and have different genetic and environmental factors, or due to different research design types or analysis methods.

When nasopharyngeal carcinoma is associated with chronic diseases, such as hypertension, diabetes, and cardiovascular disease, the risk of insensitivity to radiotherapy is increased. The reason may be that when combined with systemic diseases,



TABLE 7: The influence of various nutritional indicators on radiosensitivity ( $\chi \pm s$ ).

Nutrition index	Sensitive	Not sensitive	<i>t</i> value	<i>P</i> value
BMI	22.81 ± 2.92	22.02 ± 2.83	1.615	0.107
AMC	23.31 ± 3.02	22.10 ± 3.43	2.059	0.041
Albumin	42.94 ± 4.63	39.63 ± 6.62	3.812	< 0.001
Total lymphocyte count	1.72 ± 0.59	1.71 ± 0.52	0.298	0.767
Red blood cell	4.52 ± 0.51	4.40 ± 0.44	0.752	0.455
Hemoglobin	138.12 ± 13.81	130.32 ± 14.13	3.306	0.001
Serum prealbumin	316.72 ± 88.04	262.02 ± 94.09	3.568	< 0.001
Transferrin	2.12 ± 0.43	1.92 ± 0.39	2.559	0.013

TABLE 8: The eigenvectors of the correlation matrix of principal component analysis.

	Component		
	1	1	
AMC	0.504	AMC	0.504
Albumin	0.691	Albumin	0.691
Hemoglobin	0.591	Hemoglobin	0.591
Serum prealbumin	0.748	Serum prealbumin	0.748
Transferrin	0.602	Transferrin	0.602

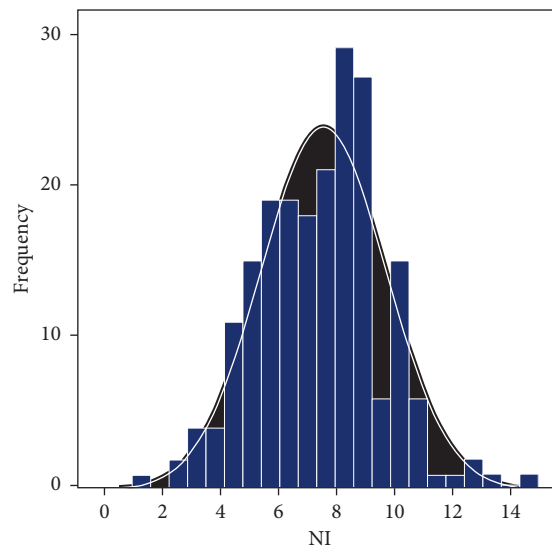


FIGURE 3: Distribution pattern of the nutrient index.

TABLE 9: Logistic regression analysis of factors affecting radiosensitivity.

Variable	<i>B</i>	<i>SE</i>	<i>P</i>	<i>OR</i>
NI	1.08801	0.32571	0.00099	2.97
T staging	-0.64944	0.2277	0.00396	0.51381
Constant	2.59281	0.80487	0.00099	13.57884

hypoxic cells can increase in the patient’s body. The latter will increase the tumor’s resistance to radiation, that is, the tumor’s sensitivity to radiotherapy decreases. Moreover, when the patient has a systemic disease, it will increase the patient’s psychological and physical burden, reduce the ability to repair normal tissues, and decrease the patient’s tolerance. At this time, extending the course of treatment or reducing the dose will directly affect the radiation effect. The results of this study show

that whether the patient has a history of chronic disease before radiotherapy is not an independent factor influencing the radiosensitivity of nasopharyngeal carcinoma.

In the univariate analysis of this study, the pathological type of nasopharyngeal carcinoma is correlated with radiosensitivity, while the pathological type in the multivariate analysis is not an independent factor influencing the radiosensitivity of nasopharyngeal carcinoma.

At present, more researches have focused on the effects of radiotherapy combined with chemotherapy on patients with nasopharyngeal carcinoma. The main methods are induction chemotherapy, concurrent chemotherapy, and adjuvant chemotherapy. Induction chemotherapy refers to the chemotherapy used before radiotherapy, which can reduce distant metastases, reduce local and regional tumor burden, and thereby reduce the local recurrence rate. Simultaneous radiotherapy and chemotherapy can synchronize tumor cells, which can not only directly kill tumor cells, but also inhibit the sublethal damage repair of tumor cells, thereby enhancing radiosensitization. Adjuvant chemotherapy can kill local residual tumor cells and distant metastases after radiotherapy, prevent local recurrence and distant metastasis, and play a role in consolidating the efficacy of radiotherapy. However, whether chemotherapy is beneficial to improve the radiosensitivity of patients with nasopharyngeal carcinoma remains controversial. Some scholars believe that concurrent radiotherapy and chemotherapy can increase the local regression rate of tumors and improve the local control rate (DFS) and survival rate (OS). The results of this study show that chemotherapy is not an independent factor influencing the radiosensitivity of NPC. The reason for this inconsistency of research results may be that different countries, regions, hospitals, and departments do not choose chemotherapy regimens, methods, and cycles the same way. Moreover, chemotherapy regimens include both single-agent and combination chemotherapies. Chemotherapy methods include induction, simultaneous, adjuvant, and a combination of the three. The length of treatment and the cycle of chemotherapy are also uneven, so it is difficult to accurately evaluate the effect of chemotherapy on radiosensitivity.

The results of single-factor analysis in this study showed that AMC, albumin, hemoglobin, serum prealbumin, and transferrin are all correlated with radiosensitivity, which is consistent with the results of most studies. The results of multivariate logistic regression analysis showed that the nutritional index (NI) was correlated with the radiosensitivity of nasopharyngeal carcinoma ( $P = 0.001$ ). Moreover, as the NI value increases, the radiosensitivity of NPC increases. Therefore, NI can be used as a predictor of radiosensitivity in patients with nasopharyngeal carcinoma.

## 6. Conclusion

The pathological type of nasopharyngeal carcinoma is correlated with radiosensitivity, while the pathological type in the multivariate analysis is not an independent factor influencing the radiosensitivity of nasopharyngeal carcinoma. NI value increases the radiosensitivity of NPC. Therefore, NI can be used as a predictor of radiosensitivity in patients with nasopharyngeal carcinoma. Finally, this paper concludes that nutritional intervention has a certain effect on the treatment of patients with nasopharyngeal carcinoma [19].

## Data Availability

The data used to support the findings of this study are available from the corresponding author upon request.

## Conflicts of Interest

The authors declare that there are no conflicts of interest.

## Acknowledgments

The work in this paper was supported by the Taizhou Hospital of Zhejiang Province affiliated to Wenzhou Medical University.

## References

- [1] T. Xie, Y. Kong, L. Shi et al., "Analysis of memory function and MRI changes in nasopharyngeal carcinoma patients after radiotherapy," *Chinese Journal of Radiological Medicine and Protection*, vol. 38, no. 2, pp. 105–109, 2018.
- [2] Y. Pan, H. Wu, and Y. Li, "Effect of recombinant human interleukin-11 treatment on prognosis of patients with radiochemoradiotherapy in the treatment of nasopharyngeal carcinoma," *Lin chuang er bi yan hou tou jing wai ke za zhi=Journal of clinical otorhinolaryngology, head, and neck surgery*, vol. 31, no. 12, pp. 945–948, 2017.
- [3] G. Li, J. Wang, H. Tang et al., "Comparing endoscopic surgeries with open surgeries in terms of effectiveness and safety in salvaging residual or recurrent nasopharyngeal cancer: systematic review and meta-analysis," *Head & Neck*, vol. 42, no. 11, pp. 3415–3426, 2020.
- [4] Q. Zhao, P. Sun, S. Qin, and J. Liu, "Acylglycerol kinase promotes the stemness of nasopharyngeal carcinoma cells by promoting  $\beta$ -catenin translocation to the nucleus through activating PI3K/Akt pathway," *Environmental Toxicology*, vol. 35, no. 12, pp. 1299–1307, 2020.
- [5] L. Xie, T. Jiang, A. Cheng et al., "MiR-597 targeting 14-3-3 $\sigma$  enhances cellular invasion and EMT in Nasopharyngeal carcinoma cells," *Current Molecular Pharmacology*, vol. 12, no. 2, pp. 105–114, 2019.
- [6] M. M. A. Jassim, M. M. Mahmood, S. H. M. Ali, and M. S. Kamal, "Interplay between EBERS and P27 tumor suppressor proteins in molecular transformation of nasopharyngeal and sinonasal carcinomas," *Indian Journal of Public Health Research & Development*, vol. 10, no. 6, pp. 894–900, 2019.
- [7] B. Eng-Zhuan, L. Munn-Sann, P. P. Chong, Y. Yoke-Yeow, and C. L. Siew-Ying, "Association of hOGG1 Ser326Cys, ITGA2 C807T and TNF-A 308G> A polymorphisms with the risk of NPC," *Journal of Molecular and Genetic Medicine*, vol. 11, no. 314, pp. 1747–0862, 2017.
- [8] L. Makni, A. Messadi, S. Zidi, E. Gazouani, A. Mezlini, and B. Yacoubi-Loueslati, "TLR2 (-196 to-174 Ins/Del) and TLR3 (1377C> T) as biomarkers for nasopharyngeal cancer in Tunisia," *Turkish Journal of Medical Sciences*, vol. 47, no. 4, pp. 1216–1222, 2017.
- [9] D. C. Ferguson, M. Mehrad, K. A. Ely, J. R. Shinn, and J. S. Lewis, "Human papillomavirus testing in head and neck squamous cell carcinoma: impact of the 2018 college of American pathologists guideline among referral cases at a large academic institution," *Archives of Pathology & Laboratory Medicine*, vol. 145, no. 9, pp. 1123–1131, 2021.
- [10] H. Kassiri, R. Dehghani, I. Khodkar, S. Karami, R. Valizadeh, and R. Kasiri, "Breast cancer and myiasis: review of the texts and a case report," *Journal of Entomological Research*, vol. 45, no. 2, pp. 373–378, 2021.
- [11] F. Y. Müsri, A. E. Bilici, M. K. Eryilmaz et al., "C-reactive protein-albumin ratio's prognostic importance in esophageal

- cancer for survival,” *Eurasian Journal of Medical Investigation*, vol. 4, no. 4, pp. 501–505, 2020.
- [12] I. H. Musa, T. H. Musa, H. H. Musa, R. M. Balila, and M. E. Ahmed, “Bibliometric analysis of the top 50 most-cited articles of esophagus cancer,” *Journal of Tumor*, vol. 9, no. 1, pp. 572–578, 2021.
- [13] R. Ahmad, M. A. Khan, A. N. Srivastava et al., “Anticancer potential of dietary natural products: a comprehensive review,” *Anti-Cancer Agents in Medicinal Chemistry*, vol. 20, no. 2, pp. 122–236, 2020.
- [14] D. M. Jorge, M. Labarrere, M. W. Rodrigues, C. L. Shields, and R. Jorge, “Simultaneous choroidal and retinal metastases from lung carcinoma,” *Retinal Cases & Brief Reports*, vol. 14, no. 1, pp. 90–95, 2020.
- [15] K. Motaparathi, J. P. Kapil, and E. F. Velazquez, “Cutaneous squamous cell carcinoma: review of the eighth edition of the American Joint Committee on cancer staging guidelines, prognostic factors, and histopathologic variants,” *Advances in Anatomic Pathology*, vol. 24, no. 4, pp. 171–194, 2017.
- [16] S. Scollon, A. K. Anglin, M. Thomas, J. T. Turner, and K. W. Schneider, “A comprehensive review of pediatric tumors and associated cancer predisposition syndromes,” *Journal of Genetic Counseling*, vol. 26, no. 3, pp. 387–434, 2017.
- [17] D. S. Tekcham, S. Gupta, B. R. Shrivastav, and P. K. Tiwari, “Epigenetic downregulation of PTEN in gallbladder cancer,” *Journal of Gastrointestinal Cancer*, vol. 48, no. 1, pp. 110–116, 2017.
- [18] I. San-Millán and G. A. Brooks, “Reexamining cancer metabolism: lactate production for carcinogenesis could be the purpose and explanation of the Warburg Effect,” *Carcinogenesis*, vol. 38, no. 2, pp. 119–133, 2017.
- [19] X. Ren and C. Su, “Sphingosine kinase 1 contributes to doxorubicin resistance and glycolysis in osteosarcoma,” *Molecular Medicine Reports*, vol. 22, no. 3, pp. 2183–2190, 2020.

## Research Article

# Enhancement of Nursing Effect in Emergency General Surgery Based on Computer Aid

Yan Lei,<sup>1</sup> Linxiang He,<sup>1</sup> and Houqiang Huang<sup>ID</sup><sup>2</sup>

<sup>1</sup>Department of Emergency, Anqing First People's Hospital of Anhui Medical University, Anqing, Anhui 246003, China

<sup>2</sup>Department of Nursing, The Affiliated Hospital of Southwest Medical University, Luzhou, Sichuan 030699, China

Correspondence should be addressed to Houqiang Huang; [huanglitogether6868@swmu.edu.cn](mailto:huanglitogether6868@swmu.edu.cn)

Received 21 December 2021; Revised 6 February 2022; Accepted 14 February 2022; Published 10 March 2022

Academic Editor: Gaurav Goyal

Copyright © 2022 Yan Lei et al. This is an open access article distributed under the Creative Commons Attribution License, which permits unrestricted use, distribution, and reproduction in any medium, provided the original work is properly cited.

In order to improve the nursing effect of emergency general surgery, this paper combines computer algorithms to carry out the intelligent management of general surgery nursing, and realizes the standardization of nursing information, the electronic nursing file, the precision of nursing workload, and the intelligentization of nursing quality control by means of informatization. This truly and objectively reflects the nursing operation and treatment situation, prevents the occurrence of some adverse events, and effectively reduces the workload of nursing care. Moreover, this paper uses a standardized software design method to define the software concept, and then conducts a detailed demand analysis of the nursing display function through detailed investigation, class work, discussion and analysis, and comparison decision-making methods. In addition, this paper compiles the software through strict coding standards, and finally designs test cases to test and improve the software. Through actual case studies, it can be seen that the computer-assisted emergency general surgery nursing method proposed in this paper has a certain progress compared with the traditional nursing method.

## 1. Introduction

The pre-examination and triage of emergency general surgery is relatively mature abroad. A large number of studies have proved the effectiveness and practicability of their respective triage standards, and the corresponding emergency triage process and path have been established for clinical use. The establishment of modern triage standards began in the 1990s [1]. Countries such as the United States, Australia, France, Canada, and the United Kingdom have successively established unified and standardized emergency triage procedures and standards.

These triage standards are all five-level triage, and patients are divided into five levels according to the degree of criticality, of which level I is the most critical and urgent patient, and level V is the mildest nonemergency patient. Regarding the evaluation of the American ESI standard, there are still some studies that indicate that the triage standard is not perfect. Although it is based on the allocation of emergency resources, it still has shortcomings [2]. First of

all, the sensitivity of distinguishing between various levels of the disease is low. Almost half of the patients are classified as Class III patients according to the allocation of emergency resources [3]. This makes it difficult to identify truly potentially critical patients and get corresponding and adequate dynamic observations. Secondly, the standard does not have sufficient research conclusions to prove the correlation between the outcome of the disease after triage and the time of triage. Finally, the completion of triage is still based on subjective triage. From factors such as lack of clinical experience, human triage errors, and system defects to triage staff's errors in the initial clinical assessment (i.e., triage), it leads to serious consequences such as misdiagnosis, delayed treatment, unreasonable use of medical resources, and increased medical costs.

Computer information technology gradually began to be applied to hospital management in the form of a single computer. In the early 1990s, hospitals began to introduce computer health information systems (HIS). The creation and adoption of clinical decision support (CDS) system tools

have changed the way medical professionals traditionally manage patient health, disease data, healthcare records, and diagnosis and treatment plans [4]. Preliminary studies have shown that this type of medical guidance may play an important role in patient management and triage, especially in clinical areas such as EDs [5]. The United States and Canada took the lead in introducing information applications into emergency triage. With the development of the Internet of Things technology, some scientific research institutions have developed what is called a wireless network disaster medical emergency response information system; electronic LED lights are used as patient triage labels, which replace traditional paper labels. In addition to comprehensive triage information, the general surgery nursing system adds critical value alarms, scope and effectiveness checks (such as allergy tests), and complex decision support (such as pregnancy calculators, ESI, etc.) compared with other triage software. Foreign information-based emergency triage decision-making tools continue to increase; scholars have begun to pay attention to the “high efficiency” brought about by information technology; the reliability and effectiveness of triage have also become a research hotspot. At the same time, triage tools are not only developed in information, but intelligent functions are gradually being designed and developed. The triage staff uses electronic shunt sensors to wirelessly collect the patient’s life status, remotely monitor the patient’s vital signs, and can be based on the classification. The patient location tracking provided by the diagnosis tag allows for triage.

In order to improve the nursing effect of emergency general surgery, this paper combines computer algorithms to carry out the intelligent management of general surgery nursing so as to improve the nursing effect of general surgery and provide a reference for the further improvement of the quality of follow-up general surgery nursing service.

## 2. Related Work

In the early 1970s, hospitals in the United States, Japan, and other hospitals began to try to apply large-scale commercial computers to hospital management, began to research and develop hospital information systems, and established HIS system prototypes. By the mid-1980s, nursing information systems began to be used in some large hospitals in developed countries. With the development and maturity of various new network information technologies, foreign nursing-related information systems have been relatively complete. With the strengthening of the degree of integration of hospital nursing information and hospital management systems, all aspects of hospital nursing can be effectively managed, and the safety of nursing behavior is protected to a certain extent [6]. The earliest application of computer systems to hospital management in China began in the early 1980s. However, due to technical limitations, it was mainly used in stand-alone applications at that time, such as outpatient systems, charging systems, material management systems, financial systems, and so on. In the mid-1990s, due to the development of local area networks and other technologies, the nursing information system

under the wired local area network environment also began to be applied [7]. In the late 1990s, with the maturity of network technology, the process of hospital informatization began to accelerate in China. In particular, after entering the 21st century, hospital information construction began to keep up with the pace of international development, and began to establish a digital hospital with clinical information as the core, including the establishment of doctor workstations and nurse workstations [8]. In recent years, with the wave of mobile IT sweeping the world, the traditional medical IT field is also undergoing rapid changes. The application of barcode recognition, sensor control, wireless applications, and other technologies in the nursing field has greatly liberated the labor force, improving accuracy and efficiency. With the help of these new technologies [9], new breakthroughs have emerged in the development of nurses’ work. Moreover, many nursing management concepts and ideas have ushered in the soil of application and blossomed. For example, the overall responsibility system of nursing system combined with the application of mobile nursing technology solves the ambiguity and simple one-sided problems of traditional functional nursing and improves nursing safety [10].

In general, the nursing system is developing rapidly toward specialization, mobility, and diversification. The nursing system has evolved from a single, submodule subordinate to HIS to an integrated mobile nursing system, that includes traditional nurse workstations, nursing medical records, nursing management, and nursing care. Specialized clinical nursing information systems are being developed for planning and nursing tasks [11]. Foreign nursing information systems started earlier and gradually developed and improved. They can integrate all electronic records generated during patient care into an organic whole, and can collect, store, and process patient execution information and nursing staff-related information. Forming a closed loop of medical order and nursing quality control [12], combined with clinical medicine and nursing professional knowledge, can analyze and research patient data, medical order data, and nursing data, which is a better quality service for patients in the treatment process. At present, most domestic hospitals have implemented inpatient nurse workstations, and some of the more advanced hospitals have implemented overall nursing information systems (including intensive care nursing systems, nursing knowledge bases, nursing plans, and mobile nurse workstations) [13].

With the continuous improvement of the level of nursing specialization, it has also promoted the development of nursing specialties. Since the introduction of the modified early warning score (MEWS) system in the United Kingdom, the observation and early warning of critically ill patients in nursing work have played a very important role [14]. The MEWS scoring method is a very simple system for evaluating the patient’s condition and prognosis. It scores comprehensively according to the patient’s objective indicators, such as body temperature, heart rate, respiratory rate, systolic blood pressure, and consciousness, so that the patient’s critical condition can be scored to achieve the

advantages of being scientific, fast, simple, and predicting the risk of the disease [15]. At present, the MEWS scoring method has been widely used in ICUs and the emergency department as a tool to assess the severity or potential risk of the disease, and provide certain early warning support for early detection, early treatment, and early rescue of critically ill patients [16], but it has not been promoted in the surgical ward. At the same time, because young nurses now account for a large proportion of the department, relatively speaking, the identification and attention to the condition of some critically ill patients has been weakened to a certain extent [17]. Nowadays, with the continuous improvement of people's living standards and the advent of an aging society, more and more general surgery patients are showing a trend of aging. However, the elderly have more basic diseases, more comorbidities, and rapid changes in their conditions. Therefore, the relevant data of the improved MEWS score table [18] is now being applied to general surgery wards, which has a positive significance for the early detection of patient condition changes and intervention, effectively improving nurses' awareness and warning of potentially critically ill patients and preventing accidents.

### 3. Computer-Aided Emergency General Surgery Nursing System

The hospital's intelligent nursing display system is a business system that applies and serves the internal use of the Arab League Central Hospital. At the same time, the hospital also uses the intelligent nursing display system as an important means and tool to promote the improvement of nursing management. From the perspective of the development of medical informatization, the construction of nursing informatization is gradually developing toward mobile, intelligent, and wearable models. The mobile nursing information system uses mobile devices such as tablet computers, PDAs, smart phones, and other portable mobile devices to collect and distribute data. It also includes the use of large-screen display devices for data display and push. This can effectively help medical staff to grasp patient diagnosis and treatment information in a dynamic, comprehensive, and timely manner, scientifically arrange and execute diagnosis and treatment and nursing plans so as to solve the query, and enter vital signs data and medical care data by medical staff anytime and anywhere. Moreover, it helps hospitals realize a patient-centered service concept and a quality-centered management model. The development of the hospital's intelligent nursing display system can enable nurses to perform medical behaviors in clinical nursing work, such as fluid infusion, physical sign collection, intake and output, treatment execution, daily care, etc., to follow the patient to complete the collection work at the bedside. Moreover, the application of mobile nursing information technology rationally optimizes the original work flow, thereby improving the efficiency and the quality of nursing work, meeting the management requirements of high-quality nursing, and handling various emergencies (such as crisis values) in a timely and accurate manner.

(1) Comprehensive nursing information integration: It connects various business application systems in the hospital through the hospital data integration platform. Moreover, it integrates multiple systems such as clinical nursing, nursing management, mobile nursing, intensive care, medical order system, inspection, cost accounting, and material management. In addition, it collects relevant data and incorporates it into the clinical data center to form a data warehouse for the main body of nursing information, which solves the problems of repeated data entry and data inconsistency in multiple systems, and displays it on demand after processing. (2) Automatic generation of nursing plan: It is a predefined nursing plan knowledge base, and intelligently formulates nursing plans based on doctors' orders, nursing evaluation results, special physical signs, and patient conditions, and displays the patient's nursing plan dynamically in real time with a graphical interface. (3) Intelligent reminder of emergencies: The system can remind various problems in nursing work in real time, and intelligently, such as drug allergy and drug contraindications, and promptly remind emergency events such as crisis value to avoid medical errors. (4) Multi-level information display: The system can use electronic whiteboards, handheld terminals, tablet computers, electronic large screens, and other intelligent terminal devices to display corresponding information to doctors, responsible nurses, head nurses, and nursing department managers as needed to meet the information needs of people at different levels.

The hospital's intelligent nursing display system should combine the development needs of the hospital's clinical business, adhere to the demand-led approach, refer to the best practices of domestic and foreign industry informatization, and explore the informatization development model with low cost, good results, and outstanding highlights. It is necessary to gradually promote the hospital's information planning and construction in clinical diagnosis and treatment, medical quality control, operation management, decision analysis and other related aspects, and introduce scientific, professional, and refined management methods and means to drive the hospital's management innovation and service innovation. At the same time, it is necessary to realize the standardization of the management process, the networking of work communication, the electronicization of documents and materials, the sharing of knowledge and experience, and the openness of public welfare information so as to realize the new work pattern of "orderly management, free communication, and perfect service" in the hospital. At present, nursing information management systems and mobile clinical information systems based on mobile nursing work, electronic nursing documents, and labeling of nursing items have been put into use in many large- and medium-sized hospitals in China. The hospital intelligent nursing display system is a part of the nursing system, and the overall goal of the system is to promote the improvement of the hospital's nursing quality capabilities. With the least participation of the nursing staff, it can provide the nursing staff with the greatest help, or assist the nursing staff to achieve the following functions: (1) It can realize the automatic check of drugs and patients to avoid

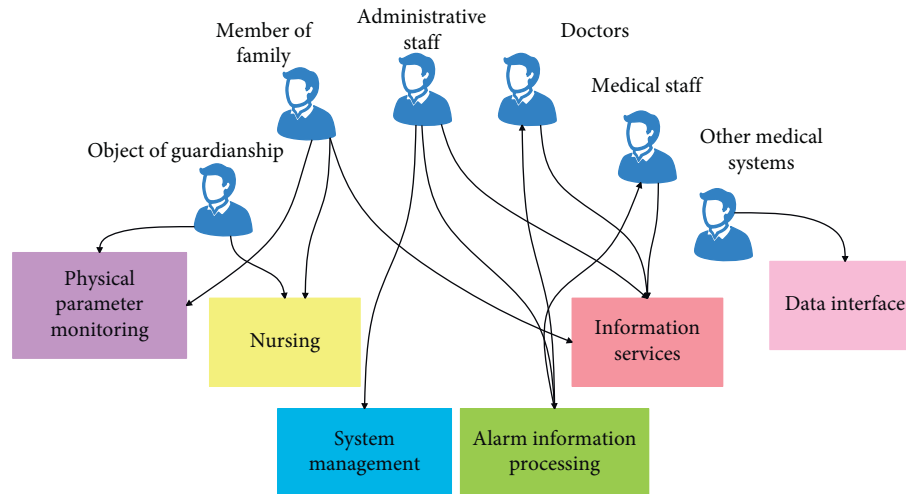


FIGURE 1: The use case diagram of a computer-aided emergency general surgery nursing system.

medical errors; (2) it can greatly reduce the workload of nursing and reduce the work intensity of nurses; (3) it can improve the efficiency and quality of nursing, and improve the level of nursing service; (4) it standardizes the clinical medical care process and improves the hospital's clinical medical care management level; (5) it provides medical and nursing staff message reminders to provide faster nursing assistance for nursing work; (6) it realizes patient review and provides comparison of average admission data for nursing management; (7) it implements a high-quality nursing information technology support platform to ensure that medical staff can communicate with each other anytime and anywhere; (8) it establishes a fair assessment mechanism to increase the enthusiasm of nursing staff. In general, the construction of the hospital's intelligent nursing display system will bring brand-new changes to nursing work, optimize the nursing workflow, and provide patients with better nursing services.

The conceptual model design is actually the realization process of the conceptual model. The conceptual model is an abstraction of the real world, i.e., it artificially processes actual people, objects, things, and concepts, extracts the necessary characteristics needed to build the system, ignores some nonessential details, and accurately describes these characteristics with various concepts.

The above is a detailed description and research of each functional module in the community intelligent remote monitoring system. Based on the analysis and abstraction of system developers, end users, and customers, it is concluded that the community intelligent remote monitoring system should include six use cases including physiological parameter monitoring, alarm information processing, nursing, information query, information management, and data interface. Figure 1 is the UML use case diagram of the system.

With reference to the above-detailed analysis of each use case of the system, we gradually refine the data objects of this part of the system, design a partial conceptual model, and determine the relationship between them. The partial conceptual model of the system is shown in Figure 2.

The partial conceptual model of the system is mainly composed of the client's basic information object, the client's relative information object, the doctor's information object, and the client's multi-physiological parameter object. The numbers on the relationship line indicate the corresponding relationship between the data objects. For example, there is a one-to-many relationship between basic customer information and multiple physiological parameter data, i.e., a customer object contains multiple physiological parameter information. Through the detailed design of the partial conceptual structure, the relationship between the data objects is truly reflected, and the foundation for the subsequent logical model design is laid.

The system hardware framework is shown in Figure 3 below. STM32 is used as the main processor, and the internal running program drives the Wi-Fi chip to send and receive data.

The driver framework of 88W8686 is shown in Figure 4 below, where the host driver (hereafter referred to as the Host Driver) is responsible for communicating with the firmware in 88W8686 (hereafter referred to as the Firmware), where Firmware is a program running in the Wi-Fi SoC chip. After the system is powered on, the processor downloads it to the Wi-Fi chip, and then the firmware can run in the SoC. Based on the ARM CPU, MAC, baseband module, radio frequency module, and hardware interface inside the SoC, functions such as hardware interface control, data service, 802.11 MAC layer management, and hardware control are implemented. There are two channels between the Host Driver and the Firmware: data channel and command channel. The data channel is used to transmit data to be sent and received, and the command channel is used to transmit control commands. The Host Driver sends the standard 802.3 frame to the WLAN Firmware in the SoC, and the WLAN Firmware processes it as an 802.11 frame and then sends it out wirelessly. After the WLAN Firmware receives the 802.11 frame, it converts it into an 802.3 frame, and then sends it to the Host Driver through the data channel.

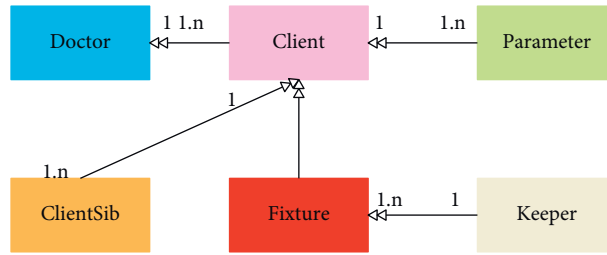


FIGURE 2: Partial conceptual model diagram.

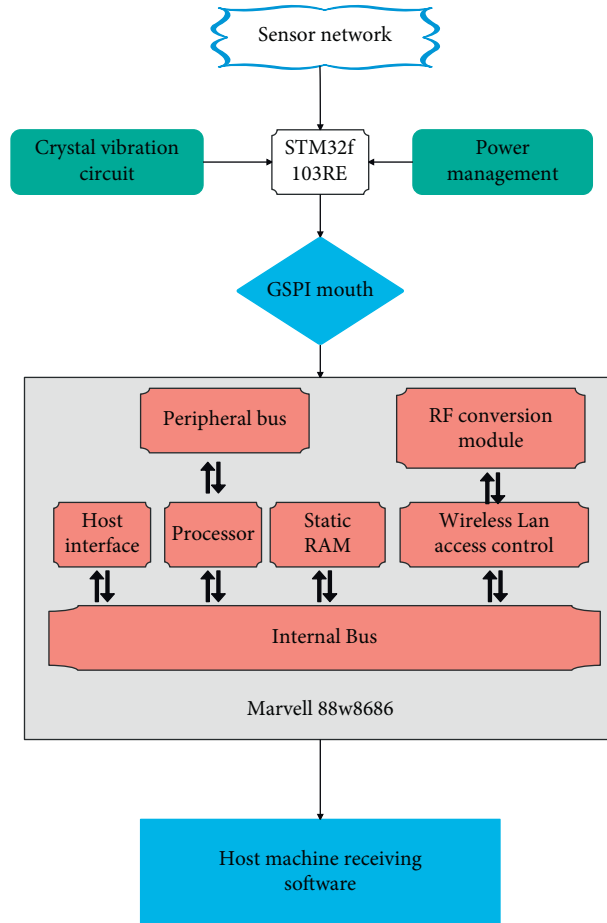


FIGURE 3: Wi-Fi system hardware block diagram.

#### 4. Analysis of Nursing Effect in Emergency General Surgery Based on Computer Aid

We select the emergency general surgery inpatients admitted to the emergency department of this hospital from June 2019 to December 2020 as the research sample. According to the method of random allocation, they are divided into the experimental group and the control group. Among them, the control group used traditional general surgical nursing methods, and the experimental group used the intelligent computer-aided nursing system constructed in this paper. In addition, other intervention methods are the same. On this basis, we collect relevant data for comparative analysis.

Risk management for patients: Medical staff need to strengthen the management of neurosurgery emergency, surgery, elderly and critical patients, and use bed guards for patients with inconvenient mobility to prevent patients from falling from beds and other injuries. Therefore, the floor should be kept dry, handrails should be added to the bathroom, related warning signs should be present in wet areas, and the wheels, brakes, and guardrails of the patient’s bed should be checked regularly. The nurse’s shift needs to be 15 minutes in advance, and the content of the shift at the bedside must be effectively verified. For patients with more serious illnesses, the nursing staff need to



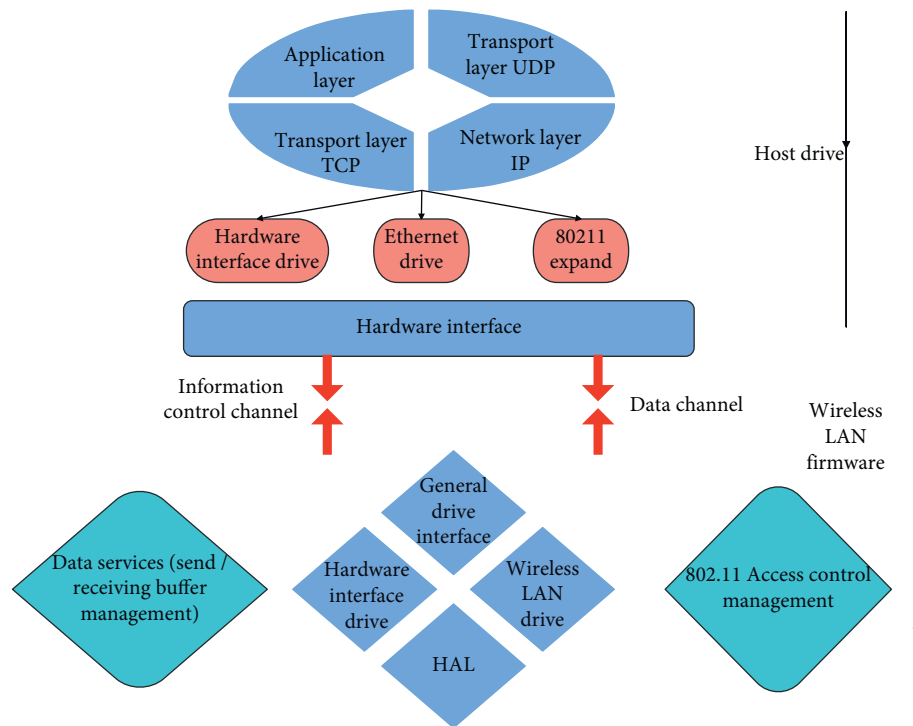


FIGURE 4: Hierarchical structure of the driver.

strengthen communication with their families and provide relevant psychological counseling.

**Risk management for nurses:** It is necessary to strengthen professional training and risk management awareness of nurses so as to effectively improve the quality of nursing work. At the same time, it is also necessary to strengthen the communication skills of nurses to promote a more harmonious relationship between the doctors and the patients. Hospital units can regularly organize nurses to conduct neurosurgery technical training and theoretical learning so as to improve the proficiency of nurses in nursing operations. At the same time, it is also necessary to strengthen the nursing level, communication level, and drug use methods of the nursing staff to improve the quality of nursing work. In addition, it is necessary to organize nurses to conduct academic exchange meetings on a regular basis to realize the sharing of information resources. For nursing staff with low qualifications, guidance and supervision need to be strengthened.

**Environmental risk management:** The environment of the nephrology ward needs to be kept clean and comfortable so as to create a comfortable and quiet atmosphere for patients to recuperate. It is necessary to effectively implement the ward visiting system to prevent patients from being disturbed in their recuperation. At the same time, the environment needs to be disinfected to prevent infections in patients.

**Risk management for the pipeline:** Patients in the Department of Nephrology generally have more

catheters indwelled, and the main purpose is to observe the patient's condition. Therefore, the catheter needs to be kept unobstructed, and a fixing device should be added to prevent the catheter from twisting and pulling. At the same time, it is also necessary to sterilize the pipelines to strengthen the operational hygiene awareness of the medical staff and prevent patients from becoming infected. In addition, the indwelling time of the catheter needs to be communicated with the physician to prevent infection caused by excessive indwelling time.

**Risk management for emergency treatment:** It is necessary to carry out effective and reasonable treatment of emergency plans for intravenous extravasation of special drugs, emergency plans for blockages, emergency plans for pressure sore prevention, emergency plans for cross-infection, and emergency plans for power outages and water cuts. At the same time, it is necessary to carry out relevant emergency drills to improve the emergency awareness of nurses, strengthen the awareness and understanding of emergency handling, improve proficiency, and effectively guarantee the quality of emergency work. On this basis, the effects of computer-aided care in emergency general surgery are calculated, and the results are shown in Tables 1–4.

It can be seen from the above research that the computer-assisted emergency general surgery nursing method proposed in this paper has a certain progress compared with the traditional nursing method. Therefore, the system of this paper can be used as an auxiliary

TABLE 1: The incidence of adverse nursing events in emergency general surgery.

No	Control group (%)	Test group (%)
1	8.65	1.85
2	7.19	1.95
3	4.59	0.69
4	5.53	0.18
5	4.52	1.21
6	4.37	1.94
7	4.12	1.12
8	3.85	1.16
9	8.60	0.86
10	6.48	1.15
11	6.66	0.23
12	2.32	0.44
13	4.88	0.55
14	8.64	0.70
15	6.38	1.46
16	4.96	0.87
17	4.33	1.91
18	4.18	0.18
19	5.36	1.19
20	5.37	0.71
21	8.27	0.59
22	7.43	0.55
23	1.99	0.67
24	1.76	0.82
25	8.89	0.95
26	4.13	0.09
27	2.48	0.92
28	1.23	0.50
29	8.93	1.03
30	3.68	0.69
31	4.88	1.44
32	2.81	0.02
33	4.49	1.83
34	5.21	0.19
35	6.80	0.95
36	2.48	1.93
37	1.65	1.08
38	1.75	0.30
39	3.84	1.96
40	7.04	0.39

TABLE 2: Completion rate of nursing measures in emergency general surgery.

No	Control group (%)	Test group (%)
1	91.62	97.63
2	93.00	97.41
3	90.16	97.55
4	91.71	95.28
5	87.09	98.68
6	85.70	94.09
7	90.84	97.15
8	93.92	94.28
9	91.50	99.73
10	92.53	99.86
11	92.20	98.95
12	91.87	99.17
13	93.63	94.09
14	87.97	94.17

TABLE 2: Continued.

No	Control group (%)	Test group (%)
15	89.87	95.64
16	93.03	98.29
17	87.92	96.48
18	92.55	98.97
19	87.01	94.80
20	90.12	98.38
21	87.74	95.22
22	91.66	95.60
23	88.53	97.18
24	85.45	97.62
25	91.95	99.01
26	92.94	98.35
27	93.08	96.24
28	91.15	97.40
29	91.17	96.33
30	92.75	98.01
31	86.31	95.10
32	93.32	97.56
33	90.18	99.63
34	86.24	94.79
35	91.82	95.74
36	89.92	99.89
37	91.85	96.86
38	92.30	98.03
39	86.73	96.78
40	85.82	98.97

TABLE 3: Satisfaction of nursing patients in emergency general surgery.

No	Control group	Test group
1	85.25	97.01
2	87.16	95.48
3	91.70	96.21
4	91.45	97.19
5	89.23	95.81
6	88.01	99.25
7	90.95	97.98
8	86.91	98.23
9	92.00	95.42
10	90.84	96.11
11	90.92	94.37
12	89.72	98.44
13	89.00	95.28
14	93.77	97.07
15	87.06	99.53
16	90.50	96.02
17	89.61	98.14
18	86.90	96.08
19	88.03	97.30
20	93.46	98.61
21	88.23	96.53
22	89.37	95.09
23	90.74	94.20
24	93.31	95.80
25	88.82	97.24
26	92.22	98.09
27	85.41	98.64
28	88.65	95.41
29	86.01	94.26

TABLE 3: Continued.

No	Control group	Test group
30	86.89	97.41
31	90.92	99.31
32	92.19	95.97
33	88.39	94.12
34	88.36	94.53
35	91.69	96.81
36	88.05	94.74
37	87.41	95.87
38	91.92	97.40
39	88.38	99.16
40	87.39	96.03

TABLE 4: Satisfaction of nursing doctors in emergency general surgery.

No	Control group	Test group
1	88.73	99.45
2	91.34	98.13
3	93.17	95.84
4	85.37	97.08
5	90.13	99.26
6	90.88	96.20
7	85.85	96.44
8	87.20	94.51
9	93.99	94.16
10	89.62	94.32
11	86.57	96.86
12	85.70	98.96
13	92.24	98.31
14	85.20	96.58
15	90.66	99.41
16	86.49	98.67
17	85.85	94.24
18	91.47	96.99
19	91.14	97.08
20	89.02	98.82
21	90.77	96.31
22	91.00	96.47
23	86.50	95.03
24	92.37	99.07
25	85.33	94.56
26	91.63	99.81
27	91.78	95.45
28	93.70	98.45
29	93.26	97.52
30	92.14	99.32
31	87.36	97.11
32	91.61	94.32
33	86.81	99.69
34	92.36	98.10
35	93.77	96.20
36	88.34	99.17
37	86.02	95.20
38	92.72	98.94
39	86.68	95.87
40	91.32	98.07

nursing system in the follow-up hospital emergency general surgery nursing to improve the nursing effect of emergency general surgery.

## 5. Conclusion

Emergency Department of General Surgery is a very important department, which is highly specialized and involves many types of diseases. In addition, the condition of some patients with craniocerebral trauma changes rapidly and the onset is more rapid; thus, medical personnel are more required to have skilled emergency handling capabilities and operational skills. The professional nature and the importance of the departments also determine the trend of nurses' high work intensity and workload. Under this highly stressful working state, the occurrence of medical care risks is also increasing. Therefore, nurses need to strengthen the analysis and management of risk factors in nursing work so as to prevent risk events. At the same time, hospital units also need to combine the items complained by patients and medical disputes, strengthen in-depth analysis and investigation of these events, understand and recognize the information content related to risk events, and evaluate the consequences of them so as to summarize the factors associated with risk events. In order to improve the nursing effect of emergency general surgery, this paper combines computer algorithms to carry out the intelligent management of general surgery nursing so as to improve the nursing effect of general surgery. Through actual case studies, it can be seen that the computer-assisted emergency general surgery nursing method proposed in this paper has a certain progress compared with the traditional nursing method.

## Data Availability

The data used to support the findings of this study are available from the corresponding author upon request.

## Conflicts of Interest

The authors declare that they have no conflicts of interest.

## References

- [1] A. Karaca and Z. Durna, "Patient satisfaction with the quality of nursing care," *Nursing open*, vol. 6, no. 2, pp. 535–545, 2019.
- [2] J. R. Bledsoe, S. C. Woller, S. M. Stevens et al., "Management of low-risk pulmonary embolism patients without hospitalization: the low-risk pulmonary embolism prospective management study," *Chest*, vol. 154, no. 2, pp. 249–256, 2018.
- [3] N. Fisher, J. Hooper, S. Bess, S. Konda, P. Leucht, and K. A. Egol, "Ninety-day postoperative narcotic use after hospitalization for orthopaedic trauma," *JAAOS-Journal of the American Academy of Orthopaedic Surgeons*, vol. 28, no. 13, pp. e560–e565, 2020.
- [4] M. Akbas, "Patient satisfaction on nursing care: the case of gynecology and obstetrics clinics," *Acta bioethica*, vol. 25, no. 1, pp. 127–136, 2019.
- [5] E. Noll, S. Shodhan, M. C. Madariaga et al., "Randomized trial of acupressure to improve patient satisfaction and quality of recovery in hospitalized patients: study protocol for a randomized controlled trial," *Trials*, vol. 18, no. 1, pp. 1–7, 2017.
- [6] G. Akbulut, E. Kant, S. Ozmen, and R. B. Akpınar, "Determining patients' satisfaction with the nursing services provided in an oncology clinic of Eastern Turkey," *International Journal of Caring Sciences*, vol. 10, no. 3, pp. 1276–1285, 2017.
- [7] A. S. Kasa and H. Gedamu, "Predictors of adult patient satisfaction with nursing care in public hospitals of Amhara region, Northwest Ethiopia," *BMC health services research*, vol. 19, no. 1, pp. 1–9, 2019.
- [8] S. Leuzzi, A. Stivala, J. B. Shaff et al., "Latissimus dorsi breast reconstruction with or without implants: A comparison between outcome and patient satisfaction," *Journal of Plastic, Reconstructive & Aesthetic Surgery*, vol. 72, no. 3, pp. 381–393, 2019.
- [9] E. S. Singer, R. E. Merritt, D. M. D'Souza, S. D. Moffatt-Bruce, and P. J. Kneuert, "Patient satisfaction after lung cancer surgery: do clinical outcomes affect Hospital Consumer Assessment of Health Care Providers and Systems Scores?" *The Annals of thoracic surgery*, vol. 108, no. 6, pp. 1656–1663, 2019.
- [10] M. Lotfi, V. Zamanzadeh, L. Valizadeh, and M. Khajehgoodari, "Assessment of nurse–patient communication and patient satisfaction from nursing care," *Nursing open*, vol. 6, no. 3, pp. 1189–1196, 2019.
- [11] B. Raju and K. Reddy, "Are counseling services necessary for the surgical patients and their family members during hospitalization?" *Journal of neurosciences in rural practice*, vol. 8, no. 01, pp. 114–117, 2017.
- [12] J. DeVore, A. Clontz, D. Ren, L. Cairns, and M. Beach, "Improving patient satisfaction with better pain management in hospitalized patients," *The Journal for Nurse Practitioners*, vol. 13, no. 1, pp. e23–e27, 2017.
- [13] K. L. Rice, J. Castex, M. Redmond, J. Burton, J. W. Guo, and S. L. Beck, "Bundling interventions to enhance pain care quality (bite pain) in medical surgical patients," *Ochsner Journal*, vol. 19, no. 2, pp. 77–95, 2019.
- [14] H. Mulugeta, F. Wagnew, G. Dessie, H. Biresaw, and T. D. Habtewold, "Patient satisfaction with nursing care in Ethiopia: a systematic review and meta-analysis," *BMC nursing*, vol. 18, no. 1, pp. 1–12, 2019.
- [15] S. M. Gijzel, J. Rector, F. B. van Meulen et al., "Measurement of dynamical resilience indicators improves the prediction of recovery following hospitalization in older adults," *Journal of the American Medical Directors Association*, vol. 21, no. 4, pp. 525–530, 2020.
- [16] H. Ozturk, N. Demirsoy, O. Sayligil, and K. L. Florczak, "Patients' perceptions of nursing care in a university hospital," *Nursing science quarterly*, vol. 33, no. 1, pp. 12–18, 2020.
- [17] E. Kavuran and N. Turkoglu, "The Relationship Between Care Dependency Level and Satisfaction with Nursing Care of Neurological Patients in Turkey," *International Journal of Caring Sciences*, vol. 11, no. 2, pp. 725–733, 2018.
- [18] N. D. Sridharan, L. Fish, L. Yu et al., "The associations of hemodialysis access type and access satisfaction with health-related quality of life," *Journal of vascular surgery*, vol. 67, no. 1, pp. 229–235, 2018.

## Research Article

# Correlation of HMGB1, PON-1, MCP-1, and Periodontal *P. gingivalis* with Amniotic Fluid Fecal Dye

Zhen-Ai Jin <sup>1</sup>, Ying Li,<sup>1</sup> Wei-Bing Chen,<sup>2</sup> Yu-Ying Wang,<sup>3</sup> Yi-Kun Zhao,<sup>2</sup> Xiang-Lan Sun,<sup>4</sup> Jia-Jun He,<sup>4</sup> Guo Jie,<sup>5</sup> and Yu-Mei Sun<sup>6</sup>

<sup>1</sup>Department of Pediatrics, Affiliated Hospital of Yanbian University, 1327 Bureau Street, Jilin, Yanji, China

<sup>2</sup>Neonatology Department, Rizhao People's Hospital of Jining Medical University, No. 126, Taian Road, Rizhao, Shandong, China

<sup>3</sup>Jilin Provincial People's Hospital, 1183 Gongnong Street, Chaoyang, Changchun, China

<sup>4</sup>Obstetrical Department, Rizhao People's Hospital of Jining Medical University, No. 126, Taian Road, Rizhao, Shandong, China

<sup>5</sup>Department of Obstetrics, Affiliated Hospital of Yanbian University, 1327 Bureau Street, Yanji, Jilin, China

<sup>6</sup>Department of Neonatology, Dalian Women and Children's Medical Center (Group), No. 1 Dunhuang Road, Dalian Liaoning, China

Correspondence should be addressed to Zhen-Ai Jin; 9000001060@ybu.edu.cn

Received 29 November 2021; Revised 23 December 2021; Accepted 28 December 2021; Published 22 February 2022

Academic Editor: Gaurav Goyal

Copyright © 2022 Zhen-Ai Jin et al. This is an open access article distributed under the Creative Commons Attribution License, which permits unrestricted use, distribution, and reproduction in any medium, provided the original work is properly cited.

**Background.** This paper aims to investigate the correlation between high mobility group protein-1 (HMG-b1), antioxidant enzyme-1 (paraoxon-1, PON-1), monocyte chemoattractant protein-1 (monocyte chemoattractant protein-1, MCP-1), *P. gingivalis*, and MSAF. **Materials and Methods.** The total sample size comprised of 73 cases in both groups. These patients were further subdivided into 2 groups: the MSAF group and the control group. 38 women were in the MSAF group and 35 women with term amniotic fluid serum were in the control group. The MSAF group was selected as a full-term singleton amniotic fluid fecal infection group. Clinical data were collected, and specimens were collected. Fecal staining of amniotic fluid and full-term amniotic fluid removes the placenta and umbilical cord blood. The expression of HMGB1 in the placenta was observed by immune-histochemical staining of MSAF and control groups. The content of PON-1 in cord blood was determined by ELISA. **Results.** Correlation between maternal and neonatal clinical data and MSAF was done; MSAF group mean gestational age was  $41.38 \pm 1.40$  weeks; control group mean gestational age was  $39.20 \pm 1.24$  weeks. This study found no correlation between the birth weight, maternal age, sex, first/transmaternal, hyperthyroidism, hypothyroidism, and anemia between the MSAF and control group with nonsignificant *P* value ( $P > 0.05$ ). However, the fatal age, gestational diabetes, gestational hypertension, umbilical cord abnormalities, placental abnormalities, and neonatal asphyxia factors were statistically different with a significant *P* value of  $<0.05$  between both groups. HMGB1 and Periodontal *P. gingivalis* are mostly expressed in placental trophoblast, vascular endothelial cells, and amniotic epithelial and interstitial cells. After HE staining of 72 placentas by HE in MSAF and control, 6 had acute chorioamnionitis (5.1 control), 32 had chronic (23.9), 35 had abnormal placentas, and three in MSAF had chorionic columnar metaplasia. In immune-histochemistry experiments, the HMGB1 expression intensity of placental tissue was higher in the MSAF group ( $P < 0.05$ ); however, the level of PON-1 was lower in the MSAF group as compared to the controls ( $P < 0.05$ ). **Conclusions.** Gestational age and placental abnormalities are clinical high-risk factors for MSAF. HMGB1, PON-1, MCP-1, and Periodontal *P. gingivalis* may be involved in the development of MSAF, suggesting an oxidative/antioxidant imbalance with inflammation, and may be one of the mechanisms for MSAF development.

## 1. Introduction

In recent years, the birth rate of high-risk pregnant women and critical newborns has been increasing, and the perinatal period of pregnant women has become the focus of attention.

Clinically, the MSAF is defined as follows: when stimulated by a variety of causes, it makes fetal intestinal peristalsis, anal sphincter tension decreases, fetal meconium with intestinal peristalsis into the amniotic fluid, originally bright, and translucent amniotic fluid presents different degrees of

turbidity, thick, and with the degree of difference, color can appear light green to dark brown change [1, 2]. The theory of the cause and mechanism of MSAF is not unified. At present, there are theories of fetal maturity and umbilical cord extrusion at birth, as well as the theory of fetal intrauterine distress put forward by many scholars. Meconium-stained amniotic fluid (MSAF) occurs when there is a passage of the fetal colonic contents into the amniotic cavity. The frequency of this condition increases as a function of gestational age. The frequency of MSAF ranges from 5% to 20% [3].

The presence of meconium predisposes to meconium aspiration syndrome (MAS) which only occurs in 5% of all neonates born to mothers with MSAF. MSAF is a risk factor for clinical chorioamnionitis, neonatal hypoxic-ischemic encephalopathy, neonatal sepsis, seizures, and cerebral palsy. Therefore, the presence of MSAF is considered a warning sign by obstetricians, even though most neonates do not have evidence of hypoxia or metabolic acidemia [4]. MSAF can lead to complications such as intrauterine hypoxia and neonatal asphyxia; due to continuous hypoxia of irreversible damage to brain nerves and other organs, such as meconium inhalation syndrome (meconium aspiration syndrome, MAS), hypoxia and ischemic encephalopathy, etc., can be life-threatening when severe [4]. Wu Meiyuan's [5] study pointed out that the amniotic fluid fecal infection is more prone to meconium inhalation syndrome, which further revealed that it is more prone to poor prognosis in newborns. At present, few related studies of MSAF and intrauterine inflammation have been reported. The etiology and pathogenesis of MSAF have not been clarified, and increasing attention has been paid to the search for MSAF markers. Through studies of the placenta and umbilical cord blood-related problems, the correlation between intrauterine inflammation and amniotic fluid fecal infection is of certain research value and significance.

Studies have pointed out that [6] MSAF patients had a chorionic amnionitis (chorioamnionitis, CA) probability of more than 50% associated with intrauterine infection. CA is one of the risk factors of intrauterine infection, and microbes entering the amniotic cavity may cause MSAF, while inflammation of the placenta may cause MSAF. Placental lesions can be classified into acute and chronic placental lesions. Acute lesions are mostly related to infection, and chronic placental lesions could be caused by bacteria, viruses, environmental pollution, and other related factors. In Chen Lifan et al. [7], the length of MSAF was found to be extremely closely related to placental lesions. Some researchers believe that intrauterine inflammation is not related to MSAF, so there is some controversy. In clinical work, intrauterine inflammation can be attributed to placental inflammation, umbilical cord inflammation, and fetal membrane inflammation. Studying its interlocality with MSAF can further investigate the occurrence mechanism of MSAF development.

HMGB1, PON-1, MCP-1, and Periodontal *P. gingivalis* are inflammatory factors studied associated with MSAF. All these factors have been involved in the occurrence of inflammation, related to oxidative damage mechanism;

however, very less studies and reports are conducted in this regard.

HMGB1, one member of the Alertin family, induces the occurrence of an inflammatory response or the repair of stress trauma to initiate host defense. Relevant studies have found that the generation and release of cytokines can change the signaling regulation inside and outside the cell, thus leading to the occurrence of inflammation and the repair after stimulation [8]. Qiu Xiaoyuan [9] believed that increased levels of HMGB1 expression can aggravate the inflammatory response in the placenta. When the body encounters an infection, HMGB1 can be secreted by immune cells. The signaling pathway is initiated by triggering an inflammatory response by binding to the Toll-like receptor 4 (Toll-like receptor 4, TLR4), as well as to the late glycosylation end-product receptor (Receptor for advanced glycation end products, RAGE).

PON-1 is a member of the antioxidant enzyme family with anti-inflammatory effects, associated with antioxidative stress and with the pathogenesis of numerous diseases. The amount of PON-1 at the site of expression is reduced, causing an oxidative stress response, leading to the occurrence of inflammation [10].

MCP-1 is a chemokine with chemotactic monocytes, macrophages, and T lymphocytes, involved in the inflammatory response, associated with apoptosis, the occurrence and progression of pregnancy diseases, and premature fetal membrane rupture.

Periodontitis in pregnancy should not be confused with pregnancy gingivitis. Pregnancy gingivitis is a common, reversible condition of gingival inflammation associated with high levels of estrogen and blooms of microbial species such as *P. gingivalis*. In periodontitis, the modification of the microbial composition is unrelated to pregnancy status or pregnancy hormones. When good oral hygiene practices are implemented, pregnancy gingivitis resolves within a few months of birth with no permanent changes in CAL. The presence of microbial invasion of the amniotic cavity by *P. gingivalis* could indicate a role for periodontal pathogenic bacteria in pregnant women with a diagnosis of threatened premature labor.

In this study, clinical risk factors of MSAF were analyzed by maternal and neonatal clinical data. The basic aim of the study was to explore the correlation of HMGB1, PON-1, MCP-1, and *P. gingivalis* with MSAF.

## 2. Materials and Methods

*2.1. Collection of Clinical Data Specimens and Data.* Clinical case data of amniotic fluid fecal-stained newborn and normal newborns born were collected from the Affiliated Hospital of Yanbian University.

Placenta and cord blood from the term women with an MSAF collection were set as MSAF groups, while women with term amniotic fluid collection were treated as control groups. Placental pathology was examined by HE staining, HMGB1 expression levels in placental tissue were measured by immunohistochemistry, PON-1 content in cord blood

was measured by ELISA, and MCP-1 content in cord blood was determined by flow cytometry.

Specimen collection has been discussed by the Ethics Committee of Affiliated Hospital, Yanbian University to collect placenta and cord blood stained with term amniotic fluid stool delivered from January 2018 to December 2019. The total sample size was comprised of 73 subjects, 38 women in the MSAF group, and 35 women with term amniotic fluid serum in the control group. After specimen collection, all the placentae were stained with HE.

Placental collection method and storage: after the delivery of the maternal placenta, the placenta was extracted and fetal membrane tissue of about 3 cm×4 cm was collected. A 4% formaldehyde solution was taken for sealing and fixation. Paraffin and wax blocks were sectioned, 4 pieces with each cut thickness of 4–6 μm, then sealed, and dried.

Process of umbilical cord blood collection: after delivery of the newborn, before breaking the umbilical cord from the mother, the umbilical cord was cut, and 5 ml of the blood from the lateral umbilical vein was collected with a pro-coagulation tube. After centrifugation and centrifugation, the upper serum was collected, recorded with specimen information and numbers, and stored in the -80 °C refrigerator.

## 2.2. Degree of MSAF and Diagnostic Criteria of CAM

**2.2.1. The Standard of MSAF.** Clinically, the amniotic fluid dung dye can be divided into 3°, from light to heavy and further, I degree, II degree, and III degree. I degree: light green, thin quality, and no faecium residue. Degree II: dark green, yellow-green, and relatively thick quality. Degree III: brown, dark yellow, thick, small amount, and visible granular meconium [11]. All the MSAF groups were stained with measured feces in this experiment.

**2.2.2. The Diagnostic Criteria for CA.** CA is further divided into acute and chronic chorioamnionitis. Acute chorioamnionitis could have neutrophils in the villus connective tissue, amniotic membrane, or chorionic plates. In chronic chorioamnionitis, lymphocytes infiltrate in the chorionic trophoblast and chorionic amniotic connective tissue [12].

**2.2.3. Main Instrument, Equipment, and Reagents.** The main instrument, equipment, and reagents used in the study have been mentioned in Table 1.

**2.2.4. Reagent. Cell Analysis Kit.** High-throughput liquid-phase protein quantification reagent of human CXCL8/IL-8, CCL5/RANTES/CXCL9/MIQ, CCL2/MCP-1, CXCL10/IP-1 cells: Becton, Dickinson, and Company.

Epidemiological histochemical experimental reagents:

- (1) Rabbit anti-human HMGB1 clonal antibody: Cell Signaling Technology reagent agent
- (2) DAB Kit: Abcam Reagent, Inc.

- (3) PV9000 Kit: Abcam Kit Company, containing reagent 1: endogenous peroxidase blocker; reagent 2: reaction enhancer; Kit 3: HRP-enhanced goat anti-mouse/rabbit IgG polymer

**ELISA Experimental Reagent.** PON1 Quantitative ELISA Kit: Shanghai Enzyme Union Biotechnology Co., Ltd. The ELISA experimental reagents have been depicted in Table 2.

## 2.3. Experimental Methods

### 2.3.1. Detection Steps of the Flow Cell Assay

- (1) Clean the flow cytometry to ensure the normal function of each instrument detection channel.
- (2) Prepare standard solution and dilution: take 4 ml standard dilution and freeze ophil dried to mix with the test tube, which is the original liquid, and rest for 10 min. Nine standard tubes were set and one was blank, and the standards were subjected to proportional fold dilutions and added to 10 tubes and labeled S1–S10. First take 300 ul from the raw liquid into the S1 tube, mix; then move from the S1 tube to 300 ul, and so on, until you move to the S10 tube. The dilution ratio and corresponding concentrations are shown in Table 3.
- (3) Prepare capture microsphere suspension: IP-10 microsphere suspension was added for 1010 ul to MCB tube, the supernatant was centrifuged for 5 min, and serum was collected. Resuspension and incubation were done in light at room temperature for 20 min.
- (4) Take serum which has to be measured and further added to the tube for the test; microsphere suspension was added to standard products and serum samples to be measured and incubated for 3h at room temperature
- (5) Washing: add washing buffer for 1 ml to each tube, and the supernatant was discarded. A 300 ul resuspension microball was added to each tube.
- (6) The final standards and samples are analyzed for statistical data.

### 2.3.2. ELISA Method

- (1) Sample serum: -80 °C, dissolved at room temperature, with shaking.
- (2) Standard product and number: take standard product reagent, prepare 10 standard holes, and mark S1–S10. The same concentration was added to each two adjacent pore droplets such as S1, S2, and 50 μl, with concentrations of 120, 80, 40, 20, and 10 nmol/mL, respectively.
- (3) Set blank holes and additional samples: set as B1 and B2, except for blank holes; add 50 μl sample to each sample hole to be tested.
- (4) HRP: add 50 μl of labeling reagent to each well.



TABLE 1: Instrument name and manufacturer.

	Instrument name	Manufacturer
1	Leica automatic slicer	Leica, Germany
2	PHY-III pathological tissue bleaching oven	Shanghai Changchang Electronics Co., Ltd.
3	Electrothermal constant temperature incubator	Shanghai Yuejin photochemical instrument Factory
4	Digital imaging equipment	Digital imaging equipment
5	Micro oscillator	Xishan Jincheng Instrument Factory
6	Foshan Zhiguang instrument Factory	Foshan Zhiguang Instrument Factory
7	Ultrapure water machine	Shanghai Yuejin photochemical instrument Factory
8	- 80°C refrigerator	Zhongke Meiling company
9	Table type low speed refrigerated multitube centrifuge	Shanghai Anting Scientific Instrument Factory
10	Micropipette	Mettler Toledo Instruments Co., Ltd.
11	BioTek reader	Biotec instruments
12	Incubator	Shanghai Xinmiao Medical Instrument Co., Ltd.
13	Eppendorf micro sampler Eppendorf	Germany
14	Flow cytometry	Beckton, Dickinson

TABLE 2: PON1 quantitative ELISA kit components.

Intracellular kit reagent	
1 Instructions	Sample dilution: 1 bottle (6 ml)
Seal plate film is 2 sheets	Color A and B 1 bottle each (6 ml)
The plate was coated with 96-well plates	Termination solution: 1 bottle (6 ml)
Standard product (concentration of 120, 80, 40, 20, and 10 nmol/mL, respectively) 5 bottles (2 ml)	Concentrate the detergent for 1 bottle (25 ml)
Enzyme labeling reagent 1 bottle (6 ml)	

TABLE 3: List of corresponding concentrations and dilution ratio of standard tubes.

Standard tube number	Corresponding concentration (pg/ml)	Dilution fold ratio
S1 (blank control)	0	0
S2	10	1 : 256
S3	20	1 : 128
S4	40	1 : 64
S5	80	1 : 32
S6	156	1 : 16
S7	312.5	1 : 8
S8	625	1 : 4
S9	1250	1 : 2
S10	2500	1 : 1

- (5) Incubation: after gently shaking, the plate membrane was sealed and incubated in a 37°C incubator for 1 hour.
- (6) Flushing: get rid of the liquid in the hole, fill with washing liquid, repeatedly wash and pat dry, and repeat 5 times in this way.
- (7) Color display with the color developer: add color developer A, B50  $\mu$ l, 37°C incubators in each well to avoid light for 10 minutes.
- (8) Color termination: gently for 50  $\mu$ l, in each well.
- (9) OD value of each well by computer.

2.4. *The HMGB1 Immunohistochemical Staining Results Were Determined.* HE staining mainly observed the morphology and pathological changes of the placenta and fetal membrane. In the placenta, HMGB1 is mainly localized in

placental trophoblast, vascular endothelial cells as well as amniotic epithelial and stromal cells. The nucleus is positive in blue, and the cytoplasm is brown; negative if the nucleus, cytoplasm, or membrane is shown in blue[13]. Color intensity: The positive intensity of positive cells in each slice was 0 colorless, 1 pale yellow, 2 brown, and 3 dark brown. The average of positive cells: the percentage of positive cells was 0, positive cell <25% 1, 25%–50% 2, > 50% was 3; the sum of positive cells and color intensity: 0–1; 2–3 (+); 4–5 (++) and 6 (+++).

2.5. *Statistical Methods.* All of the data were analyzed using SPSS 26.0 statistical software. Study data were analyzed using an independent sample *t*-test, grade data were analyzed using the nonparametric test, and  $P < 0.05$  was statistically significant. Risk factors analysis was performed using logistic regression analysis.

### 3. Results

**3.1. Comparison of Clinical Data between the MSAF and Control Groups.** The total sample size comprised of 73 subjects. In the MSAF group, there were a total of 38 subjects, 22 men, 16 females, with the mean gestational age being  $41.38 \pm 1.40$  weeks, and the control group was comprised of a total of 33 subjects, 19 men, 16 females, with the mean gestational age being  $39.20 \pm 1.24$  weeks. The gender, birth weight, maternal age, initial/transmaternal, and gestational history were nonsignificant between both the groups ( $P > 0.05$ ). However, gestational age, gestational diabetes, gestational hypertension, umbilical cord abnormalities, placental abnormalities, and neonatal asphyxia were significant between the groups ( $P < 0.05$ ), shown in Table 4.

Logistic regression analysis of the risk factor analysis in the MSAF group and gestational age and placental abnormalities were high-risk factors for amniotic fluid fecal staining, with OR being 2.639 (95%CI:1.646–4.231) and 4.506 (95%CI:1.034–19.631), respectively, and positively related (Table 5).

**3.2. Comparison of HMGB1 Expression and PON1, MCP-1, and P. gingivalis Content between the MSAF Group and the Controls**

**3.2.1. HMGB1 Expression in the Placental Tissues of Both the MSAF and Control Groups.** HMGB1 is mostly expressed in placental trophoblast, vascular endothelial cells, and amniotic epithelial and interstitial cells. The expression intensity of HMGB1 in the MSAF group was higher than in control tissues and was statistically significant ( $P < 0.05$ ) as shown in Figures 1 and 2 and Table 6.

**3.2.2. Comparison of Umbilical Cord Blood PON1 Content in the MSAF and Control Groups.** Cord blood PON1 content in the MSAF group was  $80.40 \pm 24.67$  nmol/mL and in the control group was statistically significant ( $P < 0.001$ ) as shown in Table 7.

**3.2.3. Comparison of MCP-1 Plots and Content of Cord Blood in MSAF and Control Groups.** Cord blood MCP-1 content was 271.10 (174.35–326.62) pg/mL, and the control was 104.89 (50.15–184.19) pg/mL, which was statistically significant ( $P < 0.001$ ), shown in Figures 3 and 4 and Table 8.

**3.3. Results of Placental HE Staining in Both the MSAF and Control Groups.** After HE staining of 72 placentas, six had acute chorionic amnionitis (5 in MSAF, 1 in control), 32 had chronic chorioamnionitis (23 in MSAF, 9 in controls), 5 had nonabnormal placentas, and three in MSAF had chorionic amniotic columnar metaplasia (Figures 5-8).

### 4. Discussion

MSAF refers to the fact that when the fetal fetus is stimulated differently in utero, the intrauterine fetal intestinal peristalsis

is enhanced, and when the anal sphincter is relaxed and the meconium is discharged into the amniotic fluid, this makes the amniotic fluid brown and yellow-green and then becomes cloudy and thick [14]. Fetal hypoxia causes intestinal peristalsis, the relaxation of the anal sphincter, and the release of meconium in the amniotic fluid. Meconium can also be sucked out in the first breath at birth, with studies suggesting that meconium induced direct alveolar damage through inflammatory responses and damaged lung parenchyma and endothelial cells and that 3% to 12% of infants born with MSAF would develop MAS, characterized by characteristic X-ray plaque shadows and respiratory distress and often exacerbated by pulmonary hypertension [15]. By collecting clinical data from pregnant mothers and newborns, this study found no difference between gender, birth weight, maternal age, maternal age, and maternal and gestational history, but gestational age, gestational diabetes, gestational hypertension, umbilical cord abnormalities, placental abnormalities, and neonatal asphyxia were statically significant. The gestational age and placental abnormalities were risk factors in the MSAF group and showed a positive correlation, indicating that the greater the gestational age, the more likely to develop MSAF. Lu Shaoxia et al.'s [1] study pointed out that simple amniotic fluid dung infection may not cause fetal distress. In 276 pregnant women with MSAF, the gestational week was found to be a high-risk factor for MSAF, with the incidence of pregnant women over 40 weeks, significantly greater than 38 weeks. Wang Li et al.'s [16] study showed that pregnant mothers had a higher incidence of gestational diabetes and pre-eclampsia in the MSAF group than in the normal group. MSAF can cause intrauterine oxygen and chronic hypoxia in the newborn and can cause different damage to the respiratory, circulation, and digestive systems of the nervous system of the newborn [17]. The above views are consistent with the present study. In the current study, umbilical cord abnormalities may also be the influencing factor of MSAF, spiral umbilical cord and knot, and tight winding, the umbilical cord is too short, and the incidence of placental inflammation and MSAF is significantly increased [17, 18]. MSAF can be classified into primary and secondary contamination. After the fetal membrane rupture, amniotic fluid is feces, which is primary. After the fetal membrane rupture, the amniotic fluid is clear; along with the progress of the production process, the amniotic fluid gradually changes from brightening to feces dye, for secondary pollution [19]. Secondary meconium contamination cord was associated with meconium neonatal fetal distress and other poor neonatal prognoses, and primary amniotic fluid meconium contamination was associated with adverse outcomes [20]. Severe cases can die early in the newborn [21]. Microbial invasion of the amniotic cavity in placental inflammation increases the incidence of MSAF [22]. At present, the mechanism of amniotic fluid dung dyeing is unclear, and studying the correlation of inflammatory factors and MSAF can further explore the mechanism of MSAF occurrence.

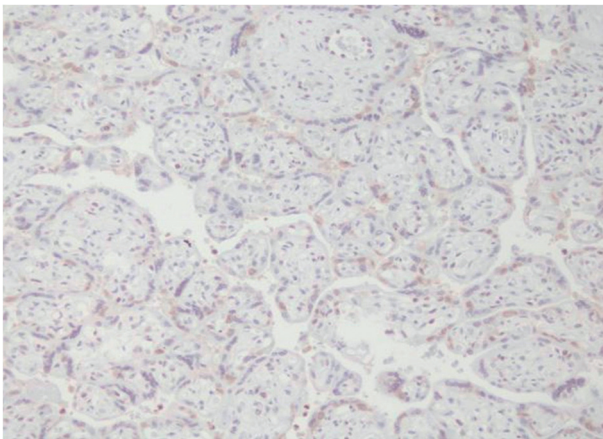
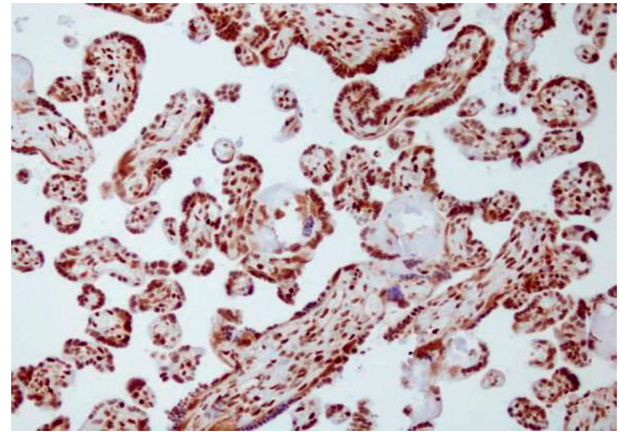
The main diagnosis basis for diagnosing intrauterine infection is that the pathological testing of CA and the placenta can more effectively detect and judge intrauterine

TABLE 4: Comparison of birth weight and maternal age of newborns in each group.

Project	MSAF group (n, %)	Control group (n, %)	$\chi^2$ (t%)Z	P
Fetal age ( $x \pm s$ )	41.38 $\pm$ 1.40	39.20 $\pm$ 1.24	7.053	<0.001
Birth weight ( $x \pm s$ )	3.55 $\pm$ 0.34	3.41 $\pm$ 0.40	1.698	0.094
Mother age ( $x \pm s$ )	29.50 $\pm$ 4.39	30.00 $\pm$ 5.11	0.309	0.759
Gender (male/female)	22/16	19/16	1.083	0.298
Early/via maternal	13/25	11/24	0.064	0.804
Pregnancy diabetes	12 (31.6)	4 (11.4)	4.323	0.038
Pregnancy hypertension	15 (39.5)	5 (14.3)	5.811	0.016
Hyperthyroidism, hypothyroidism, and anemia	6 (15.8)	5 (14.3)	0.032	0.858
Abnormal umbilical cord	9 (23.7)	2 (5.7)	4.597	0.032
Abnormal placenta	23 (60.5)	9 (25.7)	8.968	0.003
Neonatal asphyxia	17 (44.7)	8 (22.9)	3.873	0.049
History of fetal protection	9 (23.7)	7 (20.0)	0.145	0.704

TABLE 5: Logistic regression analysis of the risk factor analysis in the MSAF group.

	B	SE	Wald	P	OR (95%CI)
Fetal age	0.971	0.241	16.247	<0.001	2.639 (1.646–4.231)
Pregnancy diabetes	1.242	1.371	0.821	0.365	3.461 (0.236–50.808)
Pregnancy hypertension	0.753	1.114	0.457	0.499	2.122 (0.239–18.823)
Abnormal umbilical cord	1.139	1.217	0.876	0.349	3.123 (0.287–33.932)
Abnormal placenta	1.505	0.751	4.020	0.045	4.506 (1.034–19.631)
Neonatal asphyxia	1.295	0.782	2.742	0.098	3.653 (0.788–16.926)
Constant	-40.592	9.827	17.062	<0.001	0.000

FIGURE 1: Expression of chorionic amniotic HMGB1 (400  $\times$ ) in the control group.FIGURE 2: Expression of chorionic amniotic HMGB1 (400  $\times$ ) in the MSAF group.

infection [23, 24]. There was chronic inflammation of the placenta, compound trophoblast hyperplasia, and villus interstitial fibrosis in this experiment. There were CA, villus interstitial edema, fibrosis, and compound trophoblast hyperplasia; some studies pointed out that inflammatory cells with long span groups were mainly lymphocytes; that is, chronic inflammation is lymphocytes, and groups with short time span were neutrophils; namely, acute inflammation was mainly neutrophils [25]. In this study, it was shown that the MSAF group was more prone to placental inflammation, mainly with chronic inflammation.

HMGB1 is one member of the Alertin family, is divided in various cells, is an evolutionarily conserved DNA binding

protein that acts as Alertin, is translocated to the cytoplasm, and is secreted after injury. Extracellularly, it acts as an inflammatory cytokine [26, 27]. In this study, HMGB1 expression in placentas is higher in the MSAF group than in the control by immunohistochemical staining of both placentas. Considering that HMGB1 has been implicated in placental inflammation, high HMGB1 expression can upregulate the expression of late glycosylation end-product receptor (receptor for advanced glycation end products, RAGE), initiate a positive feedback mechanism, activate NF- $\kappa$ B, to produce a series of inflammatory factors, and exacerbate the inflammatory response in the placenta [28]. HMGB1 may be involved in the occurrence of MSAF.

TABLE 6: Comparison of HMGB1 expression intensity between the MSAF and control groups.

Group	N	HMGB1 expression intensity				Z	P
		-	+	++	+++		
MSAF group	38	1	7	11	20	6.494	< 0.001
Control group	35	18	15	2	1		

TABLE 7: Comparison of PON-1 content between the MSAF and control groups.

Group	N	PON-1 (nmol/mL)
MSAF group	38	80.40 ± 24.67
Control group	35	95.65 ± 24.33
Z		2.658
P		<0.010

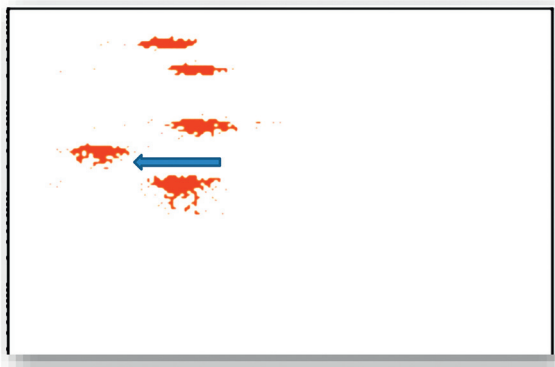


FIGURE 3: Cord blood MCP-1 content in the control group.

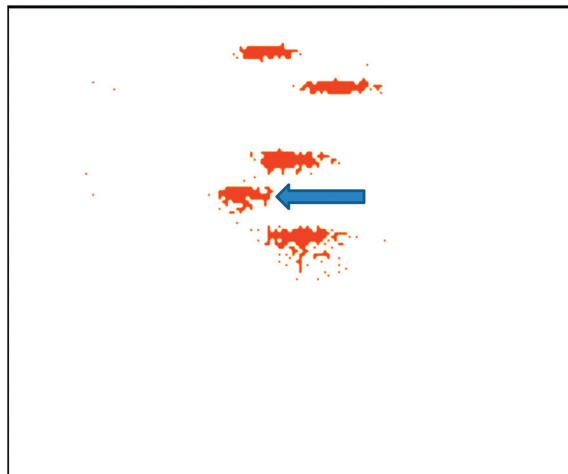


FIGURE 4: Cord blood MCP-1 content in MSAF group.

TABLE 8: Comparison of MCP-1 content between the MSAF and control groups.

Group	N	MCP-1 ( pg/mL )
MSAF group	38	271.10 ( 174.35–326.62 )
Control group	35	104.89 ( 50.15–184.19 )
Z		4.03
P		< 0.001

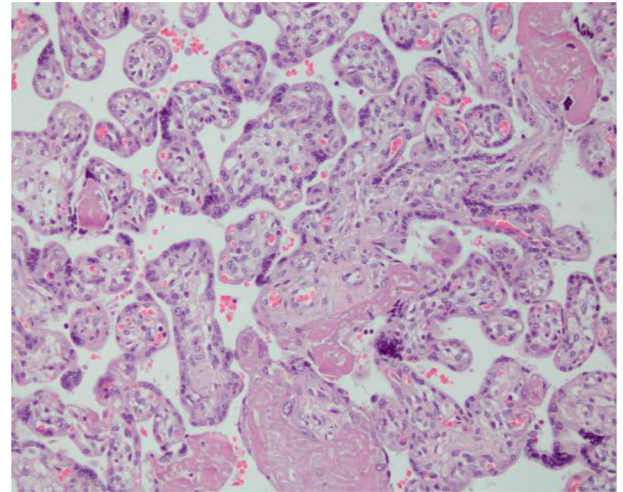


FIGURE 5: Chorioamnionitis (200 ×).

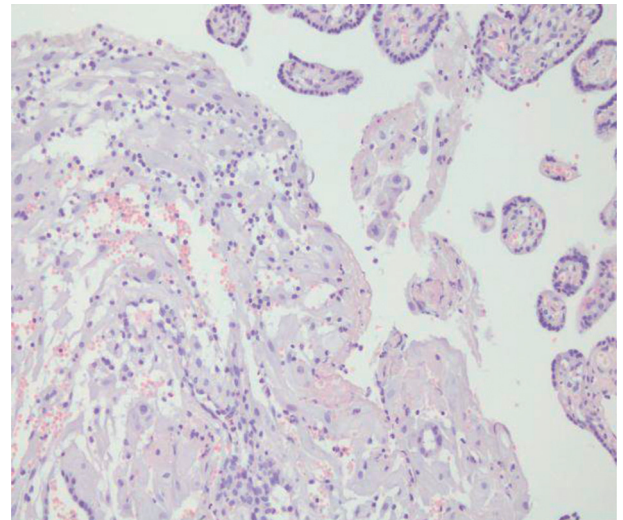


FIGURE 6: Chorioamnionitis with lymphocyte infiltration (200 ×).

HMGB1 has been associated with pregnancy complications, such as preterm birth and CA [29, 30]. Salihu et al. [31] pointed out that HMGB1 can accelerate partial cellular senescence and enhance contractility in the myometrium and expression of inflammatory genes. Endogenous hazard signals activate the Toll-like receptor-2 (TLR-2) and the Toll-like receptor-4 (TLR-4) and play a role in inflammatory diseases. HMGB1 may serve as an endogenous activator of these receptors. HMGB1 promotes neutrophils but not macrophage migration to necrotic tissue. In addition to the active secretion from inflammatory cells, HMGB1 is also passively released from necrotic cells, and HMGB1 from

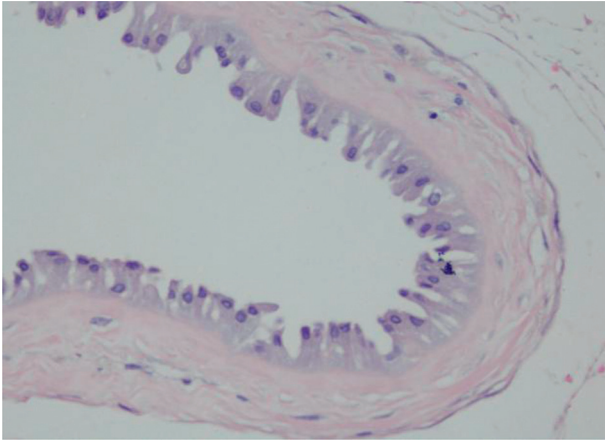


FIGURE 7: Chorioamniotic columnar epithelialization (400 ×).

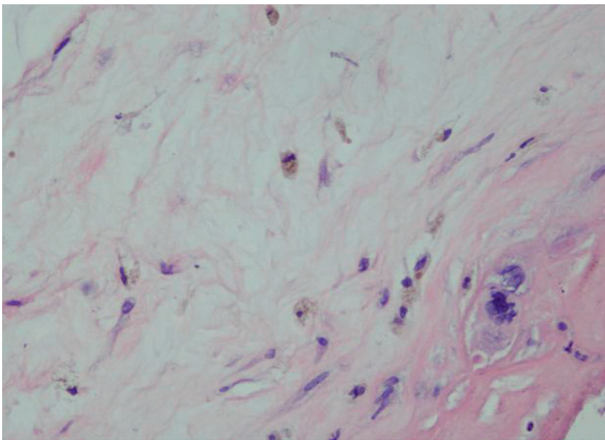


FIGURE 8: Placental chorioamnionitis edema in the MSAF group (400 ×).

cells at different sites can affect the inflammatory response after necrosis to varying degrees [32]. HMGB1 can promote the release of inflammation, with redox and endogenous cytokines-induced functional extracellular TLR4 mainly expressed in placental compound trophoblasts and fibroblasts. HMGB1 induces macrophages to produce inflammatory cytokines in a redox-dependent manner through TLR4 signaling, affecting cell proliferation, differentiation, and migration [26, 33]. All indicate a correlation with the occurrence of inflammation. HMGB1 can form an immunostimulatory complex. The inflammatory response triggered by HMGB1 may be involved in the placental inflammatory response that can induce the production of transcription factors (e.g., NF- $\kappa$ B) and trigger a local (and subsequently systemic) inflammatory response [34]. TLR2 and TLR4 are associated with MSAF, and in inflammatory cells, the Toll-like receptor (TLR) is combined with its ligand (HMGB1) through the recruitment of linker proteins to strongly activate NF- $\kappa$ B signaling, triggering inflammation [35]. The activity of HMGB1 that depends largely on its redox state, reduces HMGB1 release, and chemically modifies its redox form can improve inflammation as well as tissue damage. A positive correlation was observed between

the expression level of reactive oxygen species and the expression of HMGB1 protein [36]. In the MSAF study, HMGB1 expression in the placenta was stronger than in the control group, reliable, and oxidized.

PON-1, a member of the antioxidant enzyme family with anti-inflammatory effects, is an effective antioxidant associated with the pathogenesis of multiple diseases [37]. Multiple pathophysiological diseases are related and also have the damage of degraded organophosphate compounds to the nervous system [38, 39]. Thus, the state of PON1 in vivo can be determined by measuring the levels of enzymatic activity with different substrates [40, 41]. In this study, the PON1 gene is closely related to poison metabolism, and the strength of its activity directly affects the poison metabolism process in vivo. The oxidative stress response is involved in the development of inflammation and is an important cause of the expansion and aggravation of inflammatory response. The interaction of oxidative stress with the inflammatory response is the mechanism of disease development. Oxidative products are produced in normal physiological metabolism, while cells express endogenous antioxidants to remove free radicals and combat the harmful effects of reactive oxygen species products, keeping the oxidation/antioxidant system in a stable, balanced state [42]. PON-1 is a marker in oxidative stress metabolites. In the state of oxidative stress, the measured PON-1 content of cord blood in this study showed lower PON1 activity in the MSAF group than normal group, considering the oxidative/antioxidant system imbalance and the occurrence of oxidative stress and inflammation. Shandan et al. [43] pointed out that oxidative stress can cause placenta ischemia and hypoxia and affect the release of inflammatory factors and related enzymes. The possible involvement in the oxidative stress response in causing inflammation may have some relevance to MSAF.

MCP-1 is chemotaxis immune cells that produce corresponding antibodies after stimulation and affect phagocytosis to resist the invasion of foreign microorganisms. In recent years, studies have pointed out labor initiation, preterm birth, and pregnancy-related diseases [44, 45]. Xu Qingyun [46] suggests that elevated MCP-1 in neonatal cord blood may be involved in the development of CA. The main factor of CA is inflammatory factors through signaling; oxidative stress can stimulate inflammation and fetal edema degeneration; edema appeared in this study; there was placental HE staining; three cases had columnar metaplasia and MSAF cord blood MCP-1 higher than the control group and statistically significant difference; for placental HE staining, 3323 cases in the MSAF group had placental CA and mainly chronic chorioamnionitis. Case analysis studies studying preterm birth with MSAF indicated a higher probability of CA compared with the MSAF group [47, 48]. Liu Weiwei [14] pointed out that pregnant women in the MSAF group had a higher probability of neonatal infection than in the CA-free group; CA increased neonatal infection rate, increased intrauterine infection index in the perinatal period, and increased risk of infection during fetal delivery. Yan Lili et al. [49] pointed out that MCP-1 can drive activated macrophages and, with high MCP-1 expression,

increases cell adhesion and invasion and aggravates inflammation. In pediatric bronchial asthma, oxidative stress status is correlated with it, among which MCP-1 increases significantly between the onset and remission period in children, pointing out that oxidative stress levels are correlated with the imbalance of inflammatory factors [50]. MCP-1 may have some correlation with MSAF [9].

**4.1. Limitations.** The small sample size is limited, and increasing the sample size can improve the relevant studies.

## 5. Conclusion

The study concluded that gestational age and placental abnormalities are clinical high-risk factors for MSAF. We have found that placental chorioamnionitis may be one of the causes of MSAF. HMGB1, PON-1, MCP-1, and *P. gingivalis* may be involved in the development of MSAF, suggesting an oxidative/antioxidant imbalance with inflammation, and may be one of the mechanisms of MSAF development.

**5.1. Practical Implications.** HMGB1, PON-1, MCP-1, and *P. gingivalis* play an important role in immune responses in MSAF patients [51].

## Data Availability

The collected data have been included in the study.

## Ethical Approval

Specimen collection has been discussed by the Ethics Committee of Affiliated Hospital, Yanbian University, to collect placenta and cord blood stained with term amniotic fluid stool delivered from January 2018 to December 2019.

## Conflicts of Interest

The authors declare that they have no conflicts of interest.

## Acknowledgments

This study was supported by the Biostime Nutrition and Nursing Home “Maternal and Infant Clinical Research Special Fund” under 2020BINCLC009 and Science and Technology Project of Yanbian University.

## References

- [1] S. Lu, S. Ou, and X. Kang, “Case of clinical analysis,” *Modern Chinese Drug Application*, vol. 18, no. 21, pp. 264-265, 2015.
- [2] J. Xu, “The relationship between perinatal high-risk factors and fetal distress and neonatal asphyxia,” *Chinese Practical medicine*, vol. 10, no. 24, pp. 276-277, 2015.
- [3] S. Yue, “Amniotic fluid meconium pollution and nervous system damage,” *Chinese Clinical Journal of Practical Pediatrics*, vol. 30, no. 14, pp. 1046-1050, 2015.
- [4] L. Yin, “Study and analysis of perinatal high risk factors and fetal intrauterine distress and neonatal asphyxia,” *Journal of Aerospace Medicine*, vol. 28, no. 4, pp. 404-405, 2017.
- [5] M. Wu, “Amniotic fluid meconium pollution and neonatal prognosis,” *Women and abroad*, vol. 11, no. 18, pp. 36-37, 2016.
- [6] J. Lee, R. Romero, K. A. Lee et al., “Meconium aspiration syndrome: a role for fetal systemic inflammation,” *American Journal of Obstetrics and Gynecology*, vol. 214, no. 3, pp. e1-366, 2016.
- [7] L. Chen, C. Geng, and L. Zhang, “The relationship between contamination and duration of meconium and placental pathological changes,” *Clinical Medical Engineering*, vol. 22, no. 10, pp. 1367-1368, 2015.
- [8] M. Huang, M. Guo, K. Wang et al., “HMGB1 mediates paraquat-induced neuroinflammatory responses via activating RAGE signaling pathway,” *Neurotoxicity Research*, vol. 37, no. 4, pp. 913-925, 2019.
- [9] X. Qiu, *Significance of HMGB1 and its receptor in Chorioamnionitis-Related Preterm Birth*, Tianjin Medical University, Tianjin, China, 2017.
- [10] M. Mutlu, M. H. Korkmaz, E. Simsek et al., “Do CO2 and oxidative stress induce cancer?: a brief study about the evaluation of PON 1, CAT, CA and XO enzyme levels on head and neck cancer patients,” *Journal of Enzyme Inhibition and Medicinal Chemistry*, vol. 34, no. 1, pp. 459-464, 2019.
- [11] Y. Wu and Z. Wang, “Clinical significance and treatment of amniotic meconium pollution,” *Chinese Journal of Perinatal Medicine*, vol. 15, no. 4, pp. 203-205, 2012.
- [12] C. J. Kim, R. Romero, P. Chaemsathong, and J.-S. Kim, “Chronic inflammation of the placenta: definition, classification, pathogenesis, and clinical significance,” *American Journal of Obstetrics and Gynecology*, vol. 213, no. 4, pp. S53-S69, 2015.
- [13] S. Ni and J. Liu, “Expression of matrix metalloproteinases and tissue inhibitors and Toll-like receptors in fetal membrane tissue in patients with premature fetal membrane rupture,” *Hebei Medicine*, vol. 40, no. 1, pp. 28-31, 2018.
- [14] W. Liu, W. Zhang, and Y. Jiao, “Effect of amniotic fluid meconium contamination and chorionic amnionitis on maternal and infant infection,” *Chinese Journal of Neonatology (Chinese and English)*, vol. 34, no. 4, pp. 281-285, 2019.
- [15] G. Lista, “Neonatologists and non-vigorous newborns with meconium-stained amniotic fluid (MSAF) in the delivery room: time for hands off?” *European Journal of Pediatrics*, vol. 178, no. 12, pp. 1823-1824, 2019.
- [16] L. Wang, “Case of meconium contamination,” *Medical Information*, vol. 29, no. 33, pp. 274-275, 2016.
- [17] H. Chen and S. Chen, “Discuss the influence of amniotic fluid manure infection on maternal pregnancy outcome and correlation,” *Modern drug application in China*, vol. 13, no. 12, pp. 23-25, 2019.
- [18] Y. Zhang, “Amniotic meconal contamination and fetal intrauterine distress and neonatal asphyxia,” *Health Care Guide*, vol. 10, no. 40, p. 363, 2018.
- [19] L. Hirsch, N. Melamed, H. Rosen, Y. Peled, A. Wiznitzer, and Y. Yogeve, “New onset of meconium during labor versus primary meconium-stained amniotic fluid - is there a difference in pregnancy outcome?” *The Journal of Maternal-Fetal & Neonatal Medicine*, vol. 27, no. 13, pp. 1361-1367, 2014.
- [20] Q. Xu, “Clinical significance of primary and secondary amniotic fluid meconium contamination,” *Medical Theory and Practice*, vol. 31, no. 6, pp. 875-877, 2018.

- [21] M. Ali, A. Maruf, N. Naher, and S. Islam, "Neonatal outcome in meconium stained amniotic fluid (MSAF): a study in a neonatal high dependency unit (NHDU) of a medical college hospital," *Mediscope*, vol. 6, no. 2, pp. 65–71, 2019.
- [22] D. Paz-Levy, A. Walfisch, T. Wainstock, D. Landau, and E. Sheiner, "696: meconium stained amniotic fluid exposure is associated with a lower rate of offspring's infectious morbidity," *American Journal of Obstetrics and Gynecology*, vol. 220, no. 1, pp. S459–S460, 2019.
- [23] M. Bolten and E. Chandrarahan, "The significance of 'non-significant' meconium stained amniotic fluid (MSAF): colour versus contents," *Journal of Advances in Medicine and Medical Research*, vol. 30, no. 5, pp. 1–7, 2019.
- [24] H. Liao, "Analysis of placental disease infected with amniotic fluid dung," *Everybody Health (Academic Edition)*, vol. 10, no. 7, pp. 58–59, 2016.
- [25] J. Zheng, L. Zheng, D. Wang et al., "The relationship between amniotic fluid dyeing and amniotic cavity infection," *Chinese Journal of Infectology of the Hospital*, vol. 23, no. 8, pp. 1846–1847, 2013.
- [26] A. Raucci, S. Di Maggio, F. Scavello, A. D'Ambrosio, M. E. Bianchi, and M. C. Capogrossi, "The Janus face of HMGB1 in heart disease: a necessary update," *Cellular and Molecular Life Sciences*, vol. 76, no. 2, pp. 211–229, 2019.
- [27] H. Yang, P. Lundbäck, L. Ottosson et al., "Expression of Concern to: redox modification of cysteine residues regulates the cytokine activity of high mobility group box-1 (HMGB1)," *Molecular Medicine*, vol. 26, no. 1, p. 18, 2020.
- [28] L. Y. Huang, I. C. Yen, W. C. Tsai et al., "Rhodiola crenulata suppresses high glucose-induced matrix metalloproteinase expression and inflammatory responses by inhibiting ROS-related HMGB1-TLR4 signaling in endothelial cells," *The American Journal of Chinese Medicine*, vol. 48, pp. 1–15, 2020.
- [29] R. Menon, F. Behnia, J. Polettini, G. R. Saade, J. Campisi, and M. Velarde, "Placental membrane aging and HMGB1 signaling associated with human parturition," *Aging*, vol. 8, no. 2, pp. 216–230, 2016.
- [30] C. Hernandez, P. Huebener, J. P. Pradere et al., "HMGB1 links chronic liver injury to progenitor responses and hepatocarcinogenesis," *The Journal of clinical investigation*, vol. 128, no. 6, pp. 2436–2450, 2019.
- [31] H. M. Salihu, A. Pradhan, L. King et al., "Impact of intra-uterine tobacco exposure on fetal telomere length," *American Journal of Obstetrics and Gynecology*, vol. 212, pp. 205–208, 2015.
- [32] Y. Wang, F. Du, A. Hawez et al., "Neutrophil extracellular trap-microparticle complexes trigger neutrophil recruitment via high-mobility group protein 1 (HMGB1)-oll-like receptors (TLR2)/TLR4 signalling," *British Journal of Pharmacology*, vol. 176, no. 17, pp. 3350–3363, 2019.
- [33] B. Khambu, N. Huda, X. Chen et al., "HMGB1 promotes ductular reaction and tumorigenesis in autophagy-deficient livers," *The Journal of clinical investigation*, vol. 128, no. 6, pp. 2419–2435, 2019.
- [34] S. Rakoff-Nahoum and R. Medzhitov, "Toll-like receptors and cancer," *Nature Reviews Cancer*, vol. 9, no. 1, pp. 57–63, 2009.
- [35] S. Zhang, M. Wang, Z. Chen et al., "Expression of Toll-like receptor in children with hemophocytic syndrome," *Chinese Journal of Experimental Hematology*, vol. 27, no. 5, pp. 1664–1671, 2019.
- [36] L. Yan, S. Z. Qi, and T. Wang, "Regulation of HMGB1 expression in lung cancer cells and its application value in lung cancer screening," *Journal of Clinical Examination*, vol. 37, no. 8, pp. 625–628, 2019.
- [37] M. Alimohammadi, M. Soodi, and M. Gholami Fesharaki, "Organophosphate pesticide exposure reduced serum Para-oxonase1 (PON1) activity which correlated with oxidative stress in pesticide factory workers," *Archives of Hygiene Sciences*, vol. 8, no. 2, pp. 88–97, 2019.
- [38] S. Dong, Z. Liu, and S. Guo, "Effect of PON1 activity and AOPP levels on disease severity in preeclampsia," *Maternal and Child Health Care in China*, vol. 34, no. 12, pp. 2698–2701, 2019.
- [39] Y. Wu, "Study on diagnosis of PON1 diagnosis and disease in women with endometriosis," *Experimental and Laboratory Medicine*, vol. 37, no. 5, pp. 919–921, 2019.
- [40] X. Xiao, X. Wen, Y. Chu et al., "PON-1 reduces the molecular mechanism of myocardial oxidative stress damage by up-regulating HSPB1 expression," *Journal of Practical Shock (Chinese and English)*, vol. 3, no. 3, pp. 150–154, 2019.
- [41] C. O. Reichert, C. G. de Macedo, D. Levy et al., "Paraoxonases (PON) 1, 2, and 3 polymorphisms and PON-1 activities in patients with sickle cell disease," *Antioxidants*, vol. 8, no. 8, p. 252, 2019.
- [42] G. Lin and H. Zhao, "Effect of oxidative stress on placental life," *International Journal of Obstetrics and Gynecology*, vol. 46, no. 2, pp. 185–188, 2019.
- [43] D. Shi, Y. Wang, J. Guo et al., "Clinical study on oxidative stress, inflammatory response, and vascular endothelial injury in patients with preeclampsia," *PLA Journal of Medicine*, vol. 30, no. 1, pp. 60–63, 2018.
- [44] S. Lin, D. Ke, Y. Lin et al., "Puerarin inhibits the migration of osteoclast precursors and osteoclastogenesis by inhibiting MCP-1 production," *Bioscience, Biotechnology, and Biochemistry*, vol. 84, pp. 1–5, 2020.
- [45] C. Sun, X. Li, E. Guo et al., "MCP-1/CCR-2 axis in adipocytes and cancer cell respectively facilitates ovarian cancer peritoneal metastasis," *Oncogene*, vol. 39, no. 8, pp. 1681–1695, 2020.
- [46] Q. Xu, *Correlation between TLR-2, 4 and MCP-1 and Premature Fetal Membrane Rupture and Chorioamnionitis*, Yanbian University, Jilin, China, 2018.
- [47] D. Brabbing-Goldstein, D. Nir, D. Cohen, A. Many, and S. Maslovitz, "Preterm meconium-stained amniotic fluid is an ominous sign for the development of chorioamnionitis and for in utero cord compression," *The Journal of Maternal-Fetal & Neonatal Medicine*, vol. 30, no. 17, pp. 2042–2045, 2017.
- [48] K. Abraham, E. Thomas, and J. Lionel, "New evidence to support antibiotic prophylaxis in meconium-stained amniotic fluid in low-risk women in labor a prospective cohort study," *The Journal of Obstetrics and Gynecology of India*, vol. 68, no. 5, pp. 360–365, 2018.
- [49] L. Yan and H. Lijuan, "Changes and significance of peripheral blood MCP-1, sflt-1, sICAM-1 in patients with endometriosis," *Chinese Journal of Family Planning*, vol. 27, no. 10, pp. 1339–1342, 2019.
- [50] C. Zhu and L. Zhang, "Evaluation of serum inflammatory factor levels and oxidative stress status in children with bronchial asthma," *World Composite Medicine*, vol. 5, no. 8, pp. 33–35, 2019.